Renewable Monomers for Bio-styrene Formation using Phenolic Acid Decarboxylase

Nurfariza Bahrin

A thesis submitted in partial fulfilment of the requirement for the degree of Doctor of Philosophy in Chemistry

WARWICK
THE UNIVERSITY OF WARWICK

Department of Chemistry

July 2017

Supervisor: Professor T. D. H Bugg

TABLE OF CONTENTS

LIST OF FIGURES

LIST OF TABLES

ACKNOWLEDGEMENT

الحمد لله .. Praise be to Allah, for allowing me to undergo this journey.

I wish to express my gratitude to the financial support provided by Majlis Amanah Rakyat (MARA) for the 4 years sponsorship I have received throughout my study.

To the best supervisor I have ever had, Professor Tim Bugg, thank you for your continuous support and guidance for all these years. To my advisory panel; Dr Manuela Tosin and Dr Claudia Blindauer, Professor Martin Wills and Sukhjit as well as the Department of Chemistry in general, thank you for the all the advice, and facilities provided.

To the Bugg group members, past and present especially my seniors; Dr Rahman Rahmanpour, Dr Goran Mahmoud, Dr Paul Sainsbury, Dr Peter Harrison, Jo, Dr Zoe Mycroft, Dr Maria Duran Pena and others, many thanks for the help, friendship and fun we have shared together. Thank you to Anne Smith, Magda and some friendly faces in CBRF. Not forgetting the kind technical assistance from Alifah (Physics) and Dr Panos Efthymiadis (WMG), thank you so much.

Special appreciation goes to my parents Mr Bahrin & Mdm Rosinah, my brothers Abdul Rashid and (late) Abdul Halim, my sisters Afiqah, Hazimah & 'Amirah as well as my family in-laws, for the years of never ending encouragement and prayers to keep me going. To my dear husband Faissal and son Marwan, thank you for taking this journey with me, it has bound us closer as a little family. I couldn't do this without their support, and will be forever indebted to all of them. My grandparents (Makwo, Maktok & Tokwan) and aunts (Umi & Mak Lang) whom have all passed away while I was dealing with my final year here, may Allah bless them. I will miss you all dearly.

Finally, to all my friends here, our new friendship blossomed into beautiful sisterhood that I hope will last forever.

DECLARATION OF AUTHORSHIP

Experimental work contained within this thesis is original research carried out by the author, unless otherwise stated, in the Department of Chemistry at the University of Warwick, between April 2013 and June 2017. No material contained herein has been submitted for any other degree, or at any other institution.

Results from other authors are referenced in the usual manner throughout the text.

Your name : Nurfariza Bahrin

Date : 10 July 2017

ABSTRACT

Lignocellulose is an abundant natural polymer on earth that contains renewable resource of aromatic compound, the lignin. Many industrially valuable chemicals can be developed from lignin and this can reduce the dependency on petrochemicals.

Wheat straw contains ferulic acid as one of its building blocks, which can be accumulated as a major metabolite from growth with *Rhodococcus jostii* RHA1, a known lignin degrading bacteria in minimal media.

Using the enzyme phenolic acid decarboxylase (PAD) in engineered *E.coli*, ferulic acid was converted into 4-vinylguaiacol (3-methoxy-4-hydroxystyrene). The substituted monostyrene was then enzymatically polymerised by laccase to form a polymer that showed an adhesive property. This enzymatically generated polymer can potentially provide an alternative to synthetic process, besides providing renewable option to generate environmental friendly material in ambient conditions.

.

ABBREVIATIONS

Ala	Alanine
Arg	Arginine
EIC	Extracted ion chromatogram
ESI	Electrospray ionisation
FDCA	Furandicarboxylic acid
Glu	Glutamic acid
GPC	Gel permeation chromatography
His	Histidine
His_6	Hexa-histidine
HPLC	High-performance liquid chromatography
IPTG	Isopropyl β-D-1-thiogalactopyranoside
LB	Luria-Bertani
LCMS	Liquid chromatography mass spectrometry
MeOH	methanol
NaOH	Sodium hydroxide
PAD	Phenolic acid decarboxylase
PET	Polyethylene terephthalate
PHA	Polyhydroxyalkanoate
PLA	Polylactic acid
Poly(4-vinylguaiacol)	Poly[(3-methoxy-4-hydroxystyrene)]
Poly[(4-vinylguaiacol)-co-(4-vinylcatechol)]	Poly[(3-methoxy-4-hydroxystyrene)-co-(3,4-dihydroxystyrene)]
PS	Polystyrene
rpm	Rotation per minute
RT	Retention time
SEM	Scanning electron microscope
TIC	Total ion chromatogram
TLC	Thin layer chromatography
Tyr	Tyrosine
UK	United Kingdom
US	United States
WS	Wheat straw (milled)

CHAPTER 1 INTRODUCTION

The development of renewable resources as sources of fuels and chemicals has become increasingly important, since fossil-based resources is depleting greatly. The research and technology to convert and manipulate waste materials or agricultural by products have the potential to reduce fossil-dependent energy production [1]·[2]. Plant biomass represents a readily available and renewable, and thus versatile alternative resource, and research focused on exploring the possibilities to exploit this resource is growing [3]. Many industrially important products such as biofuel, aromatic chemicals, animal feed and others can be synthesised from lignocellulose.

1.1 Lignocellulose biomass

Plant biomass is the most abundant renewable resource in the biosphere. Focusing on cereal producing crops that makes up staple foods in many countries around the world, the amount of crop residues produced post- harvest per year are vast. Within the UK, wheat straw is generated in large scale as a byproduct of wheat plantation. Many varieties of wheat are planted, and fall into several categories i.e: control, bread-making varieties, biscuit-making varieties and animal feed varieties. According to the national statistics by the Department for Environment, Food & Rural Affairs [4], more than ten thousand tonnes of wheat were produced each year from 2011 to 2015 alone, as shown in Figure 1.

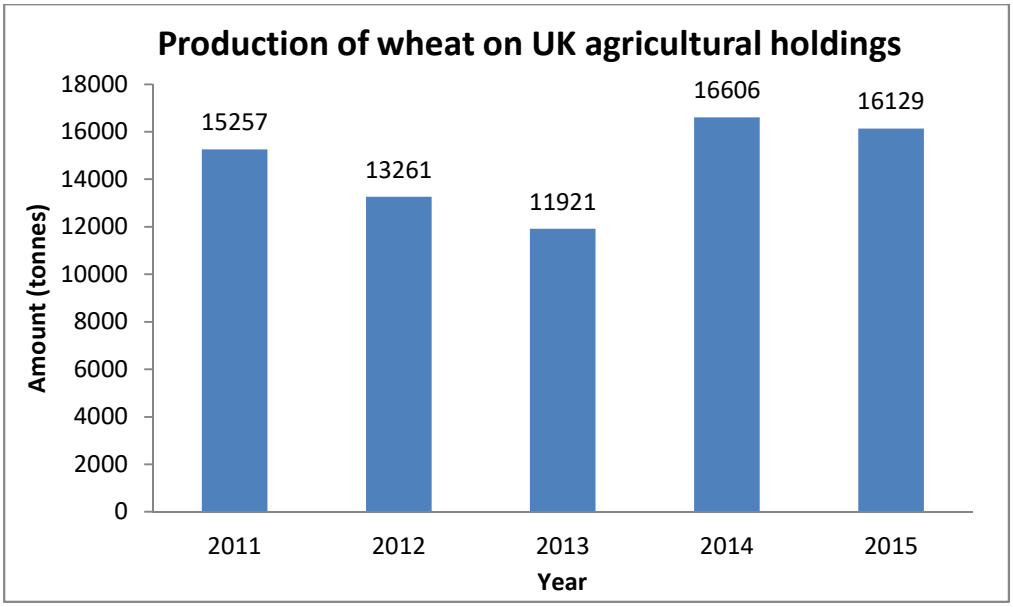

Figure 1: Production trend of wheat on UK agricultural holdings
Source: Ref [4]

Since it has been illegal to burn straw in fields, this agricultural waste has either been reused as animal bedding, returned to soil in chopped form, or sold as hay to farmers for winter uses. However, wheat straw is an attractive source for bioconversion into value added products, since it is rich in lignocellulose, and due to being non-edible, does not compete with food production.

Lignocellulose is a high molecular weight heteropolymer consisting of lignin and complex polysaccharides, namely cellulose and hemicellulose. It is generally found in all terrestrial plants, with different ratios of lignin to polysaccharide. In addition to those three main constituents, straw contains various other organic compounds including small quantities of protein, sugars and salts. It also has a waxy coating which functions as protective layer for the epidermis of the straw.

Other than that, some amount of insoluble ash including silica also exists within straw, due to its uptake from the soil. This is one of the reason why straw is very difficult to process in its raw state, since it cause bluntness to cutting machinery, interferes with pulping processes (in paper industry), reduces digestibility (in animal feed industry) and is generally difficult to burn [5]–[7].

Interestingly, there are also cases where the ratio of lignin to polysaccharides varies to quite a significant degree within a single plant species, affected by the cultivar, season, and location of the plantation [8], [9]. The lignocellulose compositions of some cereal based agricultural feedstocks are shown in Table 1.

Table 1: Composition of some lignocellulose feedstocks in cereal-based agroindustry

Feedstocks	**Lignocellulose composition (% dry weight)**		
	Lignin	**Cellulose**	**Hemicellulose**
Barley husk	19	34	36
Barley straw	6.3 – 9.8	36 – 43	24 – 33
Rice straw	17 – 19	29.2 – 34.7	23 – 25.9
Rice husk	15.4 – 20	28.7 – 35.6	11.96 – 29.3
Wheat straw	12 – 16	35 – 39	22 – 30
Oat straw	10 – 15	31 – 35	20 – 26

Source: Ref [10]

This information can be of considerable importance to exploit the crop residue, such as to determine the type of treatment to be used or product that can be valorised from each kind of crop. For most of the time, the industry would preferentially select the locally sourced material to be utilised for conversion into value added product.

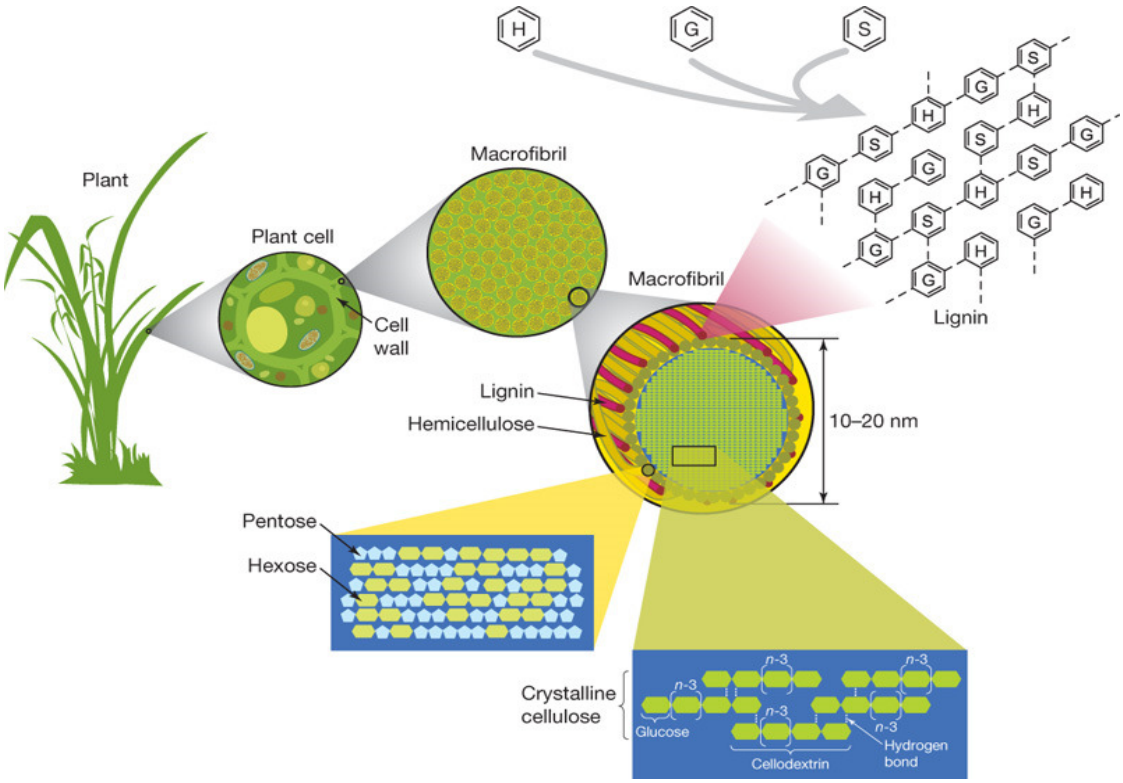

Figure 2: Generalised structure of lignocellulose.
Source: Ref [11]

Figure 2 generally depicts the building block of lignocellulose. It is mainly comprised of cellulose, a β(1–4)-linked chain of glucose molecules. This polysaccharide is strengthened by hydrogen bonds between each of its different layers providing resistance towards degradation. Then, there is hemicellulose, which consists of various pentoses and hexoses such as arabinose, galactose, glucose, mannose and xylose. Finally, lignin, the structural reinforcement of lignocellulose, is composed of three major phenolic components, namely *p*-coumaryl alcohol (H), coniferyl alcohol (G) and sinapyl alcohol (S) as shown in Figure 3.

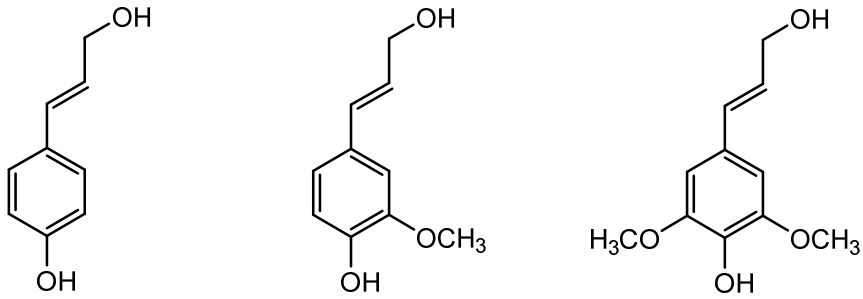

p-Coumaryl alcohol (*p*-Hydroxyphenyl, H unit) | Coniferyl alcohol (Guaiacyl, G unit) | Sinapyl alcohol (Syringyl, S unit)

Figure 3: Monolignol building blocks for lignin

Lignin is synthesised by polymerisation of these components and their ratio within the polymer varies between different plants (see Table 1), wood tissues and cell wall layers [11]. The polysaccharides within plant biomass can yield a large amount of metabolisable sugars and energy, however, access to them is hindered by the highly recalcitrant lignin [10].

1.1.1 Lignin

Lignin is by far the most abundant source of aromatic heteropolymer available in nature [9]. It made up the 20-35% dry weight of the rigid component in all terrestrial plants [10]. Industrially, it is also currently produced as a ‘‘waste stream’’ in paper and biofuel productions [3].

Brunow *et al.* (1999) introduced the idea of protolignins and how they are polymerised by branching and cross-linking. The protolignins actually referred to phenylpropanoid S, G and H units. Like Sun *et al*., they discussed the existance of linkages between protolignin and carbohydrates, which in this case are the cellulose

and hemicellulose. Also mentioned were some other types of protolignins being esterified with phenolic acids and specifically describing how grass lignins forms ester linkage with *p*-coumaric acid [12]–[14].

The lignin biosynthetic pathway involves a cascade of enzymes. Since lignin is aromatic, the starting point of its monolignol synthesis begins with the aromatic amino acid, mainly phenylalanine and sometimes tyrosine catalysed by the enzyme phenylalanine (or tyrosine) ammonia-lyase (P/TAL) [15]–[18]. A recent finding by Maeda (2016) has showed that in a grass model, there is a 'short cut' to produce cinnamate directly from tyrosine instead of phenylalanine. This was due to the readily available hydroxyl group at the *para*-position [19].

Once the monolignols are generated, it is generally understood that lignin is synthesised via the action of intracellular plant peroxidases or laccases. A single electron oxidation of the monolignol precursor generates a phenoxy intermediate (oxidised monomer). This is followed by random radical coupling of 4-hydroxyphenylpropanoids S, G and H type (Figure 3) which participate in a variety of radical dimerisation and polymerisation reactions yielding to a variety of bonds and linkages. They consist of β-aryl ether (β–O–4), phenylcoumaran (β–5), pinoresinol (β–β), biphenyl (5-5) and diphenyl ether (4-O-5). Sometimes, a cinnamaldehyde end group is found [14], [16], [20]–[24]. Altogether, the most common linkages formed are the β-aryl ether and biphenyl bonds [25]. The complexity of the overall wheat straw lignin structure is illustrated in Figure 4, as suggested by Sun *et al.* (1997) [13], [26].

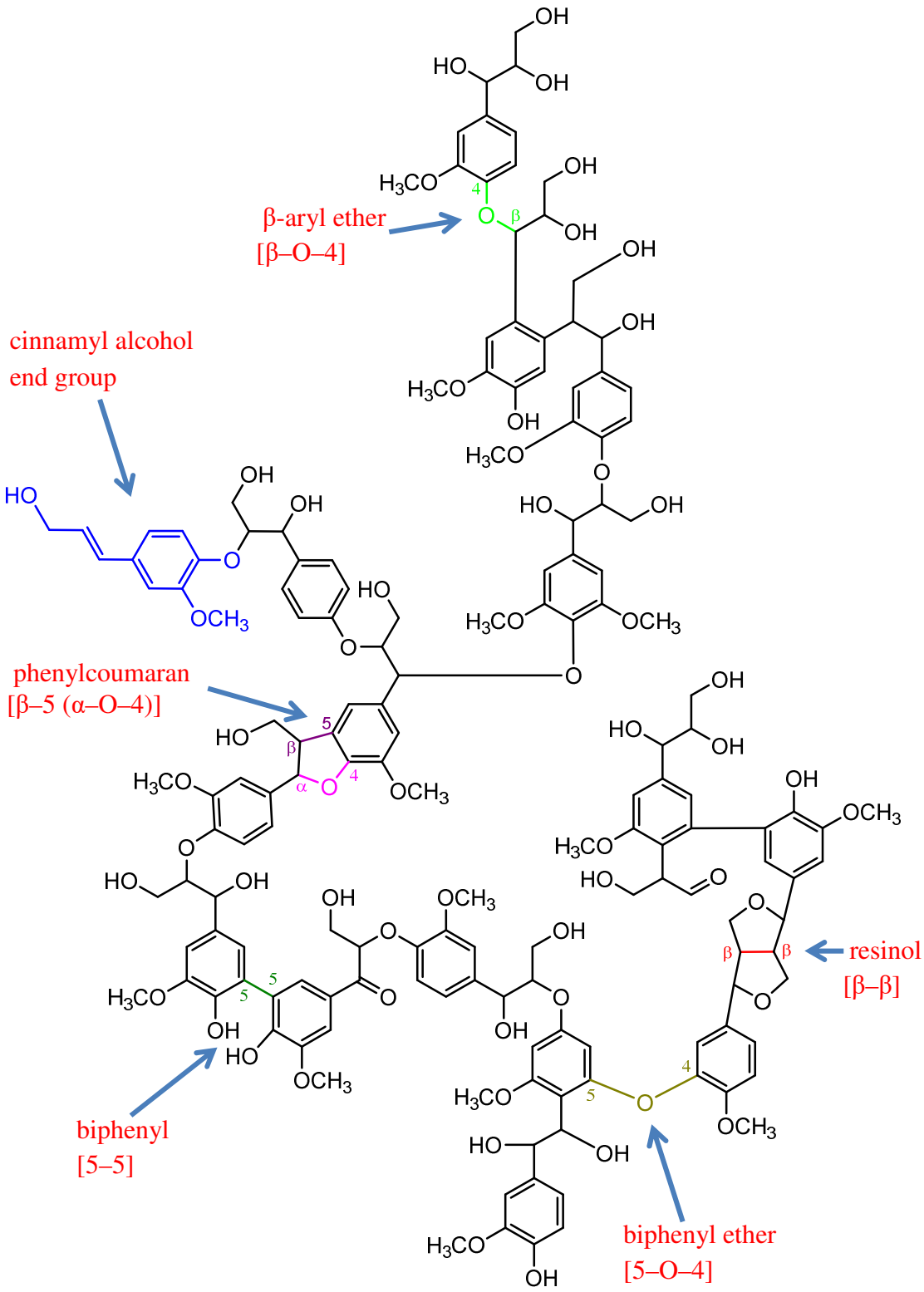

Figure 4: Schematic chemical structure of wheat straw lignin
Adapted from ref [13], [26]

In plant, lignin makes an important contribution towards the plants' wellbeing and structural development. Lignin thickens plant cell wall and therefore provides strength, rigidity as well as mechanical support for plant organs. This allows an upright growth and increase in size. Lignin, being hydrophobic, is also advantageous for the xylem and phloem tissues in plants vascular system to aid the transport of water and solutes. It also renders them insoluble in water, thus, providing resistance to the usual climatic wear and tear. Finally, lignin also provides protection against pathogens by providing a passive barrier for the internal polysaccharide layers. Furthermore, the compounds released from monolignol biosynthesis during the lignification process were found to have the ability to act as antimicrobial agents, such as against powdery mildew fungus on wheat [20], [27], [28].

As plants become mature, their lignin content increases significantly. This is due to the incorporation of H and G units which begins at the onset of lignification. The S units however, are not detected as much during this stage. Afterwards, coniferyl alcohol and increasing amounts of sinapyl alcohol are fused to form a mix of G and S units during secondary wall formation [29]. In grass cell walls, hydroxycinnamic acids are also incorporated during secondary cell wall development and lignification. While ferulic acid is the major hydroxycinnamate derivative in young grass cell walls, *p*-coumaric acid is an indicator of cell wall maturity, since it is mainly esterified to side chains of S units and its incorporation follows the same deposition pattern of syringyl units [18]. Differential distribution of lignin monomers is also observed in case of specific cell types [30].

1.1.2 Value added products from lignocellulose

There has been an ongoing research throughout the world on converting lignocellulose as renewable resource into value added products based on locally obtained agriculture byproducts. These byproducts are mainly waste that remain in the fields after the harvest. The appealing factors for using biomass for production of fuel and chemicals are that it does not compete with food for human consumption, and their large scale annual production. The USA for example would utilise corn stover, while Brazil uses sugarcane bagasse for their biofuel production [31]. Some South East Asian countries would use oil palm residues or rice straw, and the UK would easily exploit the availability of sugar beet residue, wheat, barley or oat straw. Possible "waste to wealth" products from lignocellulose are illustrated in Figure 5 [32].

As the pyramid goes higher, the value of the product generated is higher. Meanwhile, products listed closed to the base are usually produced in bulk, without much conversion processing and usually cheaper in price. Biofuel for example, needs quite a lengthy process such as depolymerisation of polysaccharides from lignin, followed by hydrolysis of the cellulose and hemicellulose prior to its fermentation. [33]–[36], [36]–[38]. The selling price however, has to compete with the existing petroleum based fuel. Thus, the value can fluctuate, depending on the market price of petroleum.

Fine chemicals on the other hand, even though requires a thorough processing, it is often sold as medium to high purity material. Therefore, their price is stable and could generate higher return compared to the cost of its starting material. Aromatic

compounds are among the expensive products that exist in cosmetic, perfumery, food and even polymer industry.

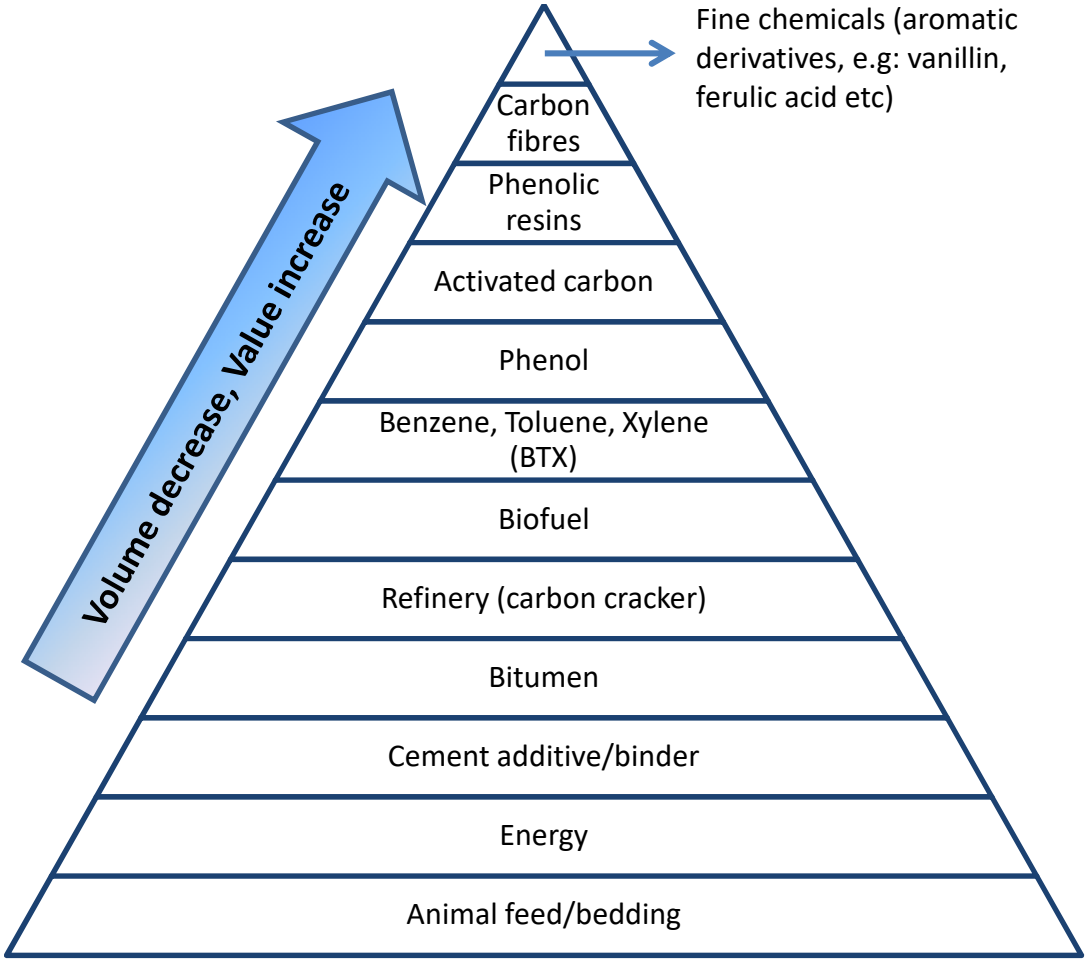

Figure 5: Value added products from lignocellulose.
Adapted from ref [32]

Lignocellulose has huge potential to be a source of renewable aromatic monomers which can then be used to synthesise green-polymers if properly broken down. Many techniques have been employed even in industrial scale to chemically or physically deconstruct lignocellulose. The most notable pretreatments are mechanical milling, steam explosion, dilute acid or alkaline hydrolysis, organosolv and ionic liquid treatment [10], [34]–[47]. A biological alternative has also been explored, which is the use of lignin degrading microorganism [7], [43].

1.1.3 Lignin degradation

Lignin degradation is essential for the Earth's carbon cycle since it hinders the breakdown of the cellulose and hemicellulose. Hence, research on lignin degradation is often aimed to remove lignin, to provide better access to the metabolisable sugars so that it can be converted to biofuel [11], [33], [36], [37], [48], [49], animal feed [6], [7], [50], [51] or kraft pulping in paper industry [52]–[55]. But it would be more beneficial to utilise the rich aromatic molecule resource in lignin to produce value added products. Lignin depolymerisation utilises a number of biochemical reactions that occur quite simultaneously. They involve the cleavage of intermonomeric linkages, demethylations, hydroxylations, side chain modifications, and aromatic ring fission followed by dissimilation of the aliphatic metabolites produced [56].

In nature, lignin can be broken down by the actions of microbial enzymes such as lignin peroxidase, manganese peroxidase, laccase and versatile peroxidase. These lignin degrading enzymes fall under the category of oxidoreductase. Notable examples are the well-researched types of haem peroxidases; manganese peroxidase, lignin peroxidase, and versatile peroxidase and laccase, a multicopper phenoloxidase. Manganese peroxidase, MnP (EC1.11.1.13) is a haem protein which represents the most common lignin-modifying enzymes secreted by almost all basidiomycetes and various soil-colonising fungi. MnP preferentially oxidise Mn^{2+} into Mn^{3+}. This reactive Mn^{3+} is then stabilised before acting as diffusible redox-mediator that attacks phenolic lignin structures, creating unstable free radicals that are easily broken down [57]. Lignin peroxidase, LiP (EC1.11.1.14), also an iron-dependent enzyme that catalyses the oxidative depolymerisation in the side chains of lignin and related compounds aided by H_2O_2. LiP also performs extended

valorisation of lignin fragments that were initially broken down by MnP [58], [59]. Versatile peroxidase, VP (EC 1.11.1.16) exhibits a unique feature of having multiple active sites. This increased its capability to oxidise different substrates under altered environmental conditions [60]. Together with MnP and LiP, it can undergo synergistic reaction to degrade lignin if all of them are produced by the same organism [61]. Laccase (EC 1.10.3.2) has been widely studied for its ability to oxidise phenolic lignin units, as well as degrading non-phenolic lignin units in the presence of synthetic mediators [58]. Laccase will be discussed in detail in a later section.

Most researches have been established around the role of white-rot and brown-rot fungi in delignification of plant materials [62]. Many white-rot fungi from the Basidiomycetes family such as from the genus *Pleurotus*, *Agaricus*, and *Phanerochaete* to name a few, has been thoroughly studied for their ligninolytic enzymes. Nevertheless, there is no commercialised lignin breakdown process yet even after more than two decades of research. This is due mainly to difficulties in fungal genetics and protein expression [63].

Even though both fungi and bacteria are able to depolymerise lignin; they have different reactivity towards lignin [2]. There is however, evidence that bacterial lignin degradation is more specific than the fungal systems making bacterial enzymes more attractive for applications in biotechnology where specific modifications of lignin would be of interest [11], [56], [64].

Lignin degrading bacteria can be isolated from nature, particularly from soil which was made up of the rich layer of decaying plant material [65]. Besides that, they also thrive in the stomach of ruminants as well as anaerobic ecosystems in sediments

[64]. Although the understanding of lignin degradation in bacteria is not as complete compared to fungal systems, bacteria are capable of depolymerising lignin into smaller aromatics for intracellular catabolism, a common trait for soil bacteria [2].

The genus *Rhodococcus* is a distinctive taxon of microorganisms that has a wide range of metabolic diversity, particularly for degradation of aromatic and aliphatic hydrocarbons, chlorinated phenolics, steroids and lignin. They are capable to breakdown xenobiotic compounds, while some of its members showed pathogenicity towards human, animal and plants [66], [67]. Their competency of performing biodegradation is comparable to pseudomonads and some other related bacteria [67]. *Rhodococci* are aerobic, Gram-positive, nonmotile nocardioform actinomycetes. They fall under the same order as streptomycetes, the current antibiotic producing organism, as well as the pathogenic *Mycobacterium tuberculosis*. They can exist as cocci or short rods to filaments with short projections, elementary branching, or, in some species, extremely branched hyphae [66].

The sequencing and annotation of the genome of *Rhodococcus jostii* RHA1 (RHA1) provided an understanding of how it could degrade a wide array of aromatic compounds by separate pathways [63]. The bacterium was originally isolated from lindane contaminated soil, proving its competency as bioremediation tool. RHA1 has a total of 34 pathways (26 peripheral and 8 central pathways) for catabolism of aromatics [68]. According to McLeod *et al*., (2006), RHA1 also has a surprising abundance of oxidoreductases, which includes many oxygenases. One of them has been identified as *dypB* gene which codes for a type of dye-decolourising peroxidase, the first bacterial lignin peroxidase. DypB is capable of chemically modifying ligninocellulose substrate while the gene's deletion mutant showed

reduced lignin degrading activity [63]. Besides that, the genome of RHA1 also contains several other hydrolases, some of which are postulated to be esterases [68].

With reports of vanillin synthesised through biotransformation by several *Rhodococcus* species and mutants from ferulic acid or eugenol published [1], [69], [70], more interest has been generated towards this versatile bacterium. Therefore, it confers an advantage for further research in lignocellulose valorisation, as well as for bioremediation.

1.1.4 Ferulic acid

Among the products of lignocellulose breakdown are the phenolic acids, which are phenol carboxylic acids found abundantly in plant kingdom. The phenolic acids, such as ferulic, sinapic, caffeic, and *p*-coumaric acids are found both covalently attached to the plant cell wall and as soluble forms in the cytoplasm [71]. Ferulic acid has been extracted from various parts of plants such as fruits, vegetables, cereals, and even the structural material of plant itself (woody or non-woody tissues). In monocotyledons, ferulic acid is neatly polymerised in the form of lignocellulose [72]–[74].

It has many reported uses in pharmaceutical, food and cosmetic industries. In the pharmaceutical industry, ferulic acid or its derivatives were found to have antioxidant property, lower cholesterol level (thus, preventing thrombosis and atherosclerosis), as well as possessing anti-microbial, anti-inflammatory and anti-cancer effect [75]–[77]. In healthcare and therapeutics, antioxidants play a major role for preventive medicine, when taken as supplements. Phenolics have antioxidant properties, due to the reactivity of the hydroxyl substituent on the aromatic ring,

which is able to form a stable phenoxy radical. Although there are several mechanisms, radical scavenging via hydrogen atom donation is believed to be the predominant mode of antioxidant activity [78]. In the food and cosmetic industries, ferulic acid is used as an antioxidant and as a precursor to produce vanillin through microbial biotransformation [77], [79].

The lignocellulose complex from grass and herbaceous crops is structurally different from those in woods (soft and hard woods) and contains ferulic acid bridges between lignin and carbohydrates (arabinoxylans) (see Figure 6a). Ferulic acid (4-hydroxy-3-methoxycinnamic acid), makes up approximately 5% of straw lignin's content. A large proportion of this residue is ester-linked to polysaccharides or hemicellulose chains, mainly with arabinose residues. Ferulic acid also forms an ether bond with phenylpropane units creating a bridge between cell wall polysaccharides and lignin as shown in Figure 6b.

In general, many alkali pre-treatments would cleave off the ester component, thus, liberating the ferulic acid residue (1–4.3%) and lignin from carbohydrates [80]. Among the alkalis that were used are sodium hydroxide, ammonia, urea or lime, either on their own or in combination with a thermal process. Concurrently, there are also other types of alkali-stable bonds to carbohydrates such as glycosidic and ether linkages, since a portion of residual lignin remains firmly attached with the alkali-treated residues [9].

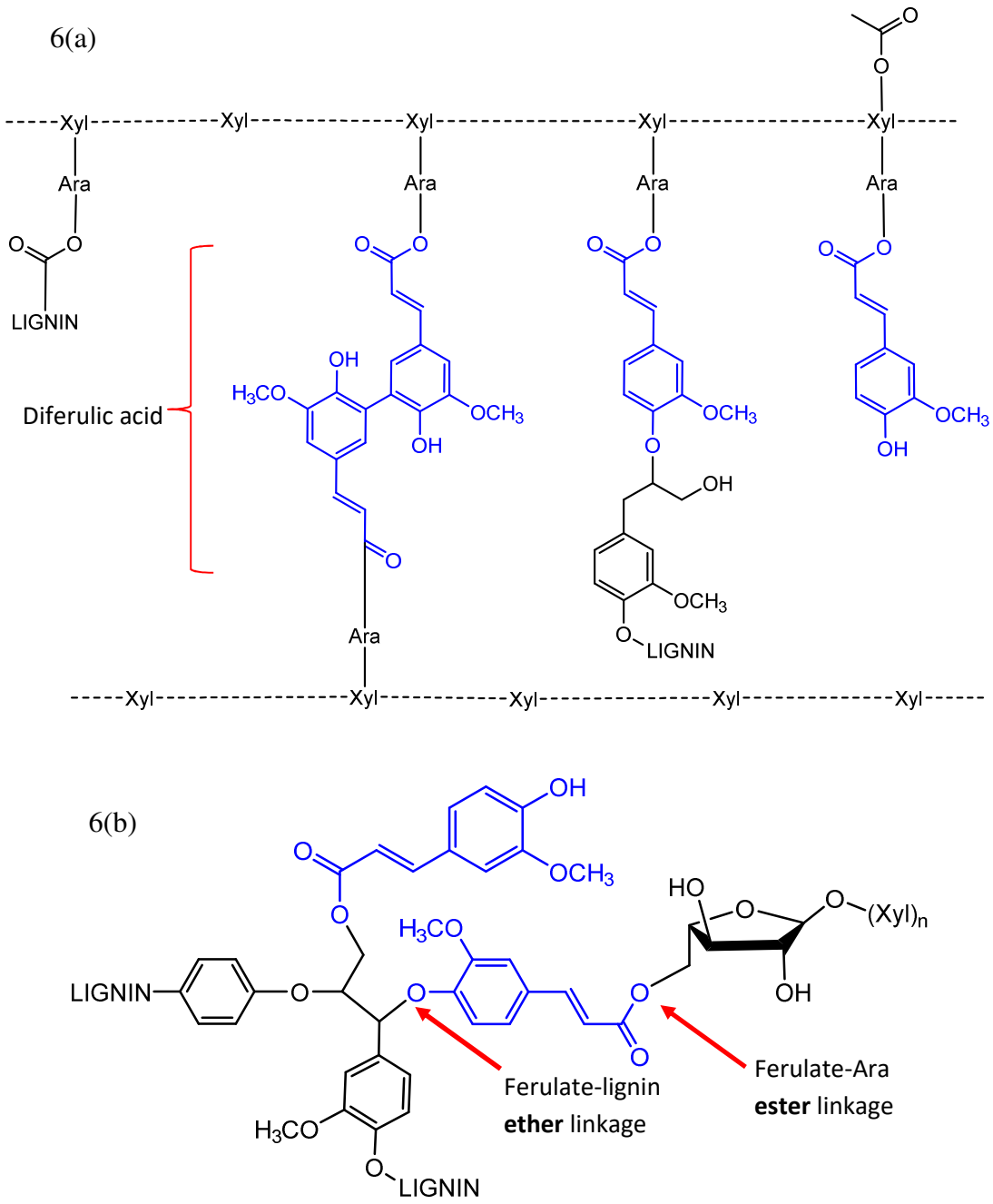

Figure 6: (a) Simplified structure of cross-linking between ferulic acid, lignin and hemicellulose in grass cell walls (b) Bonds between lignin, hemicellulose and ferulic acid.
Ferulic acids are highlighted in blue. Adapted from ref [1], [74]

According to Hatfield *et al*., (1999), dimerisation of ferulate–polysaccharide esters results in whole range of diferulates which acted like monolignols that assimilate into lignins of herbaceous plants by radical cross-coupling. Its extensive

copolymerisation with monolignols helps to anchor lignins into cell walls during the early stages of lignification. In the end, their simple dimerisation decreases the biodegradability of digestible cell walls and any further association with lignin polymer would cause severe reduction in carbohydrate availability [9], [81].

Sainsbury *et al*., (2013) for example has reported that ferulic acid was accumulated twice throughout a 7 days incubation of *Rhodococcus jostii* RHA045 (*Δvdh* mutant of RHA1) in wheat straw lignocellulose minimal media (Figure 7).

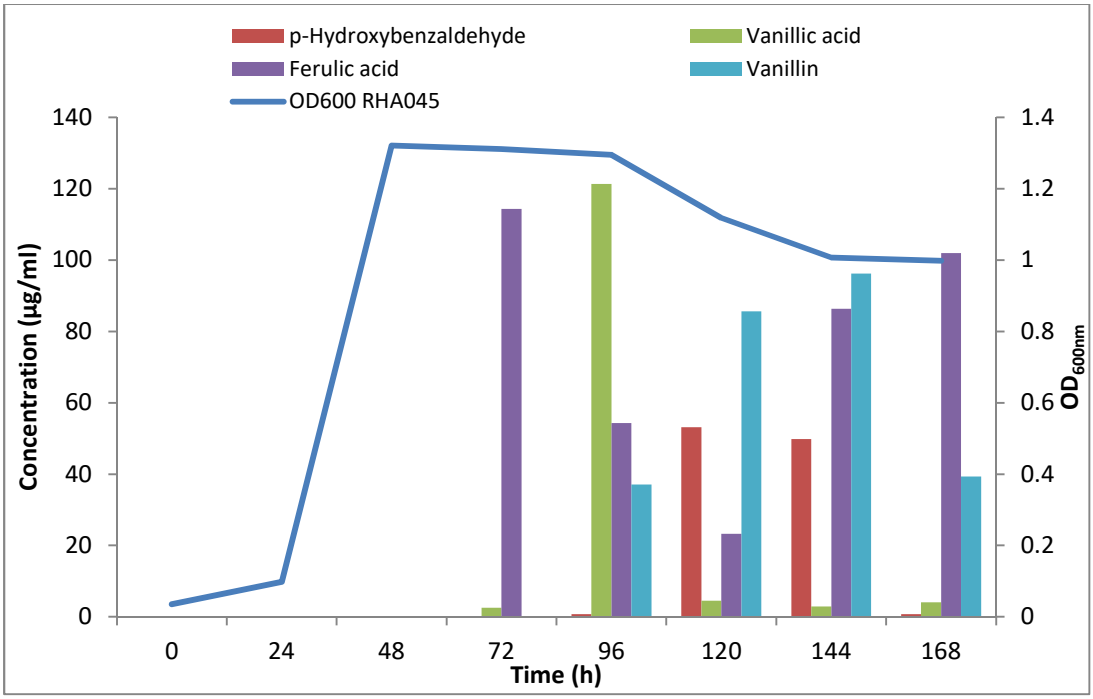

Figure 7: Time-course metabolite production from *R.jostii* RHA045 culture in lignocellulose minimal media.
Reproduced from ref [1] with author's permission.

The first liberation of ferulic acid after 4 days was proposed to be due to hydrolysis of ferulate ester linkage between lignin and hemicellulose, while the second release,

after 7 days was proposed to be due to oxidative cleavage of ether linkages [1]. Hence, there is a potential to generate ferulic acid from lignin using *R. jostii* RHA1.

Besides usage in pharmaceutical, food and cosmetic industries, ferulic acid and other hydroxycinnamic acids have been studied in the conversion into other high value chemicals as well. For example, polyethylene ferulate and polyethylene coumarate (see Figure 8) have been synthesised from ferulic and *p*-coumaric acid, which are polystyrene mimics. This has opened more opportunity to synthesise new green polymer [82]–[84].

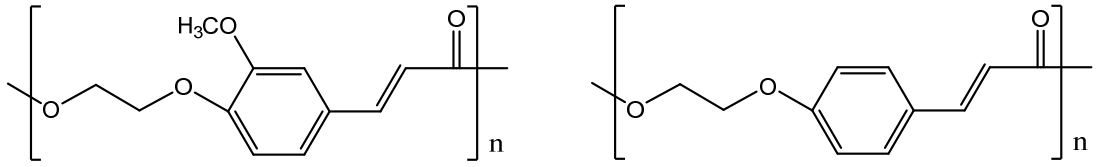

Polyethylene ferulate Polyethylene coumarate

Figure 8: Polystyrene mimics polyethylene ferulate and polyethylene coumarate synthesised from ferulic and *p*-coumaric acids.
Source: Ref [82]

Besides these, ferulic acid can also be a precursor to synthesise other polymers as well using biocatalysis. To simplify, using lignocellulose as a resource for polymers in this age is actually a proactive step towards a more sustainable future.

1.2 Phenolic acid decarboxylase (PAD)

One of the most common and important enzyme-catalysed processes are decarboxylation. For example, the most essential reaction in life involves emission of carbon dioxide in cellular respiration through the action of decarboxylase enzymes. Many of them require cofactor such as thiamine diphosphate or pyridoxal phosphate, while some do not require any [85], [86].

Phenolic acid decarboxylase, PAD (EC 4.1.1.-) is a cofactor-independent enzyme that catalyses the non-oxidative decarboxylation of phenolic acids to their corresponding *p*-vinyl derivatives. Initially, some organisms cannot tolerate the toxic effect of phenolic acids, and therefore, a number of them develop the capability to catabolise it into the less toxic vinyl phenol compounds [87].

PAD can be found across a variety of species within the class Bacilli such as *Bacillus subtillis* [88], [89], *Bacillus pumilus* [90], [91], *Lactobacillus plantarum* [79], [92], [93] and *Pediococcus pentosaceus* [94]. There have also been reports of PAD found in the yeasts *Dekkera bruxellensis* [95] and *Candida guilliermondii* [96], which is the culprit of wine spoilage, and even the baker's yeast *Saccharomyces cerevisiae* [97]. Besides that, there are also ferulic acid decarboxylase (FAD) from *Enterobacter sp*. Px6-4 [98] and *p*-coumaric acid decarboxylase [90] that catalyse the same reaction. All these enzymes possess about 15% sequence identity (albeit minor changes for the yeast counterpart), and conserved amino acids in 29 positions, based on the ClustalΩ multiple sequence alignment tool [99], [100] as shown in Figure 9.

Figure 9: Comparison of the amino acid sequences of four closely related PAD. The sequences were aligned using the ClustalΩ program. Identical residues are notated with asterisk at the bottom. Red boxes indicated the conserved active site residues. Numbers on the right correspond to the amino acid position in the protein sequence.

With reference to *B.subtilis*, this Gram positive bacterium is said to be capable of becoming a powerful protein-secreting cell factory in the future [101]. It is easily isolated from the top of soil layer. With a large number of chemicals released into the environment during their production cycle such as natural or synthetic aromatic compounds like lignin or pesticides, these microbes somehow undergo a directed evolution to metabolise these chemicals within their life cycle.

Since biotransformation of renewable feedstock has gained considerable attention recently, it is of great interest to explore the potential of this enzyme. It is known that ferulic acid has been observed as one of the intermediate in bacterial lignin degradation [1]. Accordingly, there is a possibility to produce a renewable monomer of substituted styrene (4-hydroxy-3-methoxystyrene or 4-vinylguaiacol) through the decarboxylation of ferulic acid by the enzyme phenolic acid decarboxylase.

Compared to ferulic acid, vinylguaiacol is 40 times more valuable, and it can be further converted into acetovanillone, ethylguaiacol, and vanillin [71], [102]–[104], as shown in Figure 10.

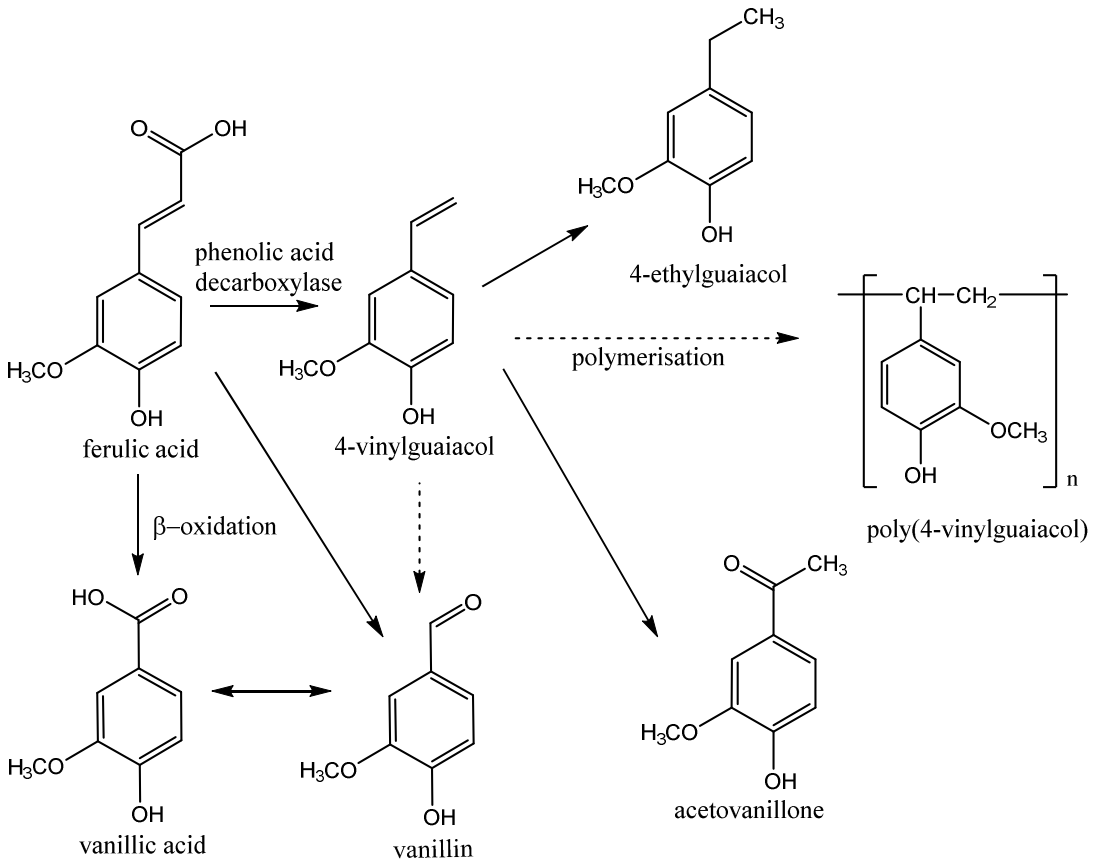

Figure 10: Chemicals derived from ferulic acid.
Adapted from ref [103], [104]

These compounds are highly prized in food, perfumery and cosmetic industries, as well as being a possible precursor for polymer synthesis. Therefore, enzymatic bioconversion of ferulic acid into 4-vinylguaiacol provides more avenue in the production of fine chemicals.

Phenolic acid decarboxylase is a homodimer, with a flattened β-barrel monomer structure that acts as the active site for the substrate (Figure 11).

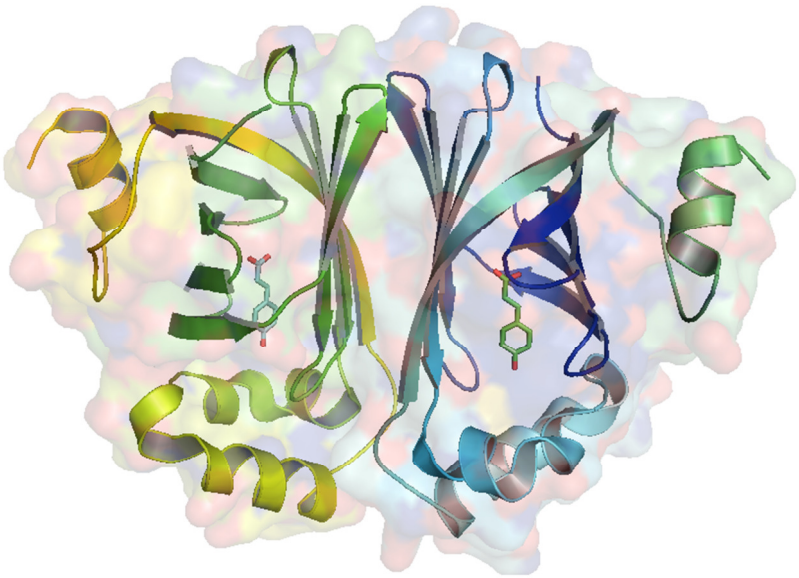

Figure 11: Crystal structure of *Bs*PAD in complex with *p*-coumaric acid (PDB:4ALB)

Several PDB entries of the PAD crystal structure from different species; *Bacillus subtilis* (*Bs*PAD, 2P8G), *Lactobacillus plantarum* (LpPAD, 2GC9) *Bacillus pumilus* UI-670 (3NAD), *Enterobacter sp*. Px6-4 (EFAD, 3NX1, 3NX2) have been deposited into the PDB database and were found to share structural homology. Based on a superimposition study, Frank and co-workers showed that Tyr11, Tyr13, Tyr31, Arg41, Glu64 are conserved in their active site region (Figure 12) and are within 3Å of the substrate cavity [87], [105]. This is also supported by the sequence alignment mentioned in Figure 9, whereby those respective amino acids are found to be aligned together.

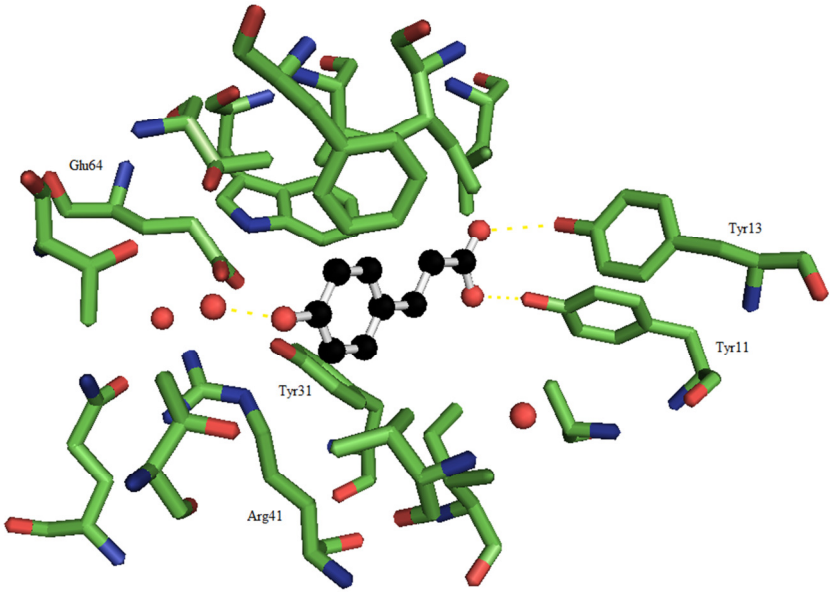

Figure 12: *Bs*PAD Tyr19Ala mutant active site's amino acid residues (PDB:4ALB)

As depicted in Figure 13, the two Tyr residues (Tyr 11 and 13) acting like a "pincer", are responsible to secure the carboxylate of the substrate in a correct orientation for the enzyme reaction. PAD performs an acid-base catalysis in which the general requirement is for the substrate to have a hydroxyl group in the *para* position [93]. As a start, the phenolic hydroxyl undergoes deprotonation by Glu64 serving as the catalytic acid-base of the active site. This promotes electron flow along the cinnamate molecule and gives rise to a quinone methide intermediate. Consequently, this intermediate allows an electron relay from the carboxylate anion which cleaves off the CO_2 and generates the *p*-vinyl phenol product [87], [93], [105], [106].

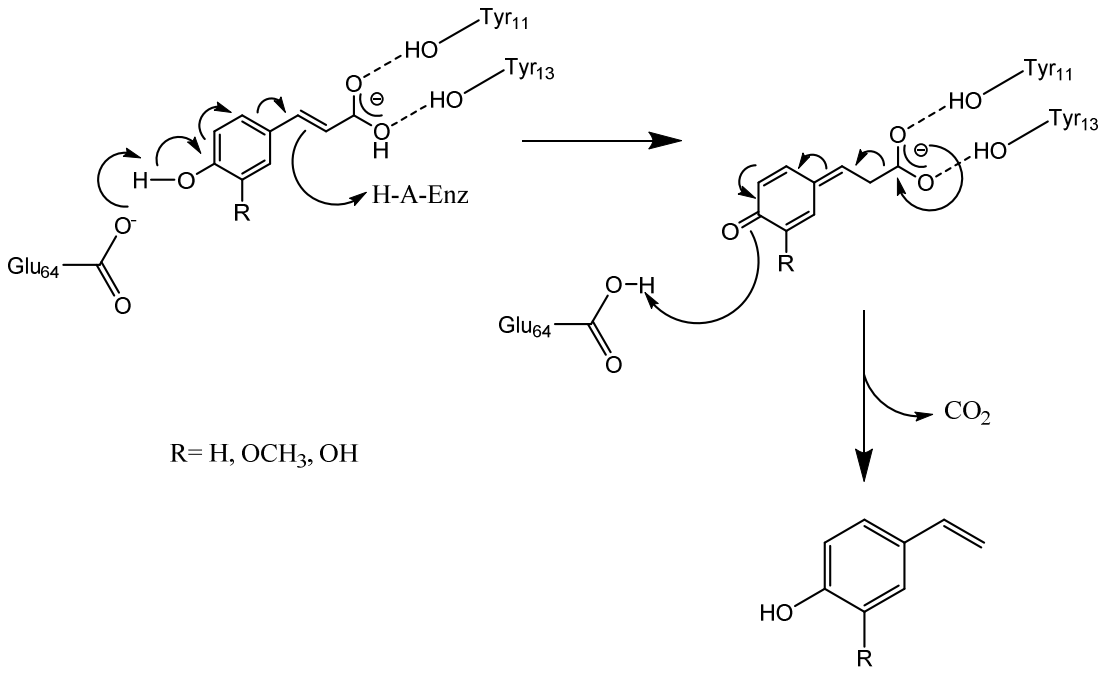

Figure 13: Reaction mechanism of phenolic acid decarboxylase
Source: Ref [105]

Both structural studies by Frank *et al.* and theoretical studies by Sheng *et al.* showed an open-close gate mechanism involving binding of the substrate into the active site, and shielding it from the reaction solvent [87], [105]. This is understandable as both the substrate and products are quite hydrophobic in nature.

The enzyme catalysed decarboxylation of ferulic acid is the most viable option for synthesis of a very useful aromatic monomer. Biocatalysis is a sustainable alternative to solve numerous setbacks resulting from chemical synthesis and plant cell culture methods. The most significant advantages of this enzyme catalysed preparation of aromatic compounds are mild reaction conditions, limited byproducts, and high substrate selectivity. High product purity is also attainable in a single step reaction [107].

1.3 Bio-based plastics

Plastics are one of the most important commodities worldwide, ranging from industrial to domestic use. International demand for polyethylene, for example, is projected to reach almost 100 million tonnes in 2018 [108]. At the same time, renewable and sustainable materials have been researched intensively throughout the world in these past two decades. Several factors are influencing this widespread cause, in which the primary aim is to decrease dependency on petroleum as raw material. Since the fossil fuel is depleting, its price fluctuates and thus, affecting the price of petrochemical-based plastics. Therefore, agriculture byproducts used as renewable material provides relative price stability.

Besides that, concern for the environment has promoted the switch towards green polymers which emphasize sustainability and biodegradability of bio-based materials. It provides many benefits for the environment, among which are the productive conversion of crop waste into value added products. At the same time, it helps to increase economic opportunities for farmers and rural communities [109], [110].

According to the UK based National Non-Food Crops Centre (NNFCC), bioplastics do not necessarily have to be biodegradable. Current plastics in use are referred to as as either ‘oxy-‘ or ‘UV-degradable’ meaning they decompose by exposure to light or air and are not yet certified as 'biodegradable'. Bioplastic is a desirable alternative polymer since they instil a positive outcome for the environment due to the renewable carbon source used to produce them. Biopolymers will break down, and some are suitable for domestic composting [111].

According to a recent Nature review article by Zhu *et al*., there are two ways to generate sustainable polymers; (1) decrease the impact of conventional production to the environment by utilising biomass to produce the existing monomers or polymers, and (2) innovate new and sustainable material or structures from renewable material [110]. Henceforth, the next subsections are the highlights of some plastic materials developed from renewable feedstock that either has been successfully commercialised or are still actively researched.

1.3.1 Poly(lactic acid) (PLA)

Poly(lactic) acid or poly-lactide (PLA) was discovered by Wallace Carothers in 1930s as polyesters while working at DuPont, USA. At that time, he could only make short chain PLA by heating lactic acid under vacuum while removing the condensed water. It was difficult to increase the molecular weight of the products using this method [112]. Later, higher molecular weight PLA was synthesised through the discovery of ring-opening polymerisation of the lactide. It was first used as co-polymer with polyglycolic acid (PGA) as a suture material and sold under the name Vicryl in the USA in 1974 [113].

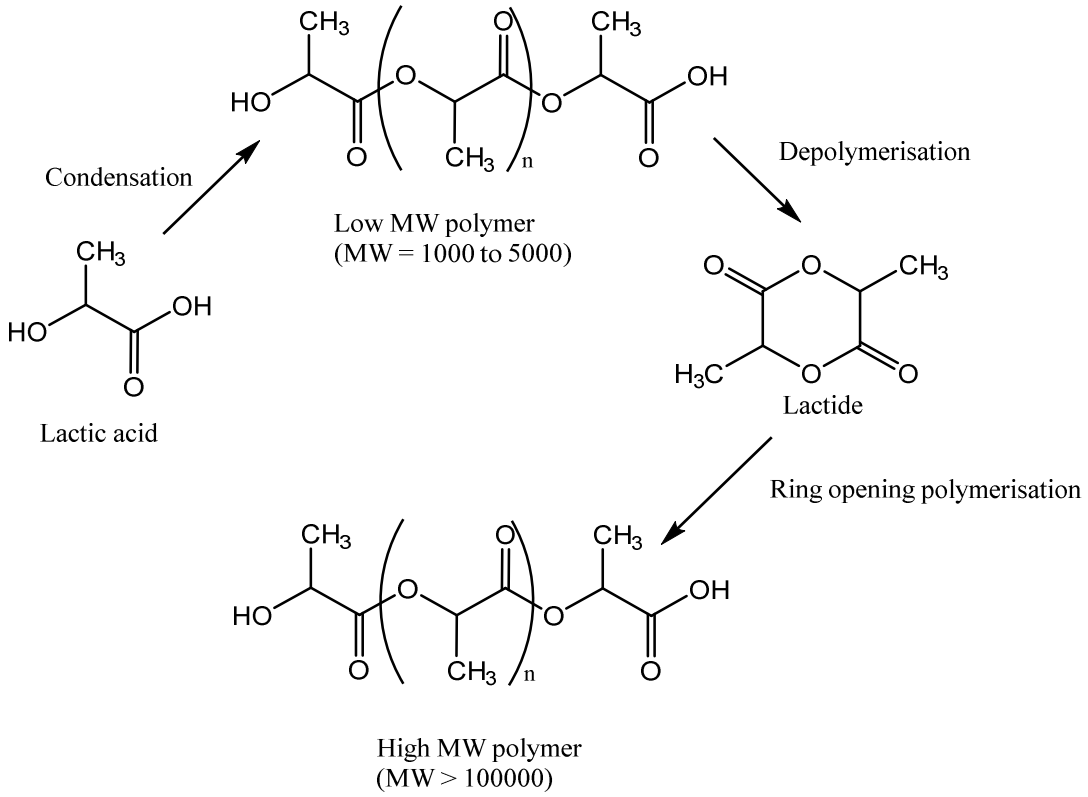

Figure 14: Synthesis of poly(lactic acid)
Source: Ref [114]

PLA is deemed to be a promising alternative to petroleum-based polymers due to its renewability, biodegradability, biocompatibility, and good mechanical properties. However, the applications of PLA were limited mostly to the medical field owing to its high production cost. It has been a widely used material in surgical procedures such as making sutures, orthopaedic implants, scaffolds, aortic stent, and as a drug carrier [115], [116].

A special attribute of PLA is its antibacterial property, thanks to lactic acid being a bacteriostatic agent. This is one of the main reasons why it has been so successful in medical field, and now, has also been introduced into food packaging and later, textiles. An antibacterial material for fresh food or ready-to-eat containers is highly sought after, especially in retail and fast food services.

For the past twenty years, synthetic textiles have been dominated by nylon, PET and polypropylene. PLA has gained some attention due to its unique properties such as hydrophilicity, good dyeability, fire resistance, antibacterial and good weather resistance. Therefore, improvements in polymerisation have allowed more economical industrial production of high molecular weight PLA for household use, commercial packaging and textile applications. Examples of more recent applications are 3D printing filament, food packaging (and cutleries), and disposable garments [115], [116].

PLA belongs to the aliphatic polyesters family. Lactic acid can be produced from the fermentation of carbohydrates, such as corn, tapioca, sugarcane or rice by *Lactobacilli*. PLA easily decomposes through simple hydrolysis, which is an advantage of PLA in promoting its speedy biodegradability, spanning between six months to two years [114]. Nonetheless, since the starchy feedstocks are bound for human (and/or animal) consumption, it is highly undesirable to be used for other non-food materials.

1.3.2 Polyhydroxyalkanoate (PHA)

Polyhydroxyalkanoate (PHA) is a type of polyester bioplastic synthesised intracellularly by a wide array of microorganisms under limiting nutrient growth condition or after pH shifts. By providing excess carbon and starving them of sulphur, nitrogen, phosphorus or oxygen, these bacteria produce PHA as an inclusion body storage compound [117]–[120]. However, these only applies to the first group or bacteria; *Ralstonia eutropha*, *Protomonas extorquens* and *Protomonas oleovorans*. The next generation, which include *Alcaligenes latus* and the genetically modified *Azotobacter vinelandii* and *E. coli,* do not require such starvation for PHA

synthesis. Until recently, more than 300 species of bacteria have been able to produce this polymer [117], [120].

A large variety of carbon source has been explored for the production of PHAs and its copolymers. Among them are fats and oils, glycerol, sugars, industrial byproducts, lignocellulose, agricultural and domestic waste materials, and yet, the list is exhaustive [117], [121]. PHAs are biologically polymerised within the bacteria by the enzyme PHA synthase and are water insoluble. Based on Table 2, they are classified based on their chain length; the short (SCL) with 3 – 5 carbons and medium chain length (MCL) which are made up by 6 – 14 carbons [118]–[120]. PHAs can form a homopolymer, such as poly(hydroxybutyrate) (PHB), poly(hydroxyvalerate) and some form copolymers. Their physical properties and rate of degradation can be controlled to some extent by manipulating the composition of the PHA monomer.

Table 2: General molecular formula of PHAs

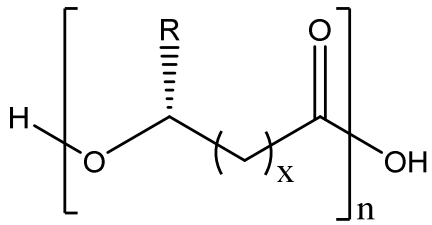

R substituent	Monomer name	Category
—H	3-hydroxypropionate (3HP)	SCL
$—CH_3$	3-hydroxybutyrate (3HB)	SCL
$—CH_2CH_3$	3-hydroxyvalerate (3HV)	SCL

——$(CH_2)_2CH_3$	3-hydroxyhexanoate (3HHx)	SCL
——$(CH_2)_3CH_3$	3-hydroxyheptanoate (3HHp)	SCL
——$(CH_2)_4CH_3$	3-hydroxyoctanoate (3HO)	SCL
——$(CH_2)_5CH_3$	3-hydroxynonaoate (3HN)	MCL
——$(CH_2)_6CH_3$	3-hydroxydecanoate (3HD)	MCL
——$(CH_2)_7CH_3$	3-hydroxyundecanoate (3HUD)	MCL
——$(CH_2)_8CH_3$	3-hydroxydodecanoate (3HDD)	MCL
x = 3	4-hydroxybutyrate (4HB)	SCL
x = 4	5-hydroxyvalerate (5HV)	SCL

Typically, x ranges from 1 – 8 and n is between 100 – 1000 depending on the degree of polymerisation. SCL- short chain length, MCL- medium chain length.
Source: Ref [118]–[120]

Since the initial discovery in the early 1900s, they have been properly characterised and successfully commercialised in several countries and are completely biodegradable. Generally, PHAs have been studied for use as nanocomposites, packaging material and thin films. For example, thermoplastic resins of P(3HB) with various copolymers for use as packaging material has been commercially sold as Biopol™ since the 1980s by Imperial Chemical Industries (ICI, now Zeneca). However, application of PHAs as commodity plastic is hampered by the production cost and availability, making the selling price not economical compared to the petrochemical based resins. Therefore, focus has been diverted into products with plastics constituting only a minor part of the product, such as the plastic film moisture barrier in food or drink cartons and in sanitary napkins [122].

1.3.3 Furandicarboxylic acid (FDCA)

In 2010, the Coca-Cola Company launched the "plant bottle" whereby their soft drinks were bottled in bio-derived ethylene glycol (EG) in combination with terephthalic acid (TA) to make their polyethylene terephthalate (PET) packaging [123], [124]. This has revolutionised renewable resourced manufacturing on a worldwide scale. In the wake of that discovery, a much better alternative have been actively sought. Avantium Chemicals in the Netherlands has been working on producing a "new" biobased monomer, furan-2,5-dicarboxylic acid (or 2,5-FDCA) on an industrial scale. The process is speculated to replace the manufacture of the widely available PET. Currently, PET is industrially produced from the petroleum-based purified TA and EG. By substituting the TA part with FDCA building block, a new PET analog, polyethylene 2,5-furandicarboxylate (PEF) was born [124].

FDCA is produced from carbohydrates that can be sourced from a variety of lignocellulosic crops or their residues [125]. At present, hydroxymethylfurfural (HMF), a type of 2,5-disubstituted furans served as a popular starting material for FDCA monomer [126]. Nevertheless, the starting point of HMF begins with cellulose (and starch) which can be potentially edible. Hence, the more attractive route to produce FDCA is preferably from non-palatable feedstock; hemicellulose, which generates xylose and arabinose [127]. Figure 15 describes a cascade of chemical reactions to produce FDCA. Besides chemical oxidation, enzymatic oxidation of HMF have also been discovered recently by McKenna and co-workers using galactose oxidase and aldehyde oxidase, making the process more environmental-friendly [128].

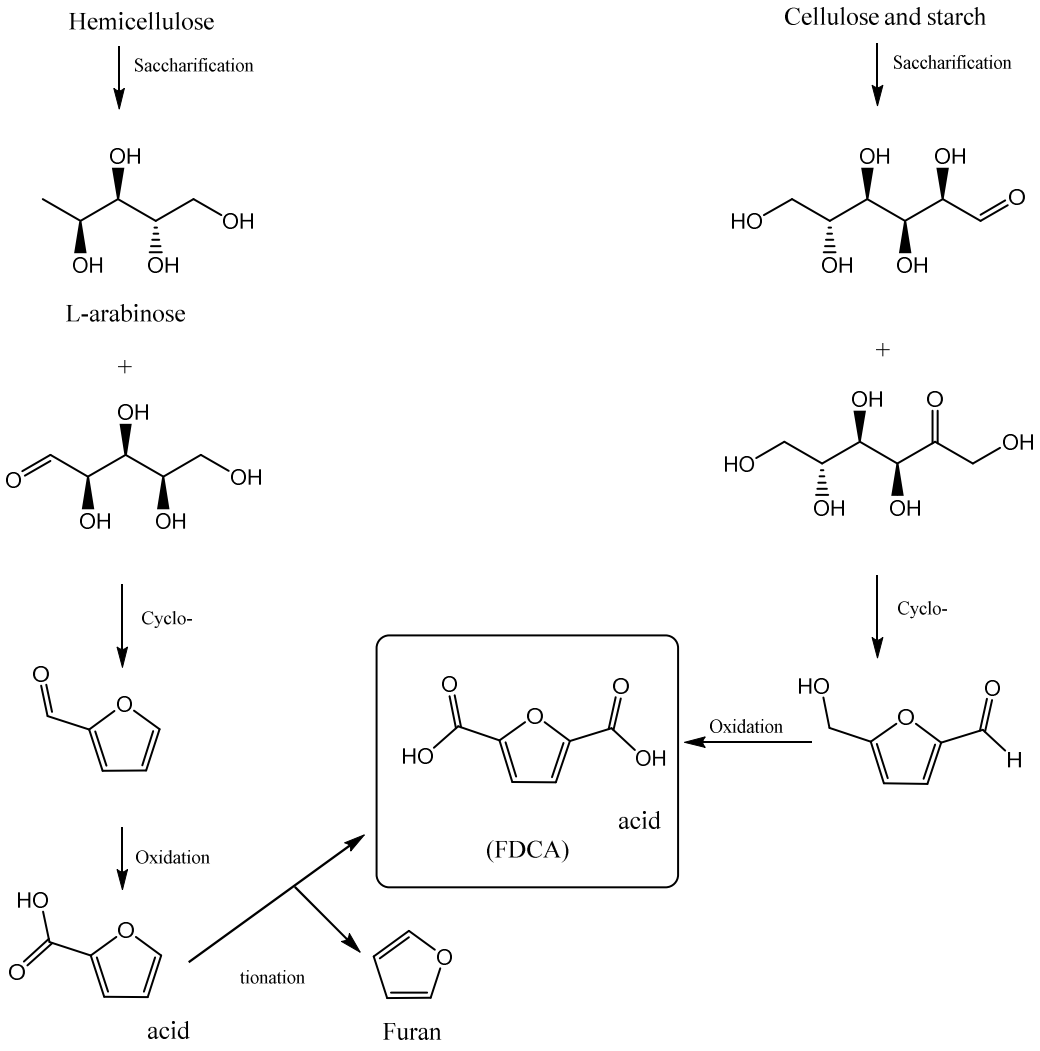

Figure 15: Synthesis of furandicarboxylic acid from lignocellulose
Source: Ref [127], [129]

Recent progress on the application of FDCA in a range of polyesters has shown that polymer properties are mostly analogous in comparison with TA [129]. Avantium themselves has been in partnership with the Coca-Cola Company and Danone working on making PEF soft drinks bottles termed as “Green bottle” which has already been in commercial circulation. Besides that, Avantium also has plans for producing fibers for textiles and carpets from FDCA [124].

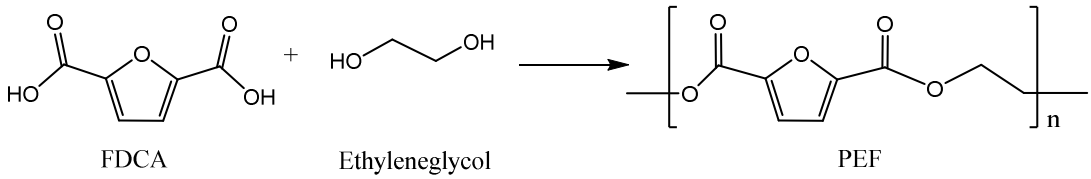

Figure 16: Polyethylene furandicarboxylate polymer from furandicarboxylic acid and ethylene glycol

To conclude, if both monomers of PEF (see Figure 16) are made from completely renewable resource, i.e. EG synthesised from bioethanol and FDCA, then, the resulting polymer can definitely replace the petrochemical based PET. This green product, if fully commercialised on a global scale for the production of bottles alone, will definitely bring a great outcome to the environment.

1.3.4 Bio-polystyrene

Styrene is a significant monomer compound and a multifaceted commodity petrochemical. The global demand for styrene is expected to reach 41 million tonnes by 2020, which is more than USD 28 billion market in the US alone [130]. It is polymerised in the manufacture of materials for transportation packaging (packaging peanuts and protective mould) and food utensils (drinking bottles, cutleries and plates).

Styrene was first discovered to self-polymerise in air since the mid nineteenth century. While in industrial scale, styrene has been made from fossil fuel as the starting material. The conventional method of styrene production (Figure 17) is to synthesise ethylbenzene first by reacting ethylene with benzene using aluminum chloride as catalyst. It is then followed by dehydrogenation of the benzene group of

ethylbenzene leading to the formation of styrene. With the addition of free-radical initiators or heat, polystyrene (PS) is produced in bulk, commercially, as early as 1931 by the BASF chemical company [131].

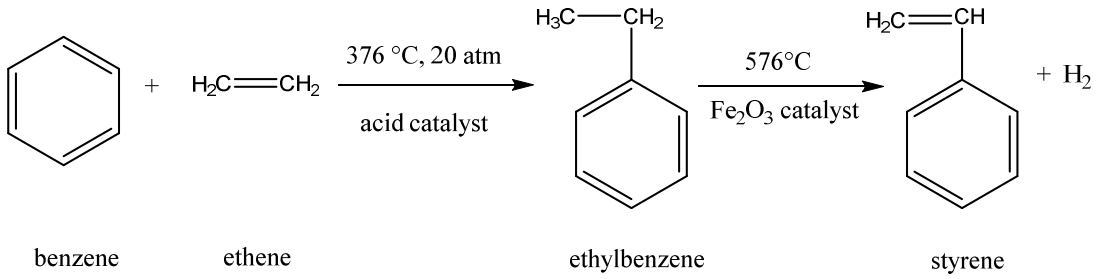

Figure 17: Conventional production of styrene in industrial scale

However, this process confers a few disadvantages such as the use of very high temperature, and concern for uncontrolled side-reactions. It was also regarded as one of the most energy intensive reactions among all commodity chemicals. Furthermore, with the impending depletion of fossil resources, there is a growing need to produce the polymer in a more sustainable way, and this can be solved using renewable alternatives.

Lignin contributes to 30% of the organic carbon on earth, and thus is the only renewable aromatic monomers that are easily accessible from agricultural waste. Since the breakdown of lignin would yield many phenolic acid derivatives, there are prospects for their valorisation into functionalised materials that are suitable as substitutes for petrochemical-derived polymers. The rich phenolic acids resource found in lignin can be converted into styrenic monomers by enzymatic

decarboxylation reaction, as illustrated in Figure 18. This green process does not require high temperature and more environmental friendly [132]–[134].

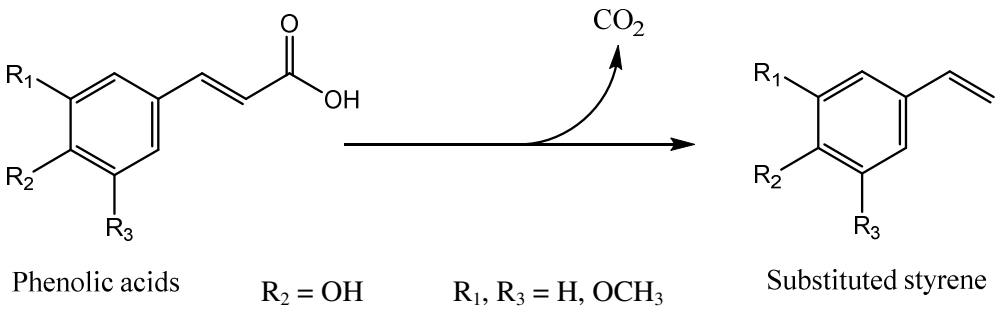

Figure 18: Conversion of phenolic acids into styrene

Another alternative method to produce styrene through biological means has also been recently explored. Taking inspiration from monolignols being synthesised via shikimate pathway, some research have been conducted to make styrene derivatives using glucose as starting point [130], [133], [135]–[138]. Using genetically modified *E.coli*, one or more genes involved in conversion of glucose into substituted styrene were co-expressed such as phenylalanine/ tyrosine ammonia lyase (P/TAL), followed by enzymatic decarboxylation as well.

In addition, polystyrene alone is merely a non-functionalised aromatic hydrocarbon polymer. To serve as attachment point of reagents and synthesis substrates, polystyrene must be derivatised [139]. This is the advantage of using naturally occurring phenolic acids since they are readily substituted without any further chemical derivatisation. By combining the biological degradation of lignin and

enzymatic cleavage of the carboxyl group in these phenolic acids, a renewable resource of substituted styrene can be made available.

1.4 Laccase

Laccases (benzenediol:oxygen oxidoreductases, EC 1.10.3.2) are blue multicopper oxidases that catalyse the oxidation of a variety of aromatic substrates alongside the reduction of molecular oxygen to water (Figure 19). They exist in a wide range of organisms, ranging from tree bark and fungi to insects and some bacteria [140], [141].

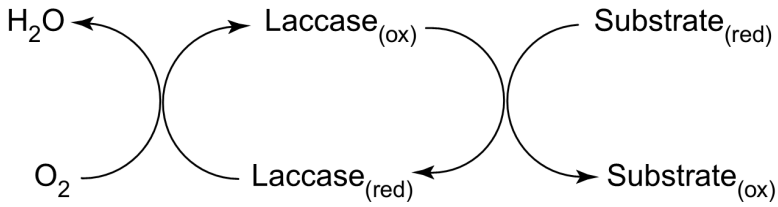

Figure 19: Schematic representation of laccase-catalysed redox cycles

Laccase has broad substrate specificity and is a versatile enzyme, with varying activities towards lignin [142]. There have been many reports suggesting it being involved in the depolymerisation [25], [143]–[145] as well as the polymerisation of lignin [146]–[159].

The majority of the fungal laccases are extracellular monomeric globular proteins with three β-barrel domains and weighing approximately 50–70 kDa or larger. The structure includes a typical metal content of one type-1 (T1) copper (Cu1), one type-2 (T2) and two type-3 (T3) copper ions (Cu2 and Cu3), with Cu2 and Cu3 arranged

in a trinuclear cluster [59], [140]. Structure-wise, the T1 site is placed in the third domain and the active site is positioned in a small cavity close to the T1 site, whereas the T2–T3 site is located between the first and the third domain (Figure 20) [59], [160].

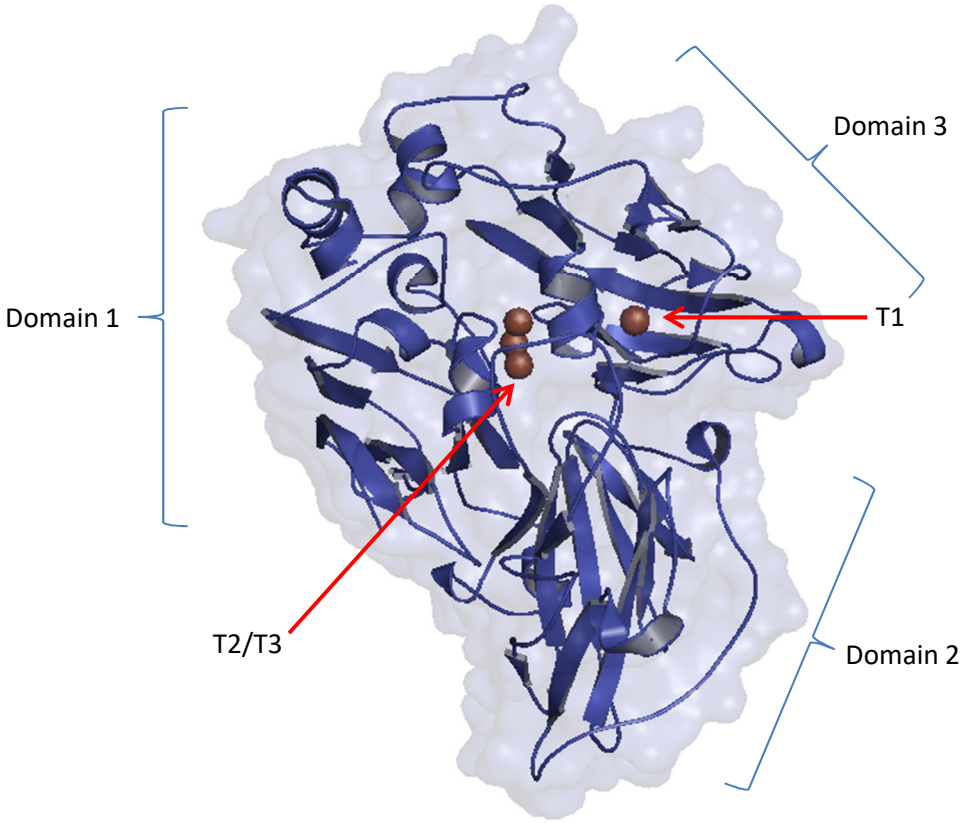

Figure 20: Crystal structure of laccase from *Trametes versicolor* (PDB:1GYC)

According to Thurston (1994), laccase is able to oxidise polyphenols, methoxy-substituted phenols, diamines and an array of other compounds [142]. Phenols are typical laccase substrates because their redox potentials are low enough to allow subtraction of one electron by the Cu1 from phenolic-OH groups. In the case of lignin model compounds, phenolic substrates are oxidised to phenoxy radicals,

which can spontaneously polymerise via radical coupling or rearrange themselves, leading to formation of quinones [59], [161].

Due to their high capacity for nonspecific oxidation and their ability to utilise molecular oxygen as an electron acceptor, laccases are useful biocatalysts for a wide range of biotechnological applications. So far, laccases have an appreciable application in bioremediation, especially in treatment of industrial plant wastewater that contains xenobiotic compounds such as a variety of textile dyes and pesticides. They are also used in pulp and paper mill effluent delignification and bio-bleaching, enzymatic modification of fibers, enzymatic removal of phenolic compounds in beverages and fruit juice processing, as well as biosensor and biofuel cell construction [140], [141], [162], [163].

In nature, laccase from white rot fungi are able to utilise the products of lignin breakdown which were initially thought to be inhibitory compounds, due to laccase being resistant to them. At the same time, laccase has already been established as one of the enzymes involved in radical coupling of monolignols during the early stage of lignification in plants [163]. This could mean that it is capable of polymerising any phenolic compounds through its oxidative radical reaction without the need of extreme conditions. Further usage of laccase in polymerisation will be discussed in the next section.

1.5 Biomimetic polymeric adhesives

Recently, there have been biomimetic inventions in organic synthesis, inspired the catechol-containing polymers for surface adhesion, adapted from polydopamine in the mussel foot protein. This bioadhesive allows strong attachment of mussels onto rock surface in watery environment, as shown in Figure 21 [164], [165].

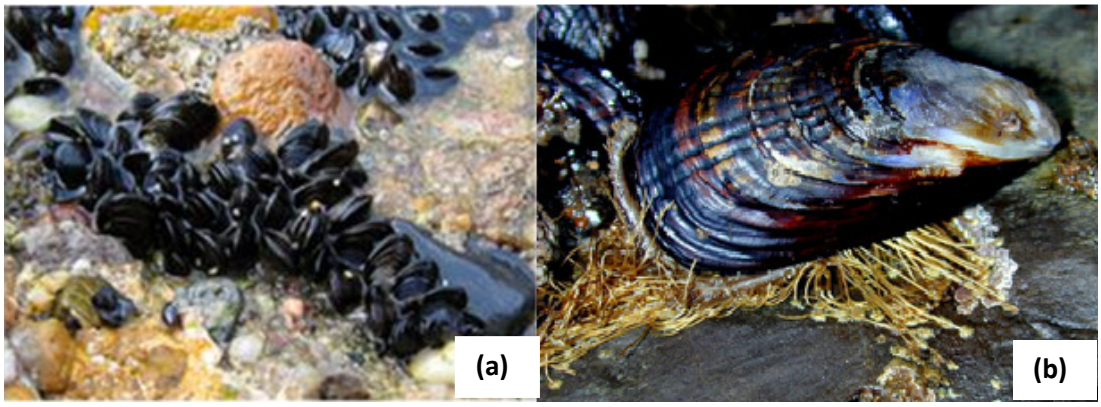

Figure 21: Mussels attachment to rocks
(a) Mussels clump together and attached to rocks in watery environment (b) Individual mussel with byssal thread protruding out and sticking onto rock surface

Mussels from the genus *Mytilus sp*. utilise a special polyphenolic compound that is protein based for their adhesive component. It provides them with a strong and lasting holdfast attachment to surface even in aquatic environment for support against the ocean's tides. This mussel foot protein, secreted through the byssal thread, contains DOPA (3,4-dihydroxy-L-phenylalanine) that forms a plaque on the substrate interface [166]–[174]. Since it is difficult to obtain the bioadhesive material in large amount from the original source, simplified polymer mimics have been chemically synthesised using a polystyrene backbone and 4-vinylcatechol (3,4-

dihydroxystyrene) to take the place of the protein polyamide chain as illustrated in Figure 22.

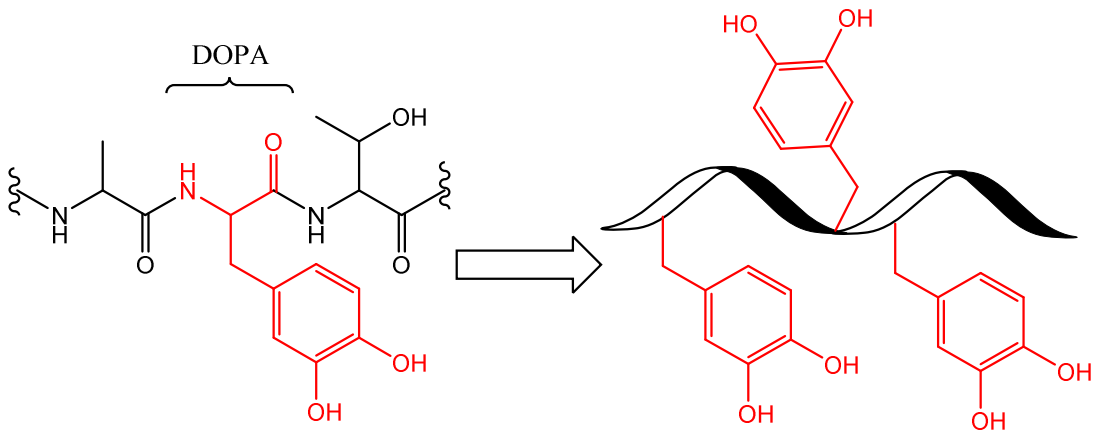

Figure 22: Catechol containing adhesive mimicking polydopamine
Source: Ref [167], [174]

It was shown that poly[(3,4-dihydroxystyrene)-co-styrene] polymers exhibit adhesive properties analogous to that of the proteins after which they were modelled. The styrene-catechol copolymers also display enhanced adhesion upon cross-linking. Adhesive performance was benchmarked against commercial glues as well as the genuine material produced by live mussels where some was found similar to cyanoacrylate "Krazy Glue" [167], [174].

This chemically synthesised biomimetic adhesive showed similar strong attachment to a large variety of surfaces, just like its biological counterpart from mussels. It was found to be an interesting polymer for surface coatings and adhesion. Development of new strategies to synthesise catechol-containing polymers are vast. The most common approach is to employ functionalisation of polymers with dopamine or other catechol-containing reagents like dihydrocaffeic acid to improve the polymer properties [175].

1.6 Aims of project

Since the degradation of lignin can provide a source of ferulic and caffeic acid, the enzymatic conversion into substituted styrene monomer 4-vinylguaiacol (3-methoxy-4-hydroxystyrene) and 4-vinylcatechol (3,4-dihydroxystyrene) respectively can potentially be converted into a sustainable form of "bio-styrene". In addition, it has been proven through chemical synthesis that 4-vinylguaiacol can be polymerised, and the resultant oligomer [poly(3-methoxy-4-hydroxystyrene)] has been found to be quite easily biodegradable [176]. Rather than doing it synthetically, this reaction can be done *in vitro* by enzymatic process with the addition of redox enzymes to create radical polymerisation, as illustrated in Figure 23 [177], [178]. The resulting polymer can be a renewable alternative for the conventional polystyrene.

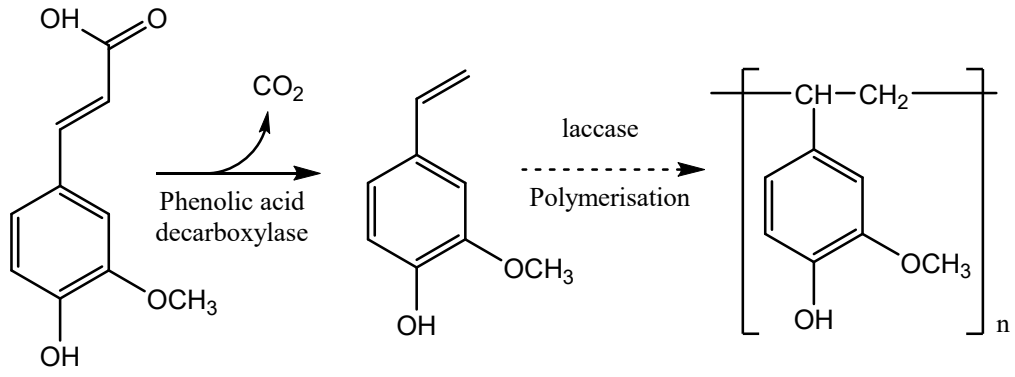

Figure 23: Proposed scheme for the production of polystyrene from ferulic acid. Adapted from ref [177], [178]

Besides being useful as packaging and building material, polystyrene also has been proven to be useful as adhesive. At the moment, the widely distributed phenolic resins are made up from phenol and formaldehyde and are usually used as adhesives [108]. According to Carraher (2012), oligomers and low molecular weight polymers cannot be used for high strength applications. However, low molecular weight amorphous polymers can be used for coating and adhesive (polymer chain length of less than 100) [179]. This material could also be very useful for medical applications such as bone cements, dental composites, and surgical glues [167].

It is hoped that the resulting biologically synthesised polymer can be used in many applications such as renewable plastic and adhesive material without depending on petrochemicals. In addition, it will also be an effective way to recycle the abundant biomass available from agriculture waste. In conclusion, a future bio-based economy should ideally be visualised as an integrated biorefineries where biofuels, platform chemicals and novel materials such as bioplastics will be manufactured alongside each other [123].

The aim of this project is to use the enzyme phenolic acid decarboxylase to convert ferulic acid and other *p*-OH cinnamates into *p*-vinyl derivatives. They can then be polymerised enzymatically using peroxidase or laccase enzymes, yielding renewable substituted polystyrene.

Specifically, this research will focus on the following:

1. Expression of *Bacillus subtilis* PadC, coding for phenolic acid decarboxylase, followed by purification and kinetic characterisation.

2. Expression of phenolic acid decarboxylase gene in a mutant of bacterial lignin degrader host. Constructs will then be grown on minimal media containing lignocellulose, with the aim of converting ferulic acid to 4-vinyl guaiacol bio-product.

3. Testing of enzymatic radical polymerisation of substituted monostyrene formed by biocatalysis with phenolic acid decarboxylase product using laccase. The resulting polymer will be characterised gel permeation chromatography to measure its molecular weight. Also, possible co-polymerisation will be explored by varying the ratio of the enzymatically generated monostyrenes.

CHAPTER 2 PURIFICATION AND CHARACTERISATION OF PHENOLIC ACID DECARBOXYLASE

Ferulic acid can be a precursor for conversion into many high value chemicals, such as the 4-vinylguaiacol (3-methoxy-4-hydroxystyrene), which is a substituted styrene. The conversion of ferulic acid to 4-vinylguaiacol is catalysed by phenolic acid decarboxylase, encoded by the gene *padC* from *Bacillus subtilis*. The first aim of the project was to express, purifiy and characterise this enzyme.

2.1 Expression in *Escherichia coli* and purification of phenolic acid decarboxylase

The gene *padC*, coding for phenolic acid decarboxylase from *Bacillus subtilis*, was inserted into a TOPO cloning vector pET200 by Dr Elizabeth Hardiman in 2012 [88]. It was transformed into *Escherichia coli* BL21 competent cells by heat shock and expressed in Luria Bertani medium (LB) containing 35 µg/mL kanamycin. After induction with 0.8 mM IPTG and an overnight incubation at 16°C, the cells were harvested and lysed by high pressure cell disruptor. The cell lysate was then purified by immobilised metal affinity chromatography (IMAC) resin as an N-terminal His_6 fusion protein.

Figure 24 shows the SDS-PAGE of the expressed protein as a major band with an apparent molecular weight of 23 kDa.

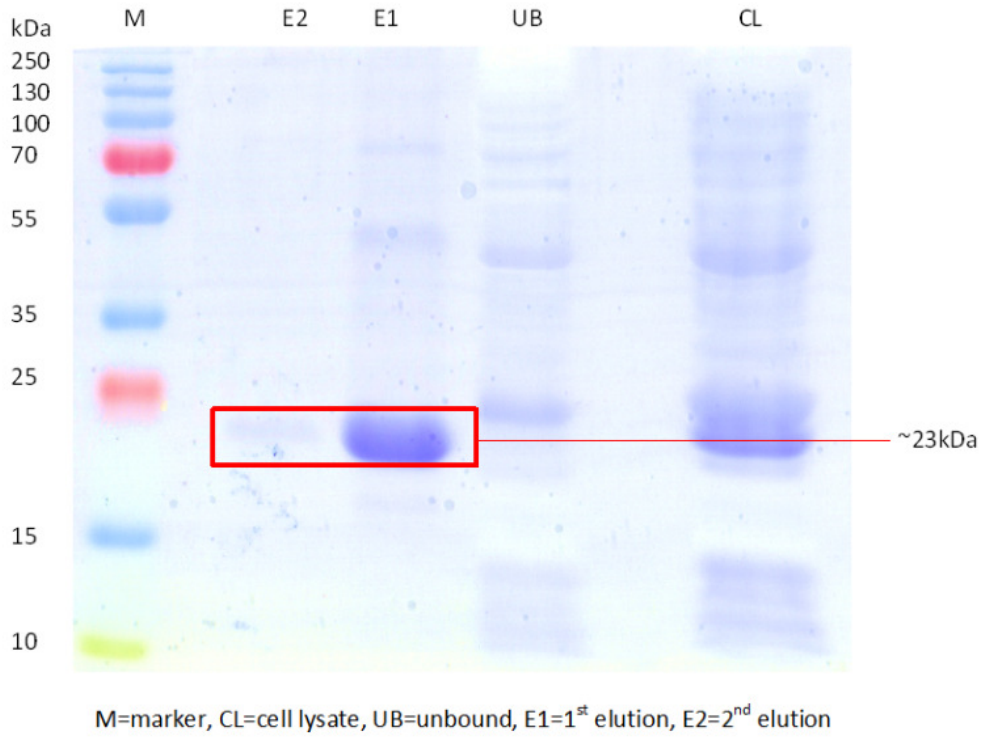

Figure 24: SDS-PAGE of purified phenolic acid decarboxylase from the transformed *E.coli*

Approximately 170 mg of protein was obtained from a total of 1 L *E.coli* culture harbouring the *padC* construct. The protein was dialysed against 50 mM sodium phosphate buffer pH 7.4 as preparation for enzyme assays.

2.2 Assay of phenolic acid decarboxylase

A series of UV-Visible spectra ranging from 200 – 400 nm were used to study the time-course of the enzyme reaction, initially with ferulic acid as substrate. Depletion of peaks due to ferulic acid at 280 nm and 310 nm and appearance of peak due to 4-

vinylguaiacol product at 260 nm were observed for 5 min at room temperature. The total 1 mL reaction mixture contained 0.98 mL 50 mM sodium acetate buffer pH 5.0 and 0.1 mM ferulic acid (Sigma) that were mixed by inversion in a quartz cuvette. The reaction was initiated by the addition of 10 µL phenolic acid decarboxylase (from 0.8 mg/mL aliquot). Buffer solutions containing ferulic acid but without enzyme were used as a negative control, while ferulic acid with a series of different concentrations was used to prepare of a calibration curve at 315 nm.

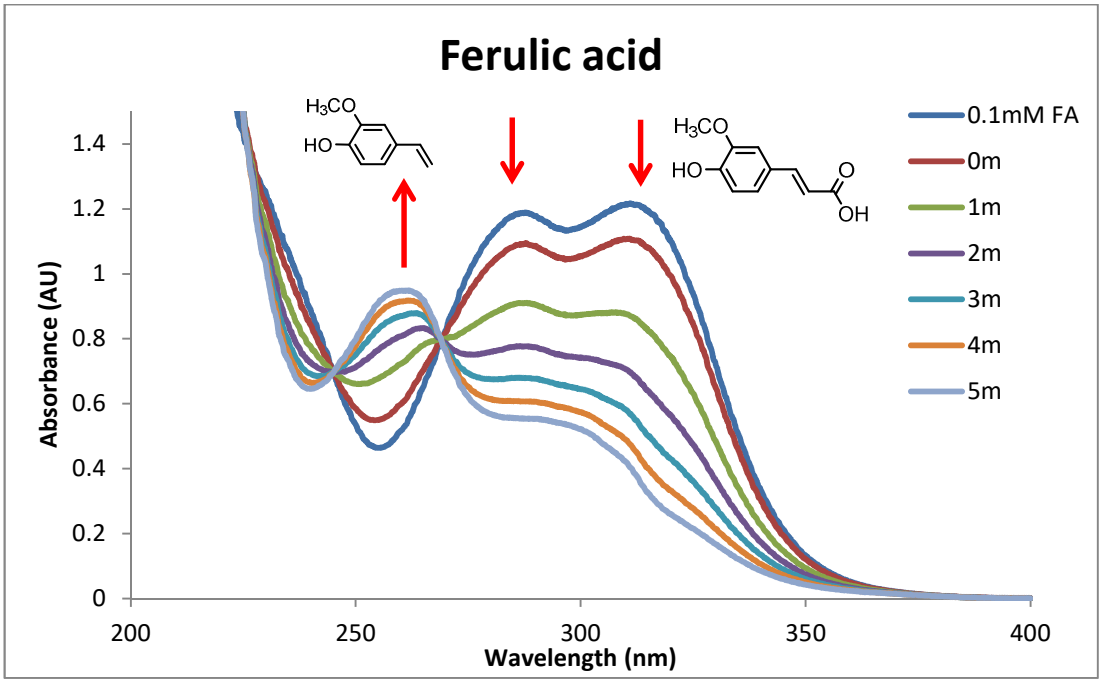

Figure 25: UV-Vis spectrum of the phenolic acid decarboxylase assay with 100µM ferulic acid as substrate taken at 1 min interval

From Figure 25 above, it is seen that ferulic acid has two maximum absorption peaks, both are within UV range at 280 nm and 310 nm. These peaks gradually decrease over time (indicated by arrows) while a new peak at 260 nm appeared for the enzymatic conversion product as soon as the reaction was initiated by the

addition of PAD. To confirm the compound produced, several of the completed assay reaction mixtures were pooled into a vial and subjected to solvent extraction with three times equal volume of ethyl acetate. The organic layer was collected and evaporated, followed by resuspension in 0.5 mL methanol. Reversed phase high performance liquid chromatography (HPLC) with variable wavelength ultraviolet (UV) detection on Agilent Series 1200 system was carried out using Agilent reversed-phase Zorbax Eclipse XDB-C18 column (130 Å, 250 mm x 4.6 mm) at a flow rate of 0.8 mL/min, with monitoring at 260 nm. The HPLC solvents were water/0.1% trifluoroacetic acid (solvent A) and methanol/0.1% trifluoroacetic acid (solvent B). The applied gradient was 10% B for 5 min; 10–15% B over 10 min; 15–25% B for 8 min; and 25–100% B for 19 min, at a flow rate of 0.8 mL/min.

This enzymatically generated 4-vinylguaiacol was analysed alongside the commercially available standard from Sigma, which was also dissolved in methanol for comparison. Figure 26 shows the resulting HPLC chromatogram, displayed as the retention time versus intensity of absorbance at 260 nm. It indicates the similar retention time (RT) at 37 minutes for both enzymatically generated and authentic 4-vinylguaiacol.

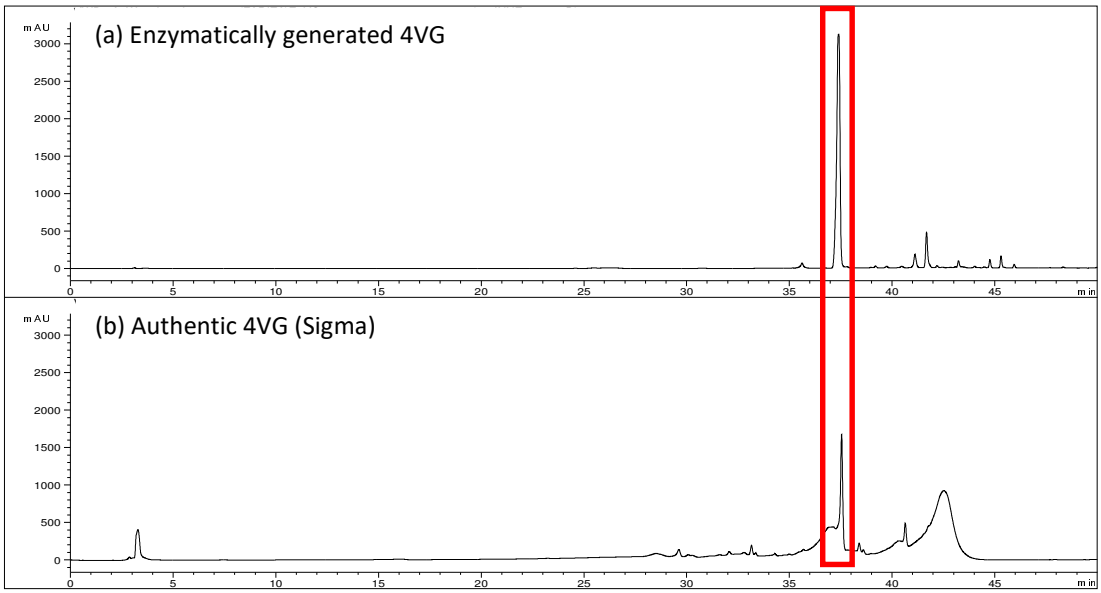

Figure 26: HPLC trace for (a) Enzymatically generated 4-vinylguaiacol (b) Sigma authentic 4-vinylguaiacol

This experiment is followed on using other cinnamic acids tested in a similar UV-Vis enzyme assay to test the substrate specificity of the enzyme.

2.3 Substrate specificity of phenolic acid decarboxylase

A UV-Vis scan for a wavelength between 200-400 nm was carried out to monitor the activity of phenolic acid decarboxylase against different substrate analogs varying from 2-, 3- and 4- methoxycinnamic acids, 3- and 4-hydroxycinnamic acids, 3,4-dihydroxycinnamic acids, as well as 4-hydroxy-3,5-dimethoxycinnamic acid. Based on the scans, only two other compounds showed a positive reaction towards the enzyme; 4-hydroxycinnamic acids (*p*-coumaric acid) and 3,4-dihydroxycinnamic acids (caffeic acids), as illustrated in Figure 27.

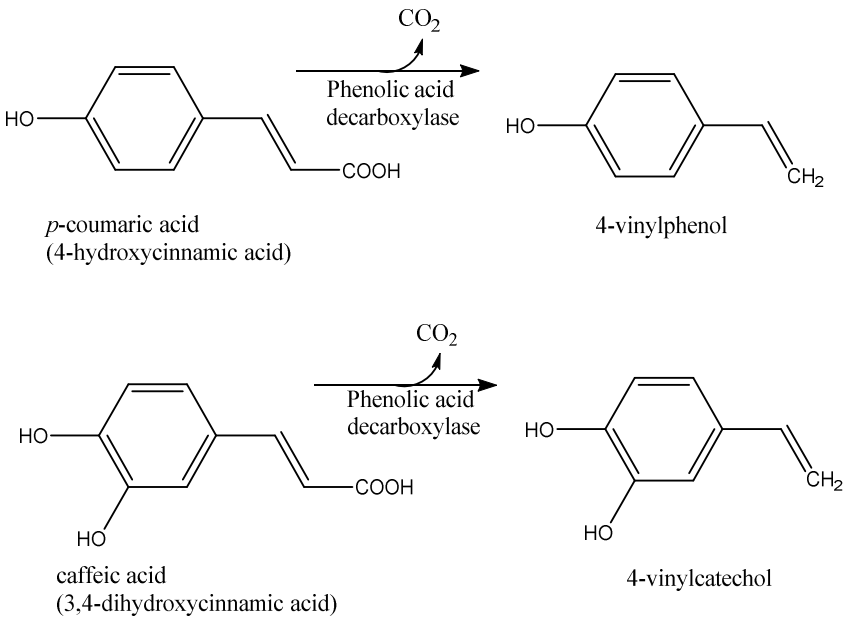

Figure 27: Reaction of phenolic acid decarboxylase with different substrates

These compounds also showed disappearance of substrate peaks together with the formation of new product peaks. For the assay with *p*-coumaric acid, it can be seen from Figure 28a the substrate peak (λ_{max}=286 nm) was depleted after the enzyme addition and shifted into a new peak at 256 nm signifying the product. However, for caffeic acid (Figure 28b), no distinct new peak appeared, but the reaction could be monitored by the lowering of substrate peaks over time.

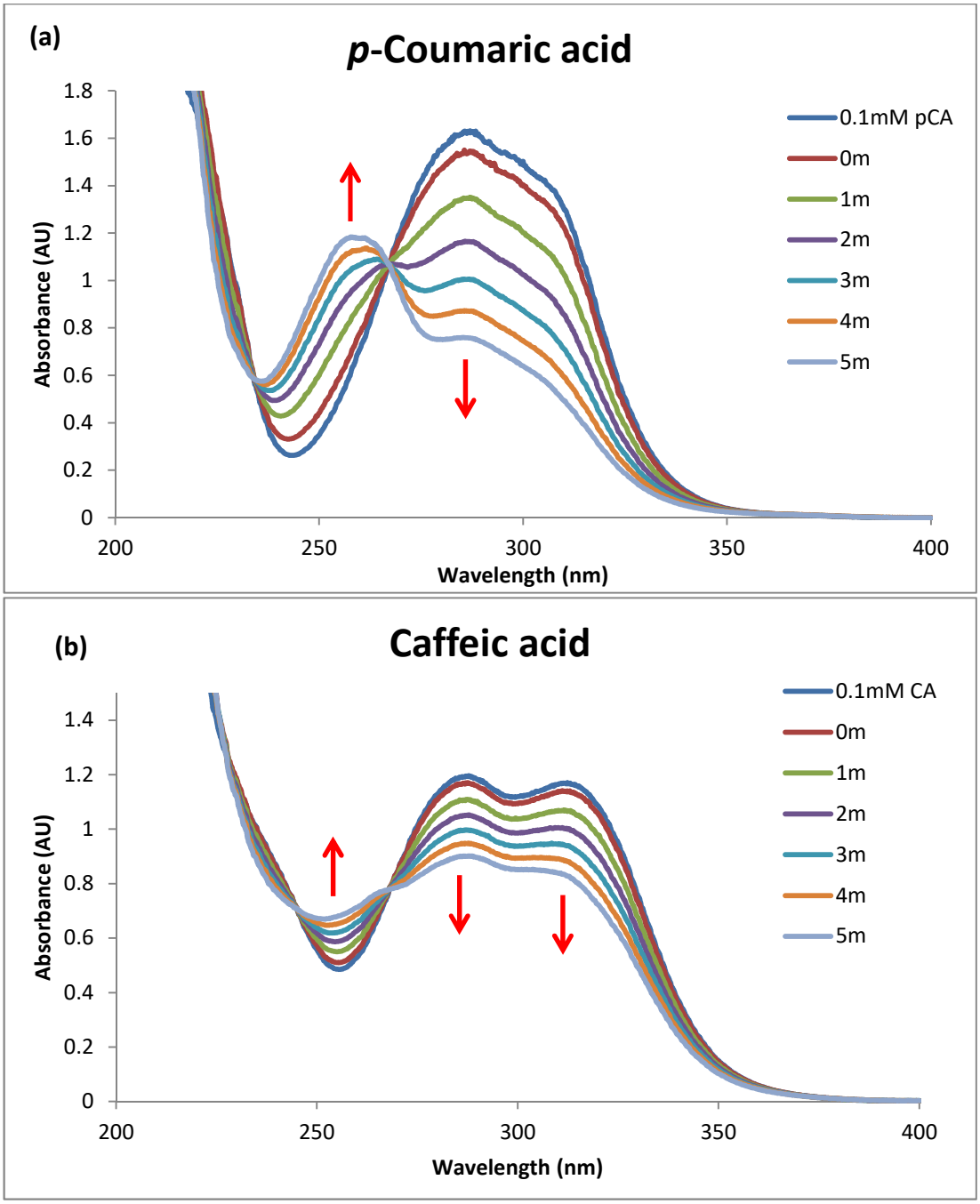

Figure 28: UV-Vis spectra for the assay of phenolic acid decarboxylase with (a) *p*-coumaric acid and (b) caffeic acid taken at 1 min interval

For 4-hydroxy-3,5-dimethoxycinnamic acid (sinapic acid) and 4-methoxycinnamic acid however (see Figure 29a and b), no reaction were observed, where the substrates' maximum absorption remained unchanged for the whole assay duration even after the addition of enzyme.

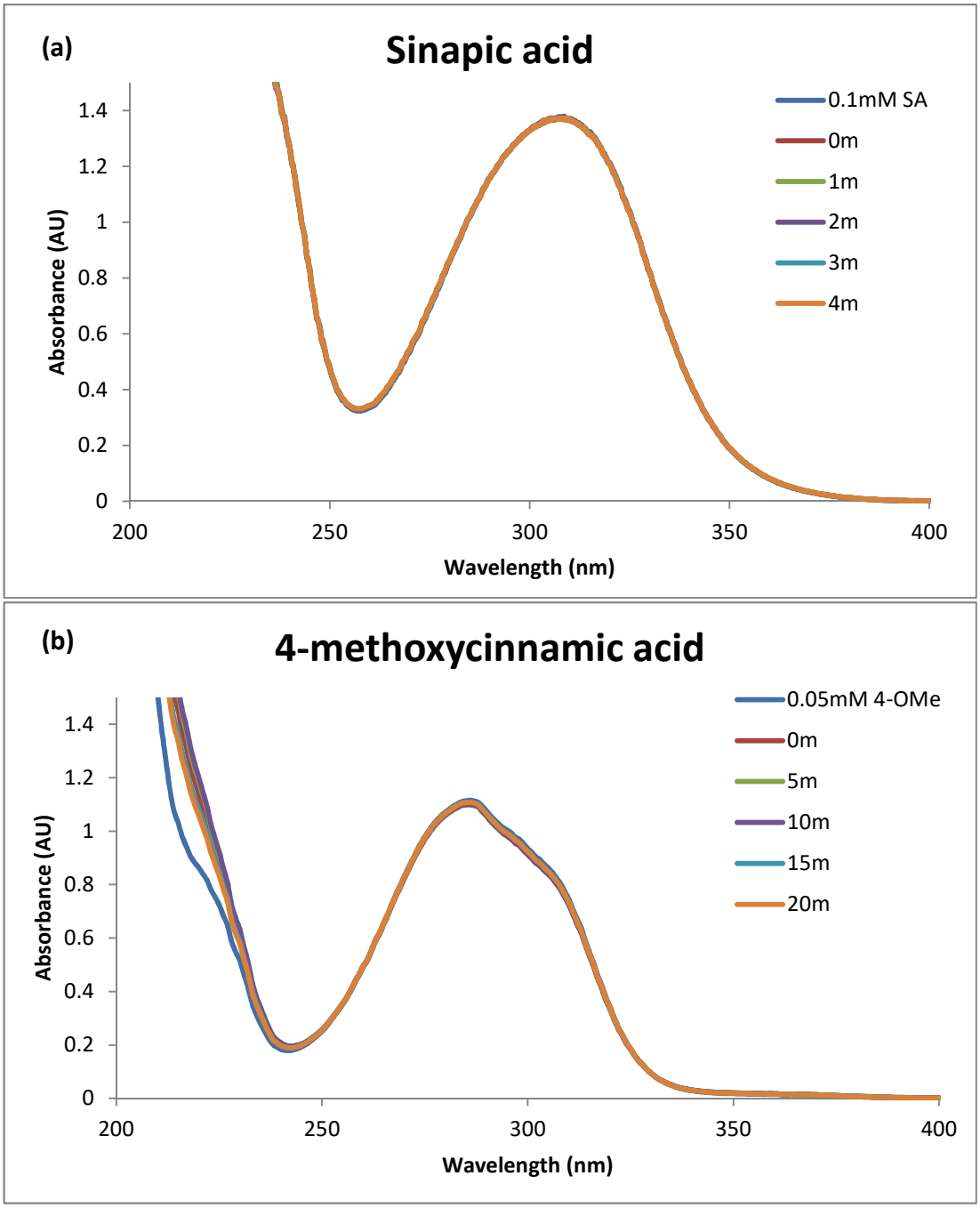

Figure 29: UV-Vis spectra for the assay of phenolic acid decarboxylase with (a) sinapic acid and (b) 4-methoxycinnamic acid taken at 1 min interval

No changes in absorbance were also seen for all the other substituted cinnamic acids tested, 2- and 4- methoxycinnamic acids as well as 3-hydroxycinnamic acids (results not shown).

A simple conclusion can be made out of these observations; all three substrates (ferulic, *p*-coumaric and caffeic acids) with a positive result towards the enzyme reaction have similarity of bearing a hydroxyl group at the *para*- position, except sinapic acid however, did not follow this trend.

Some research has suggested that the phenolic acid decarboxylase enzyme works by attacking the hydroxyl group in *para*- position. This is important in order to stabilise the transition state by forming a quinone methide intermediate for decarboxylation (refer to Figure 13 in section 1.2) [87], [93], [96], [105], [106].

2.4 Kinetic profiles

Using the previously described assay method, the effect of varying pH on enzyme activity was investigated for ferulic acid and caffeic acid as substrates. To determine the optimum pH, assays were performed in a series of buffers covering the pH range 3.0–8.0 with 0.5 pH intervals. The pH profiles indicate that this phenolic acid decarboxylase has an optimum pH between 4.5 – 6.0 for ferulic and caffeic acids as substrates (Figure 30), comparable with pH optima of other PADs (see Table 3).

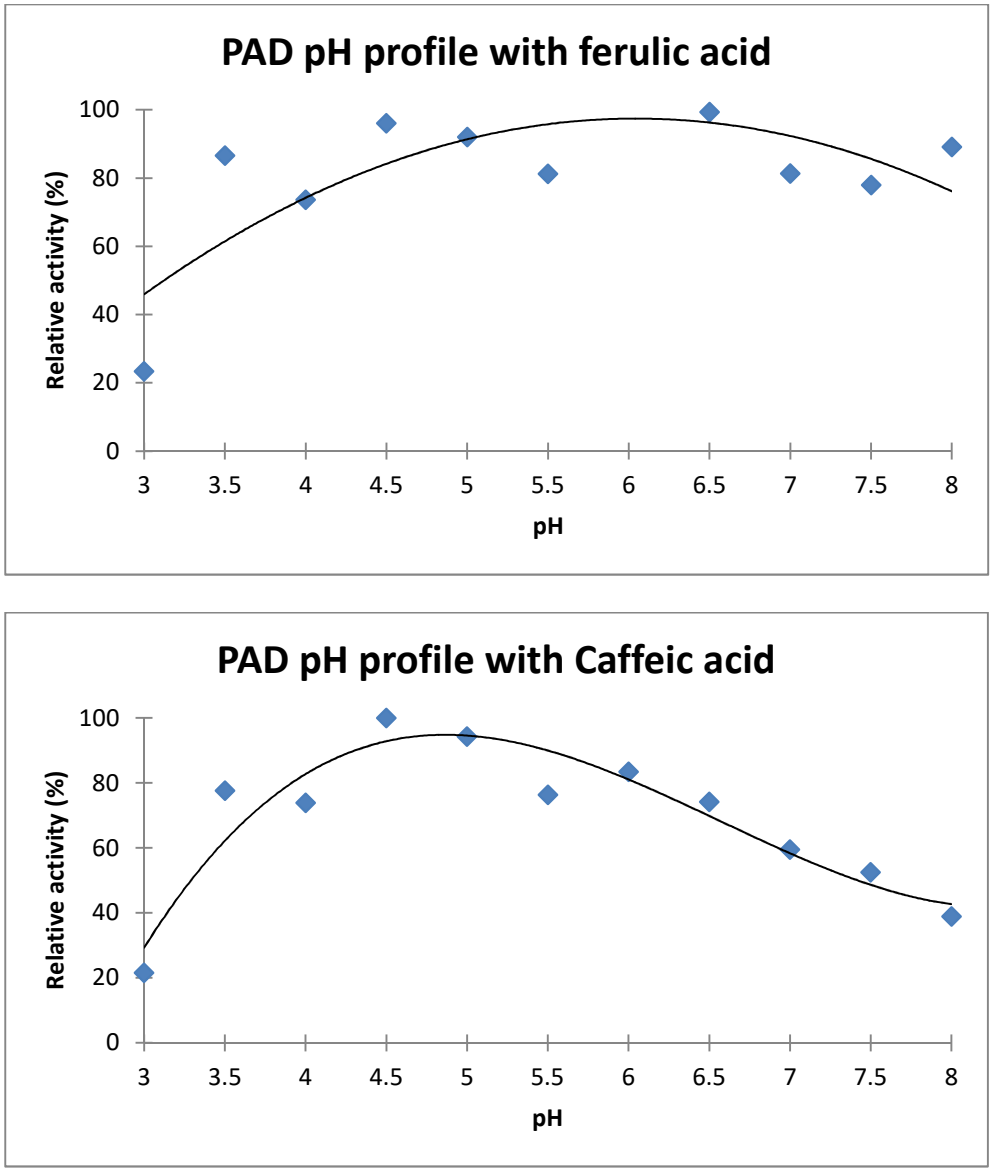

Figure 30: The pH-rate profile for PAD reaction with ferulic and caffeic acids

Kinetic parameters for phenolic acid decarboxylase were determined by Michaelis–Menten equation. The experiments were carried out with a variety of substrate concentrations under optimal reaction conditions for 5 min, and then kinetic properties were estimated from the the Lineweaver-Burk plot. Changes in absorbance were monitored at 315 nm for ferulic acid and at 285 nm for caffeic acid for both experiments. Figure 31 shows the steady-state kinetic plots for both ferulic and caffeic acid, with values shown in Table 3.

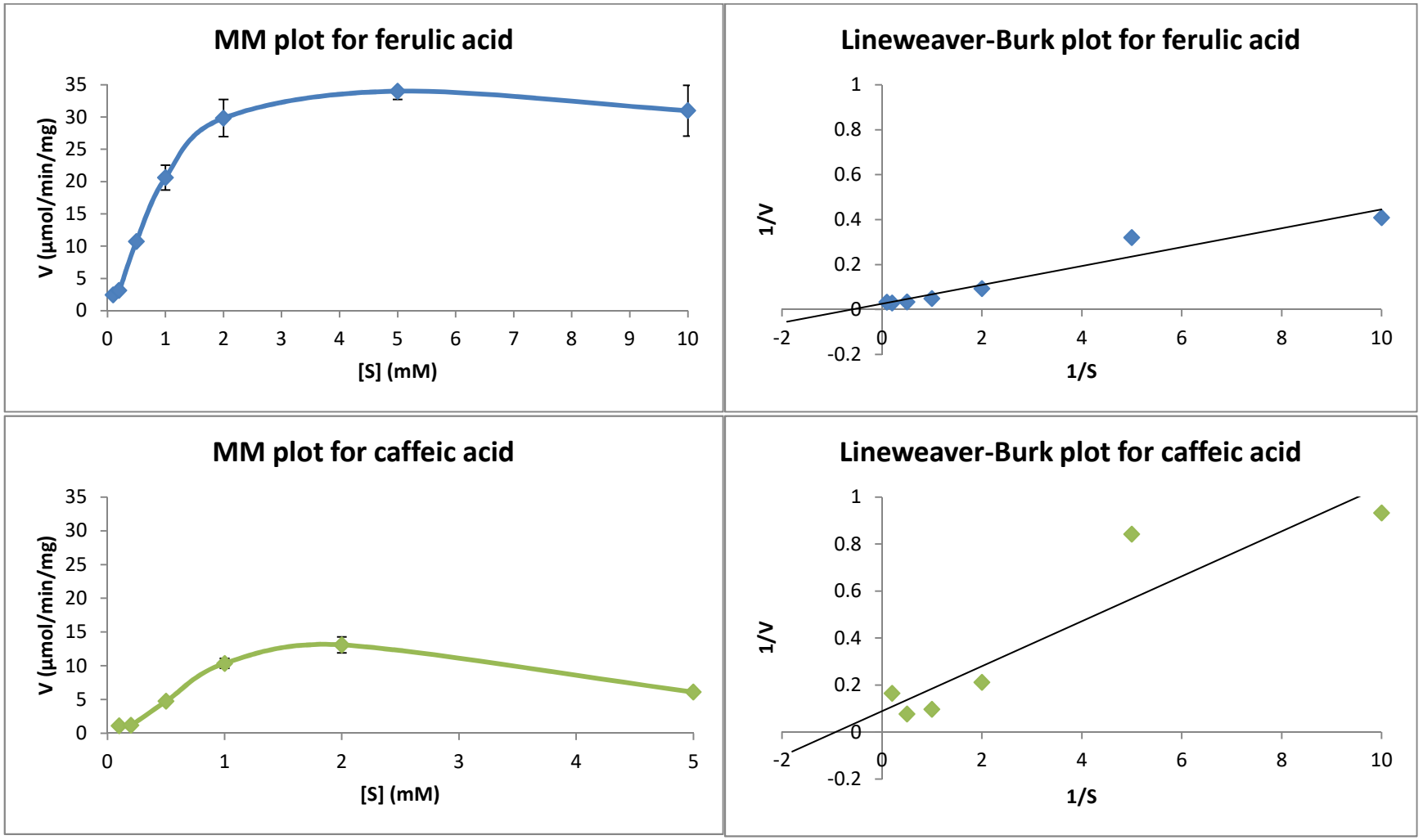

Figure 31: Michaelis-Menten and Lineweaver-Burk plots for PAD reaction with ferulic acid and caffeic acid

Table 3: Kinetic parameters for some phenolic acid decarboxylases produced by engineered *E.coli*

Enzyme	**Organism**	**Substrate**	**Optimum pH**	**K_m (mM)**	**V_{max}**	**MW (kDa)**	**Reference**
Ferulate and *p*-coumarate decaboxylase	*Bacillus pumilus*	Ferulic acid *p*-coumaric acid	5.5 5.5	1.03 1.38	0.19 mmol/min/mg/L 0.22 mmol/min/mg/L	23	[90]
Ferulic acid decarboxylase	*Enterobacter* sp. Px6-4	Ferulic acid	NA	2.36	10.10 µM/s	23	[98]
Ferulic acid decarboxylase	*Pseudomonas fluorescens*	Ferulic acid	7.3	7.9	NA	20.4	[180]
Phenolic acid decarboxylase	*Bacillus subtilis*	Ferulic acid *p*-coumaric acid Caffeic acid	5.0	1.1 1.3 2.6	280 µmol/min/mg 265 µmol/min/mg 180 µmol/min/mg	22	[88]
Phenolic acid decarboxylase	*Candida guilliermondii*	Ferulic acid *p*-coumaric acid	6.0 NA	5.32 2.66	NA NA	20	[96]
Phenolic acid decarboxylase	*Lactobacillus brevis* RM84	Ferulic acid *p*-coumaric acid Caffeic acid	6.0 (also highly active at 5.5 – 7.0)	0.78 0.98 0.96	464 µmol/h/mg 598 µmol/h/mg 609 µmol/h/mg	20	[71]
Phenolic acid decarboxylase	***Bacillus subtilis***	**Ferulic acid** **Caffeic acid**	**6.0** **4.5**	**1.68** **1.07**	**39.9 µmol/min/mg** **11.2 µmol/min/mg**	**23**	**This research**

Listed in Table 3 are some of the known K_m and V_{max} values of phenolic or ferulic acid decarboxylase from various microorganisms. Cavin *et al*., [88] mentioned that the PAD exhibited relatively high activity within broad pH range and this can be seen previously from Figure 30 where the enzyme is shown to be only significantly less active at pH 3 and 8. As for the substrate concentration, the K_m values for ferulic and caffeic acids in this work are close to 1 mM, which fall within the K_m range for *Bacillus* species indicated in Table 3 aforementioned. It is also observed that phenolic acid decarboxylase shows a characteristic of substrate inhibition when the substrate concentration is beyond 3 mM for caffeic acid, illustrated by the downward slope of the Michaelis-Menten plot. For ferulic acid, further addition of substrate concentration up to 10 mM did not increase the reaction velocity any further. V_{max} values per mg protein however, were much lower compared to the listed references.

2.5 Whole cell bioconversion of ferulic acid into 4-vinylguaiacol

As discussed in Section 1.1.1, it was understood that lignin biosynthetic pathway involves the production of monolignols that originated from aromatic amino acids with the aid of phenylalanine or tyrosine ammonia-lyase (P/TAL). In 2011, McKenna and Nielsen have researched on producing up to 260 mg/L styrene from an engineered *E.coli* containing the genes responsible for converting glucose into phenylalanine, then to cinnamic acid which was then enzymatically decarboxylated into styrene, as depicted in Figure 32 [137]. This was later followed by Kang *et al.*, using a similar procedure with tyrosine overproducing strain. It produced other substituted cinnamic acids (*p*-coumaric acid, caffeic acid and ferulic acid) which were converted into their respective styrene derivatives by phenolic acid

decarboxylase with titer of 4-vinylphenol, 4-vinylcatechol and 4-vinylguaiacol reaching 355, 63, and 64 mg/L respectively [138].

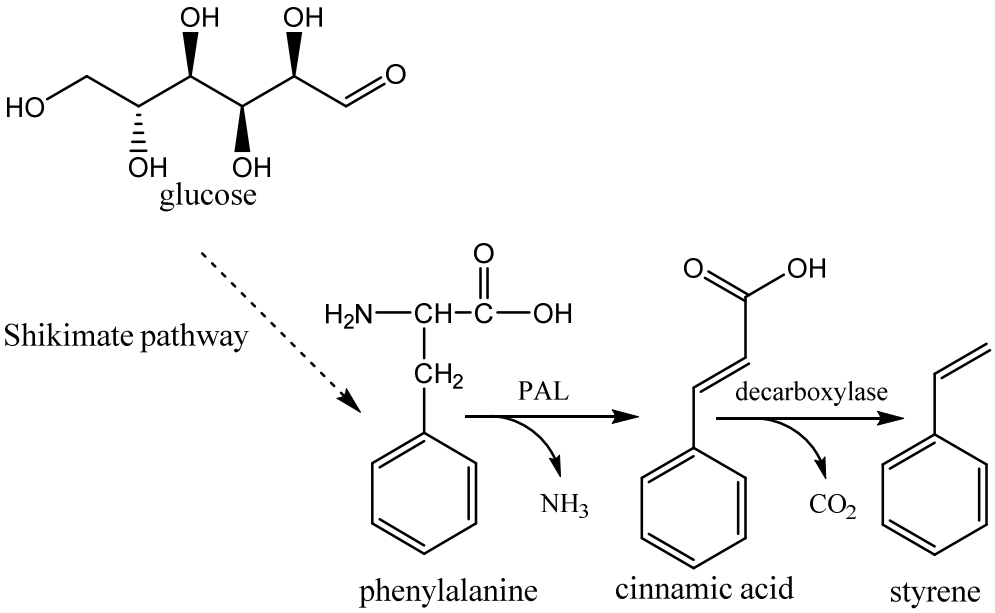

Figure 32: Styrene biosynthesis by engineered *E.coli*
Adapted from ref [137]; PAL phenylalanine ammonia lyase

In this experiment, whole cell suspension of *E.coli* BL21 bearing the plasmid pET200_*padC* was prepared in 100 mL LB containing 35 µg/mL kanamycin as described previously for protein expression. Upon reaching the OD_{600nm} of 0.8, the culture was centrifuged for 20 min at 5000 rpm to remove the LB. The cell pellet was then resuspended in M9 minimal media, supplemented with glucose, kanamycin and induced with 0.8 mM IPTG prior to further incubation at 16°C. All the process were done while maintaining the sterile condition of the culture. After 15 hours, ferulic acid was added to the medium to a final concentration of 2 mM and further incubated for 30 hours. One millilitre sample was taken out at various time points for metabolite analysis by HPLC-UV.

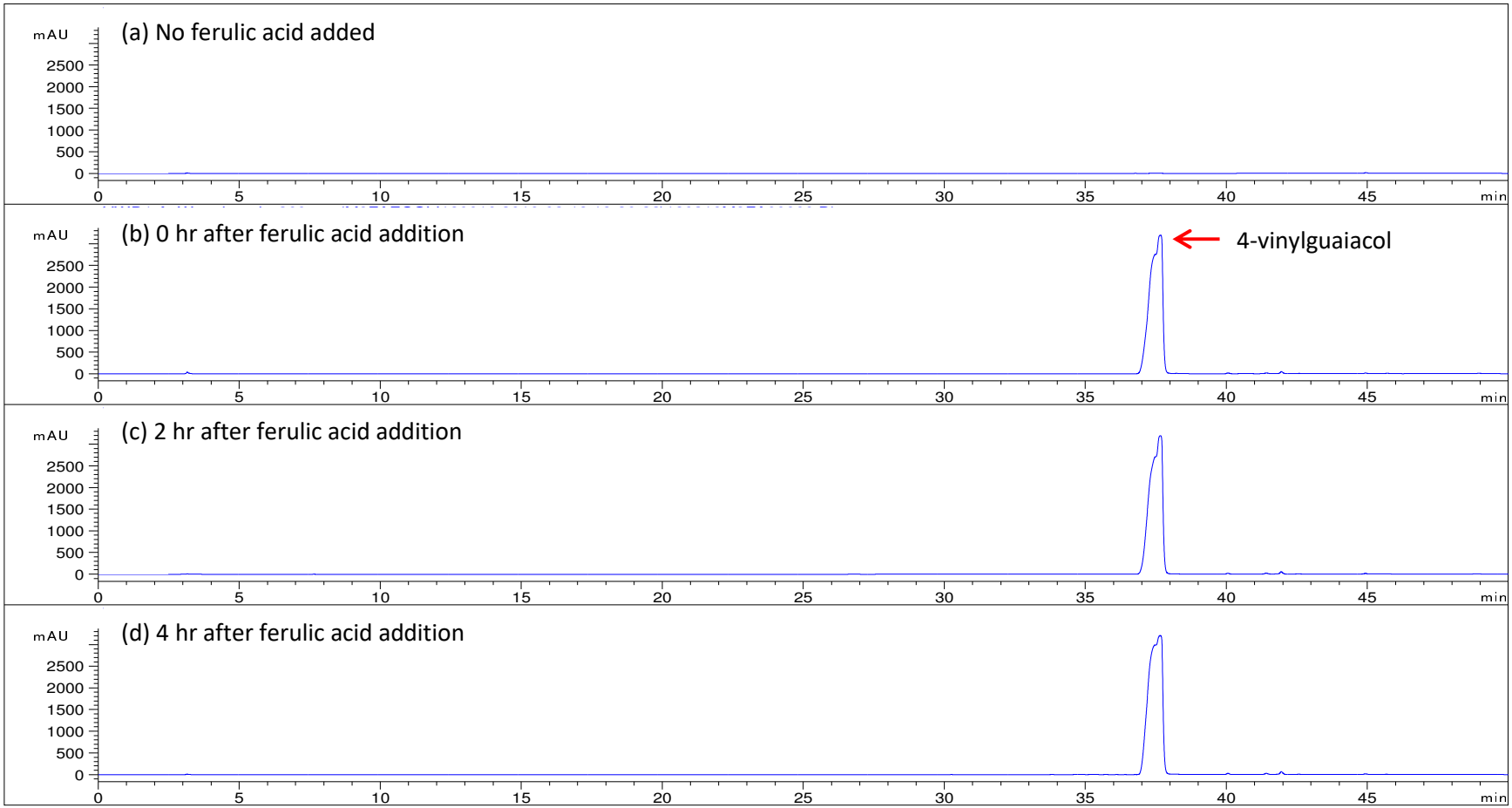

Figure 33: HPLC trace of 4-vinylguaiacol produced from *in vivo* PadC bioconversion

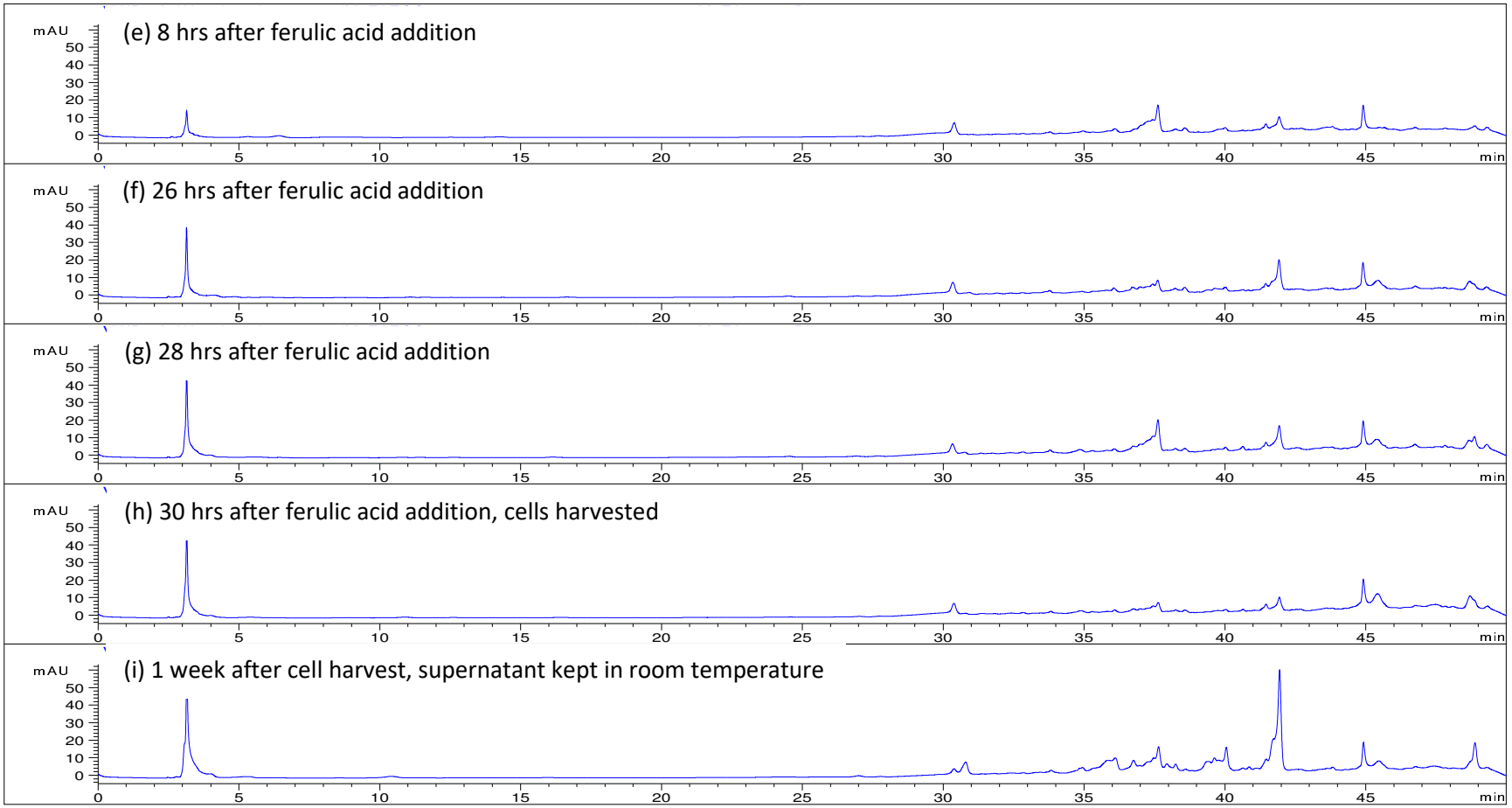

Figure 33 (continued): HPLC trace of 4-vinylguaiacol produced from *in vivo* PadC bioconversion

Figure 33 (a – d) showed the HPLC trace for the samples in which within the first 4 hours, high accumulation of 4-vinylguaiacol was seen at RT 37 min (matching those in Figure 26), with none observed in the culture without ferulic acid addition. Instant conversion was seen directly after the ferulic acid feeding, in which about 3.2 g/L of 4-vinylguaiacol yield was produced based on an estimation using authentic compound calibration. However, in the subsequent time points, from 8 hours to one week after cell harvest, (Figure 33 e – i), the peaks dramatically dropped into very low absorbance, that was almost undetectable. Kang *et al*., have also experienced an unexplained disappearance of 4-vinylguaiacol peak after 12 hours culture in *E.coli* bearind the padC plasmid [138].

Therefore, it can be understood that the ferulic acid added into the culture medium can be taken into the cells and converted by *in vivo* enzymatic reaction to produce 4-vinylguaiacol which is then available in the medium. Nonetheless, the compound produced via this method is best harvested within the first few hours after ferulic acid addition.

To simply conclude, it is true that the yield produced through this whole cell bioconversion is high, and the downstream process is more straightforward, in which, the product can be easily extracted by organic solvent from the culture supernatant. On the other hand, the bioconversion using extracted enzyme was quite laborious due to the requirement to purify the enzyme. Nevertheless, the product formed via this process can be obtained in a more controlled manner and can be easily scalable accordingly.

CHAPTER 3 EFFECTS OF PHENOLIC ACID DECARBOXYLASE OVEREXPRESSION IN *RHODOCOCCUS JOSTII* RHA1

Lignin is the most abundant natural aromatic resource in the biosphere. After harvesting agricultural crops, many of the residues remain underutilised. As explained in Section 1.1.3, some bacteria, including *Rhodococcus jostii* RHA1 are able to degrade lignin into some aromatic metabolites. Through gene deletion, RHA1 mutant lacking vanillin dehydrogenase gene (*Δvdh*) was designed by Professor Lindsay Eltis (UBC, Canada) as *R.jostii* RHA045, which was unable to grow on vanillin [181]. Sainsbury *et al*., have previously shown that treatment of wheat straw lignocellulose by *R. jostii* RHA045 strain containing a *Δvdh* gene deletion was able to accumulate vanillin (96 mg/L culture) and ferulic acid (up to 86 mg/L) [1].

Potentially the insertion of the *padC* gene encoding phenolic acid decarboxylase into this strain would allow the generation of 4-vinylguaiacol via biotransformation.

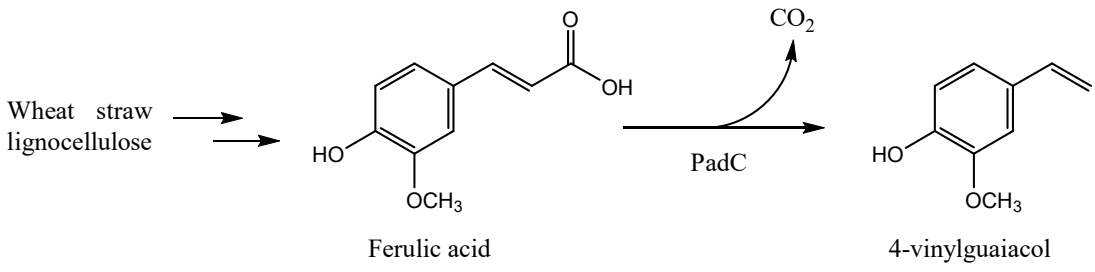

Figure 34: Biotransformation of wheat straw lignocellulose into 4-vinylguaiacol

This was first tested with wild-type *R. jostii* RHA1, and then with the gene deletion strain RHA045.

3.1 Overexpression of PAD in *Rhodococcus jostii* RHA1 in M9/lignocellulose media

Overexpression of phenolic acid decarboxylase was carried out using the lignin degrader *Rhodococcus jostii* RHA1 inserted with pTipQC2 vector. The plasmid, as illustrated in Figure 35 contains *padC* gene under the control of an inducible promoter, for which the inducer is thiostrepton [182], [183].

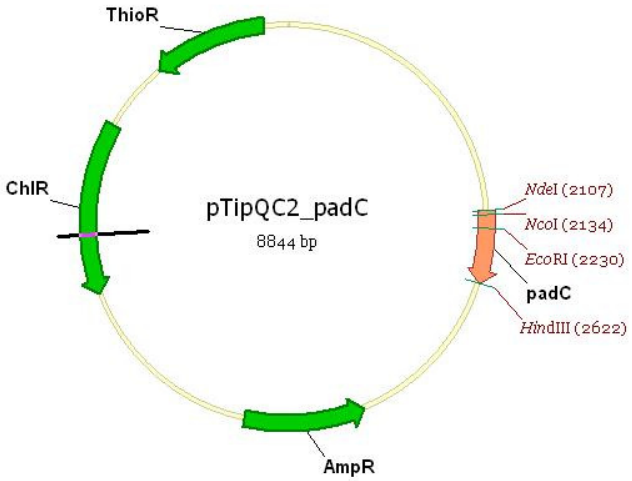

Figure 35: PadC expression vector in pTipQC2 plasmid

From LB agar, one colony was picked for a starter culture in LB, which took approximately 2 days to be viable enough for growth in minimal media. It was then inoculated into M9 minimal media supplemented with 1% w/v milled wheat straw and 0.2% (w/v) glucose in the presence of 35 µg/mL chloramphenicol. Enzyme production was induced with 1 µg/mL thiostrepton on the second day of fermentation. The culture was grown in an orbital shaker at 30°C for 10 days.

The growth profile was charted as shown in Figure 36 by taking an absorbance reading at 600 nm from a 1 mL sample every day for 10 days. A control experiment

was also conducted in which the culture medium was not inoculated with the bacterium.

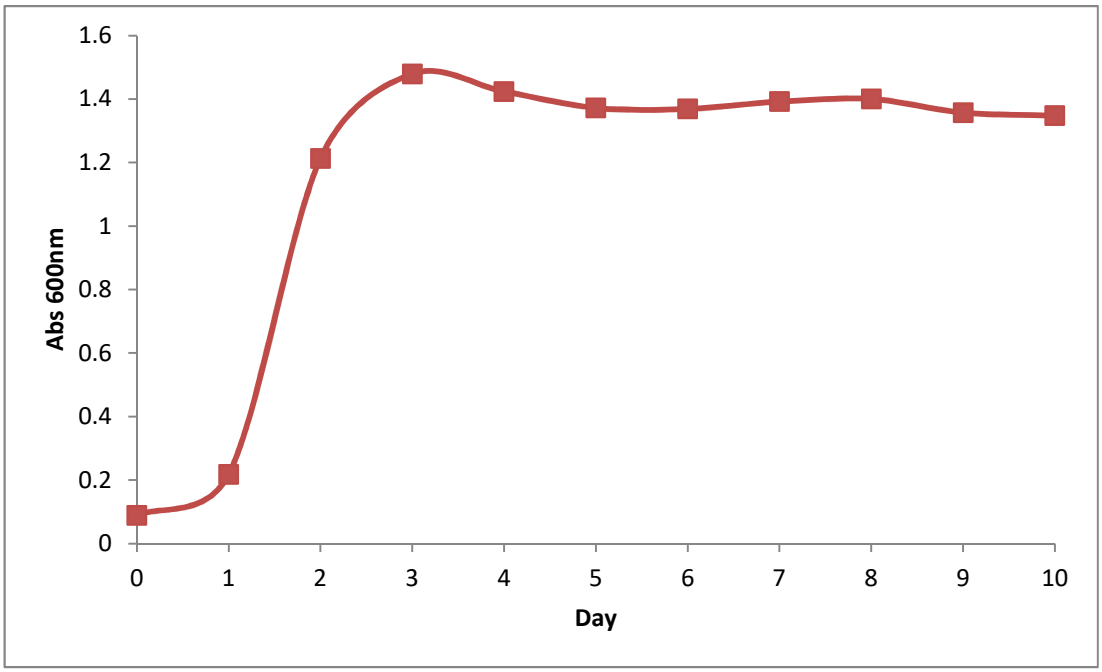

Figure 36: Growth profile of *Rhodococcus jostii* RHA1 in M9/lignocellulose media

Based on the growth profile (Figure 36), the log phase was reached between day 1 and 2 of the culture, and it stayed in stationary phase until the 10th day of incubation. Unlike *E.coli* that has a short doubling time [184], *Rhodococcus jostii* is a slow growing microorganism. The log phase lasted for 2 days, after which no significant increase in growth was observed. M9 minimal media could provide all the essential nutrients required for cell growth, and the milled wheat straw, being rich in lignocellulose served as a carbon source when supply of glucose is exhausted. Upon breakdown, hydroxycinnamic acids will be available in the media, providing substrate for PAD.

Following cell harvest after the end of incubation period, the collected samples were sedimented at maximum speed (13000 rpm) using microcentrifuge for 5 mins to remove solid residues. The recovered supernatants were prepared for metabolite analysis by extraction with an equal volume of ethyl acetate for three times, and upon complete evaporation, it was resuspended in methanol. Thin layer chromatography, TLC (70% CH_3Cl/MeOH) revealed the presence of UV-absorbing spots; two for authentic ferulic acid (R_f = 0.33 and 0.53), and one spot each for the authentic 4-vinylguaiacol and the culture supernatant at R_f = 0.81 and 0.78 respectively.

Later, the prepared methanol extracts were subjected to reversed-phase HPLC using Agilent Series 1200 system. The HPLC solvents were: water/ 0.1% trifluoroacetic acid (Solvent A) and methanol/ 0.1% trifluoroacetic acid (Solvent B). The gradient applied was: 10% B over 5 min; 10–15% B over 5–15 min; 15–25% B over 15–23 min, 25-100% B over 23-42 min, 100% B over 42-45 min and from 45-49 min back from 100% B to 10% B with 10% B for the 50^{th} minute. Resulting chromatograms are displayed as the retention time versus intensity of absorbance at 260 nm in Figure 37, which were compared against authentic standards procured from Sigma and an enzymatically generated 4-vinylguaiacol (Figure 38).

Based on the chromatograms, the highest peak was eluted at 33.9 min for all the culture supernatants tested, including the one for no bacterium control, which co-elutes with authentic ferulic acid (retention time 33.7 min). Authentic 4-vinylguaiacol eluted at 37.8 min, similar to the enzymatically generated 4-vinylguaiacol. Thus, it is initially postulated that only ferulic acid is produced, not 4-vinylguaiacol. The observation that ferulic acid is also seen in the control containing no bacteria suggests that it is released non-enzymatically from wheat straw lignocellulose, via hydrolytic cleavage of ferulate esters, perhaps via autoclaving of the wheat straw.

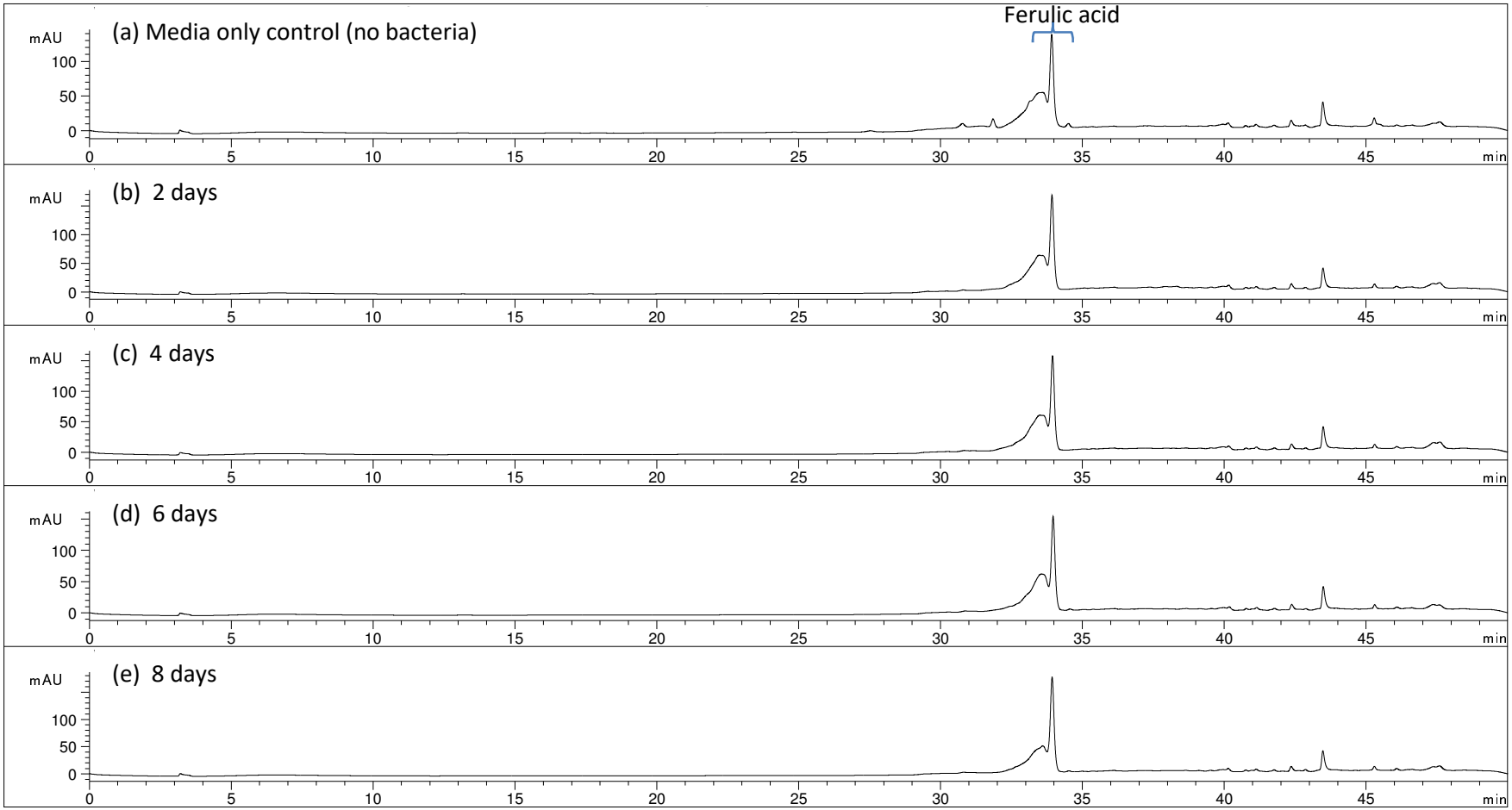

Figure 37: HPLC chromatogram at 260 nm of the time course RHA1 culture expressing PAD in M9 minimal media supplemented with milled wheat straw

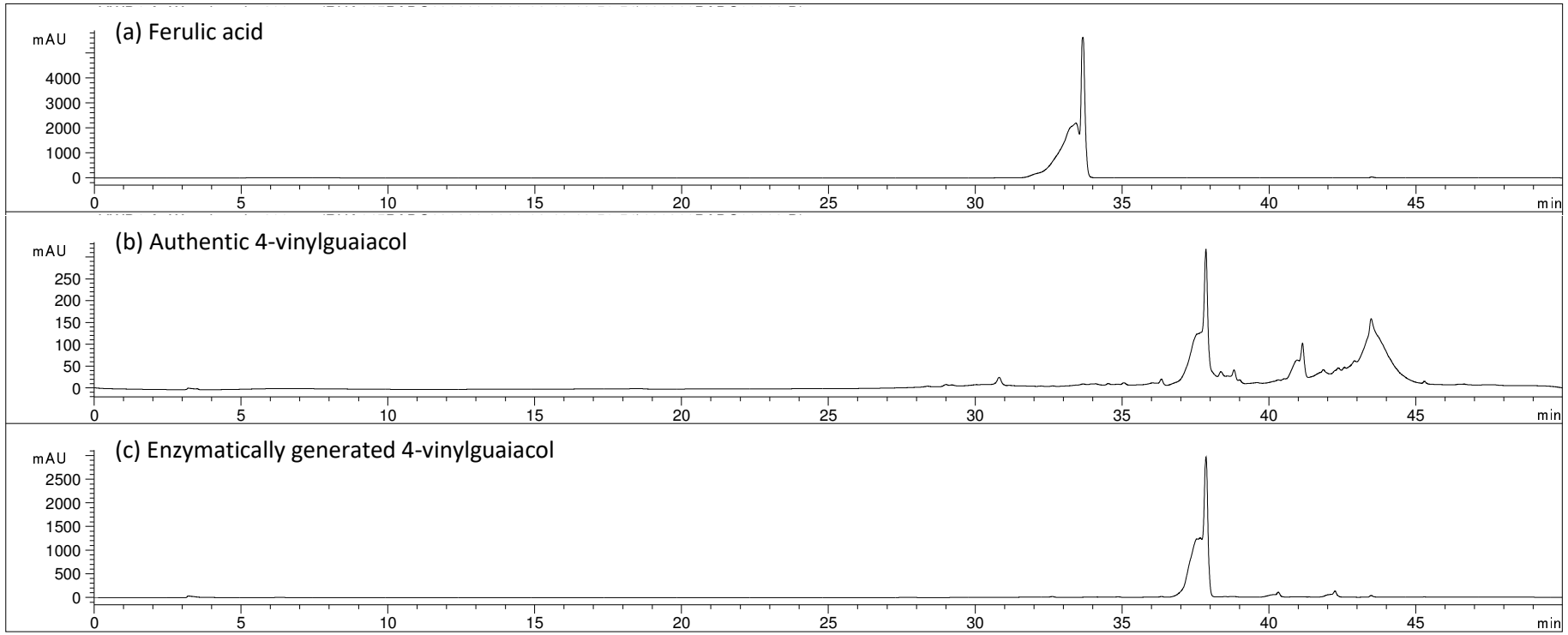

Figure 38: HPLC chromatogram at 260 nm authentic (a) ferulic acid, (b) 4-vinylguaiacol and (c) enzymatically generated 4-vinylguaiacol

Using a calibration of authentic compound, the resulting ferulic acid concentration was charted as follows.

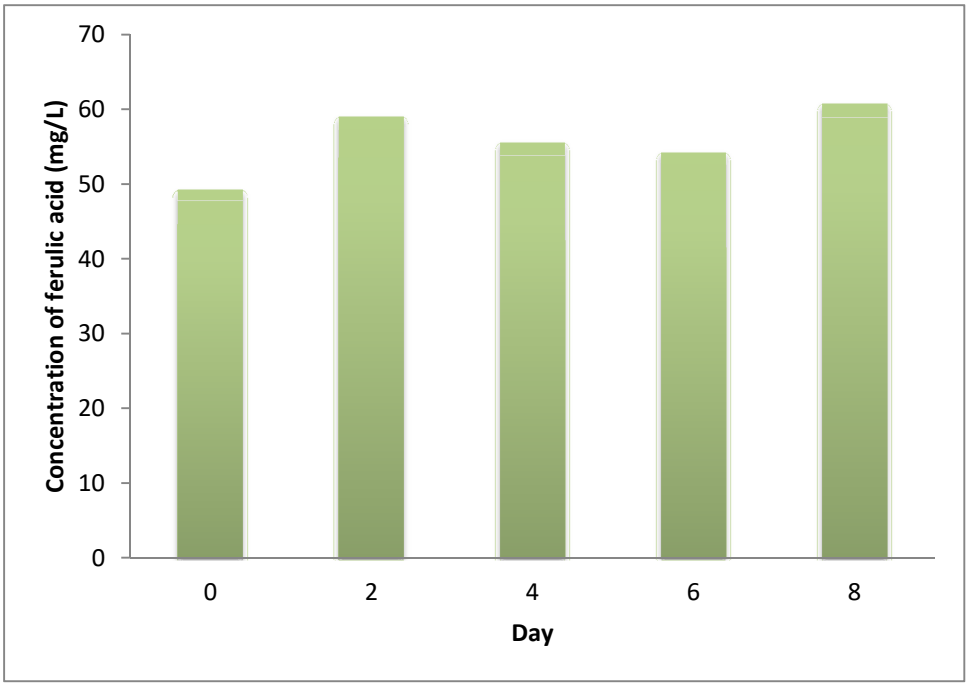

Figure 39: Concentration of ferulic acid in culture supernatant of *R.jostii* RHA1 with the *padC* gene insertion throughout the incubation period

A maximum of 60.72 mg/L (0.31 mM) of ferulic acid was accumulated from the 8 day culture (see Figure 39), and if compared to the no bacteria control, there was not much increase in concentration. The appearance of ferulic acid in the control can be explained by the possibility of autoclave treatment; in which high temperature and pressure that was exerted to the substrate could have led to the release of ferulic acid from the milled wheat straw. Hendriks and Zeeman have explained on how treating lignocellulose in the temperature above 100°C can have the capability to solubilise the hemicellulose backbone, which, in this case in sensible since ferulic acid is linked to hemicellulose [42]. A combination of 121°C and 15 psi pressure could undoubtedly result in the release of ferulic acid into the media.

Similar patterns were also recorded for LCMS run in positive mode, following the same gradient as the RP-HPLC described before, but carried out at 1 mL/min flow rate, thus, resulting in a slight shift in retention time observed, and also with similar major peak behaviour seen in the chromatograms.

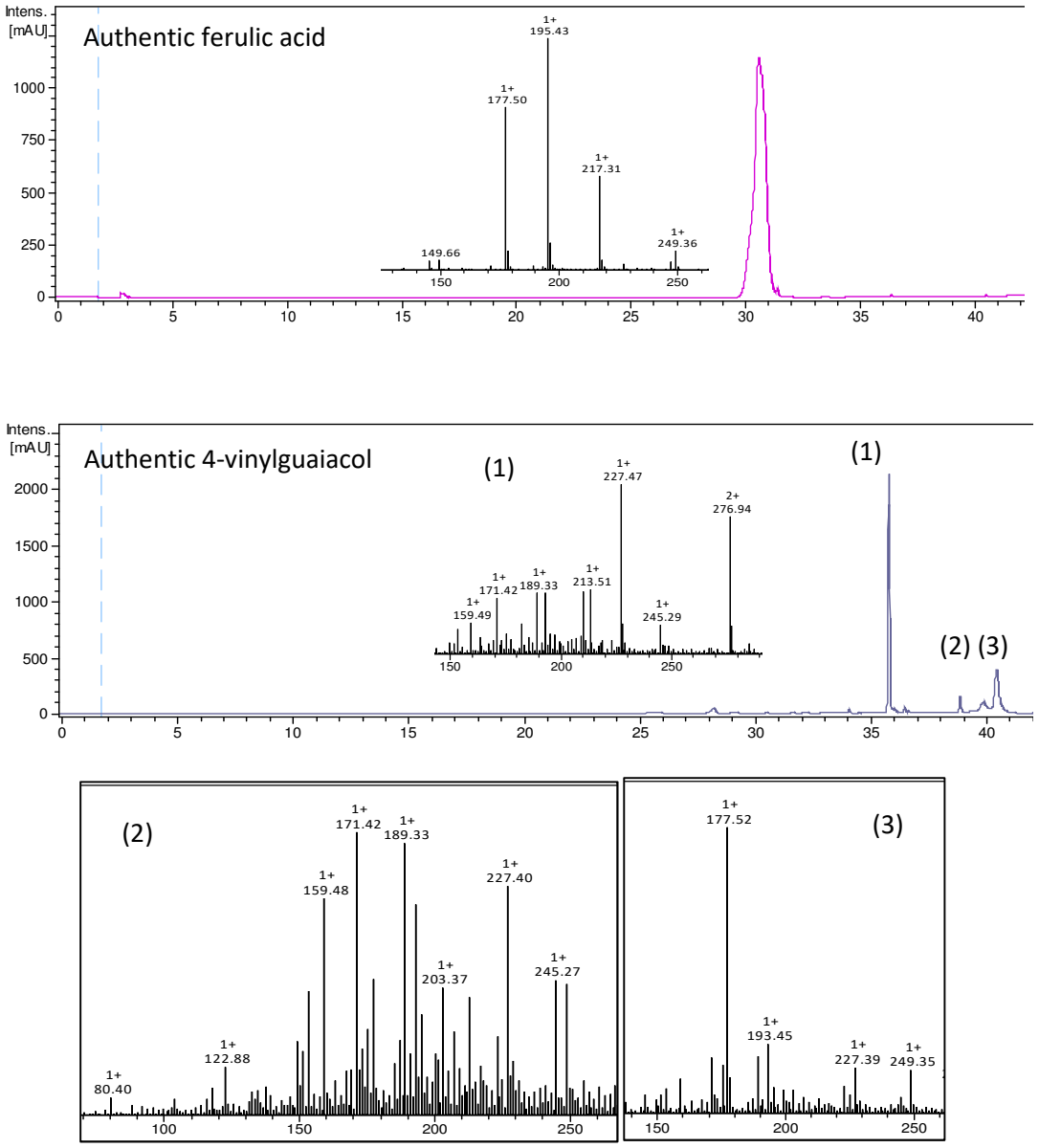

Figure 40: LCMS chromatograms at 260 nm for authentic ferulic acid and 4-vinylguaiacol compounds.
(1) TIC for peak at RT 36 min; (2) TIC for peak at RT 39 min; (3) TIC for peak at RT 40.5 min

In Figure 40, the authentic ferulic acid showed a peak with a retention time, RT of 31 min with the inset showing a total ion chromatogram (TIC) for m/z 195.45 and 217.51, corresponding respectively to the MH^+ and MNa^+ adducts of ferulic acid. While for the authentic 4-vinylguaiacol, three peaks were observed, at RT 36, 39 and 40.5 mins. The corresponding TIC however, did not show an exact mass for 4-vinylguaiacol (MW 150.17), but there was a peak at m/z 189.3 observed in peaks 1 and 2 which might correspond to the MK^+ adduct (m/z 189.3 MK^+).

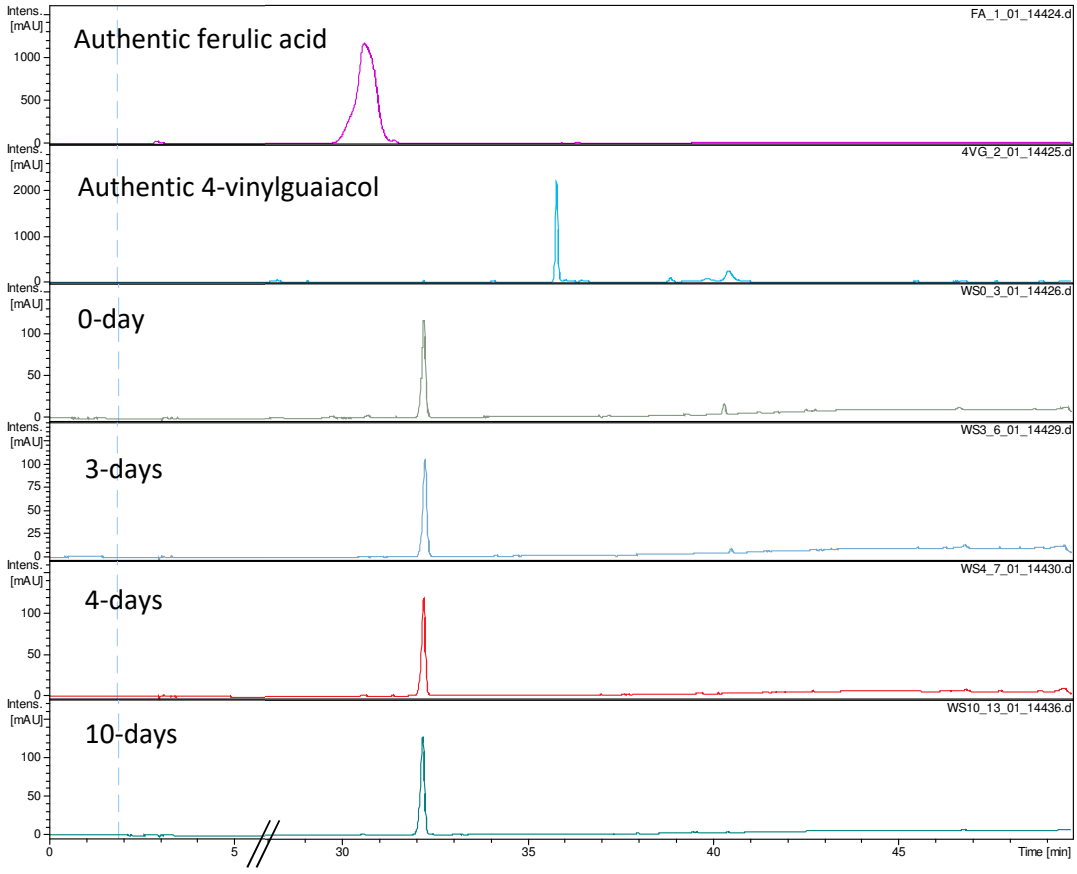

Figure 41: UV chromatogram at 260 nm using LCMS for the time course RHA1 culture expressing PAD in M9 minimal media supplemented with milled wheat straw

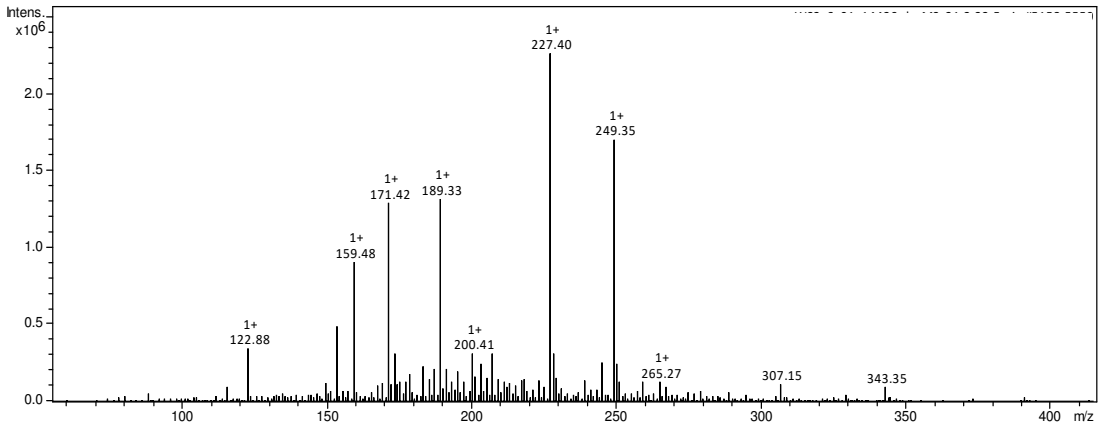

Figure 41 (continued): The corresponding mass spectrum for the UV chromatogram of all the fermented wheat straw culture extract at retention time 32.3 min.

Figure 41 illustrated the UV chromatograms at 260 nm of the different timepoints in incubation, aligned with the two authentic compounds, and their (the culture extract) corresponding total ion chromatogram. All the extracts contain a peak at retention time 32.3 min, in between those of the authentic ferulic acid and 4-vinylguaiacol. Many mass peaks (shown in the continued Figure 41) matched that of the authentic 4-vinylguaiacol (of RT 36 min), in which only one of them make sense, i.e: m/z 189.3 that is the positively charged potassium adduct for 4-vinylguaiacol.

The LCMS data suggests that a new species is formed in the bioconversion, however, the retention time does not match that of 4-vinylguaiacol. The identity of this species is not known.

3.2 Overexpression of PAD in *R. jostii* RHA1 in M9/ferulic acid media

Overexpression of PAD was again, carried out using the lignin degrader *Rhodococcus jostii* RHA1 carrying the plasmid construct pTipQC2_*padC*. All other culture methods were the same as previously described in Section 3.1, however, instead of using wheat straw lignocellulose, it was supplemented with the commercially available, authentic ferulic acid to investigate the true ability of bioconversion with the pure substrate. Two types of ferulic acids were used, 0.1% w/v each of the ferulic acid (Fluka) and *trans*-ferulic acid (Sigma, with 99% purity). Enzyme production was induced with 1 µg/mL thiostrepton on the second day of fermentation. The incubation was carried out for 4 days, in a 30°C shaking incubator.

Samples for analysis was prepared by extracting 2 mL of the 4 days culture supernatant with equal volume of ethyl acetate for three times, and upon complete evaporation, it was resuspended in methanol. The samples were analysed by RP-HPLC as described previously, and the resulting chromatograms at 260 nm are shown in Figure 42.

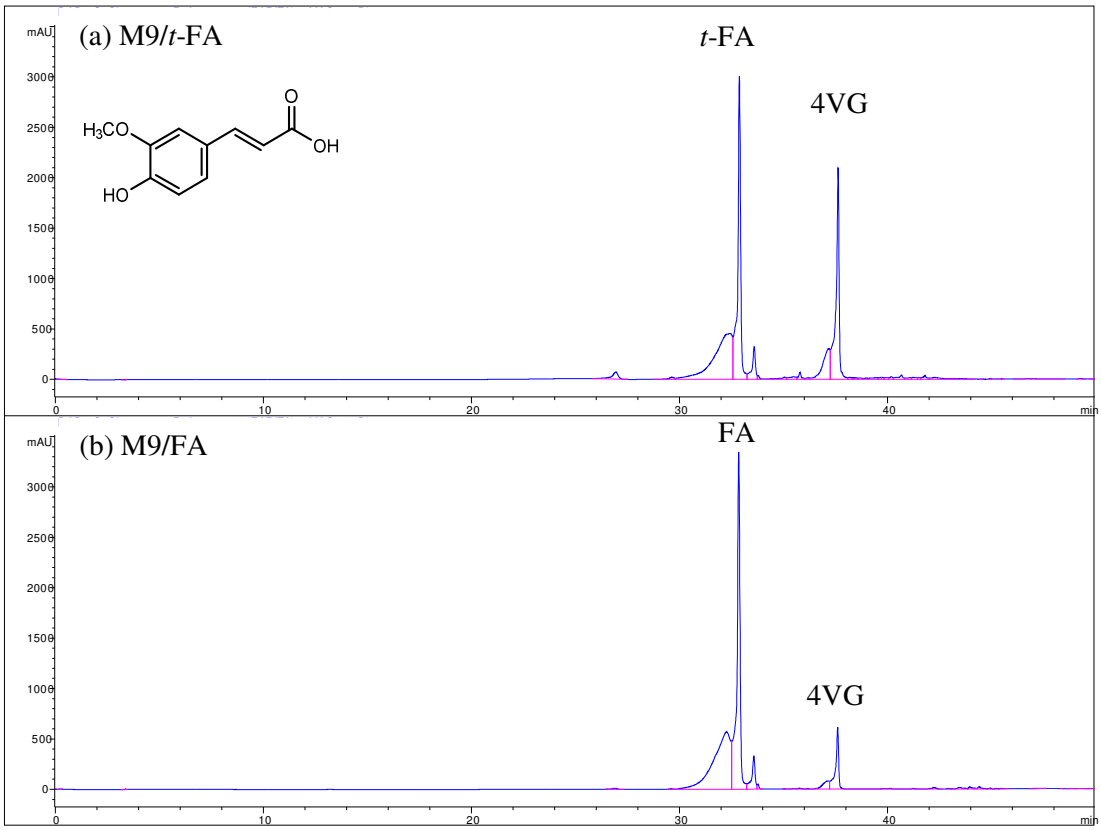

Figure 42: HPLC chromatograms of the extracted culture supernatant of *R.jostii* RHA1 pTipQC2_*padC* grown for 4 days in M9 medium supplemented with 0.1% w/v ferulic acid

*The *t*-FA was 99% pure *trans*-ferulic acid (Sigma); FA was laboratory grade ferulic acid (Fluka)

The peak at retention time 37 min is similar to both the enzymatically generated and authentic 4-vinylguaiacol (Sigma), especially for the *t*-ferulic acid culture. The 0.1% w/v concentration of ferulic acid added to the 50 mL total volume of M9 medium gave a final molar concentration of 5.15 mM. The observation that 4-vinylguaiacol is generated in this experiment suggests that a high concentration of ferulic acid is needed, due to the rather high K_m for PAD. It was reported that some kinetic studies have showed the K_m value for PAD could range from as low as 0.8 mM to as high as 7.9 mM [180]. Previous experiment in Section 2.4 with the purified PAD from *E.coli* resulted in a K_m of 1.68 mM for the *trans*-ferulic acid used. Considering the 2 mL extract used in the HPLC sample preparation, 4-vinylguaiacol yield from the two

experiments were estimated to be 3.28 g/L for *trans*-ferulic acid (Sigma) and 0.94 g/L for ferulic acid (Fluka).

This experiment demonstrates that in principle PAD can be used to generate 4-vinylguaiacol successfully in this culture media. However, it also explains that a higher concentration of ferulic acid was required for the bioconversion to proceed effectively.

3.3 Overexpression of PAD in *R. jostii* RHA045 in M9/lignocellulose media

Phenolic acid decarboxylase was previously overexpressed in the wild type *R.jostii* RHA1 by insertion of pTipQC2 vector containing *padC* gene. Production of 4-vinylguaiacol was not observed from HPLC chromatogram. To further investigate, overexpression of phenolic acid decarboxylase was carried out using the *Δvdh* knockout mutant, *Rhodococcus jostii* RHA045 by insertion of the aforementioned plasmid since the mutant was shown to accumulate ferulic acid [1]. The plasmid was transformed into electrocompetent *R. jostii* RHA045 cells by electroporation (at 1.8 kV), and the recombinant cells were isolated on LB agar containing 50 µg/mL chloramphenicol. It was grown in M9 minimal media supplemented with 1% w/v milled wheat straw and 0.2% (w/v) glucose in the presence of 35 µg/mL chloramphenicol. Enzyme production was induced with 1 µg/mL thiostrepton on the second day of fermentation. The growth profile was charted in Figure 43 by taking an absorbance reading at 600 nm from 1 mL sample every day for 12 days, in which the log phase was observed between day 2 and 3 of the culture.

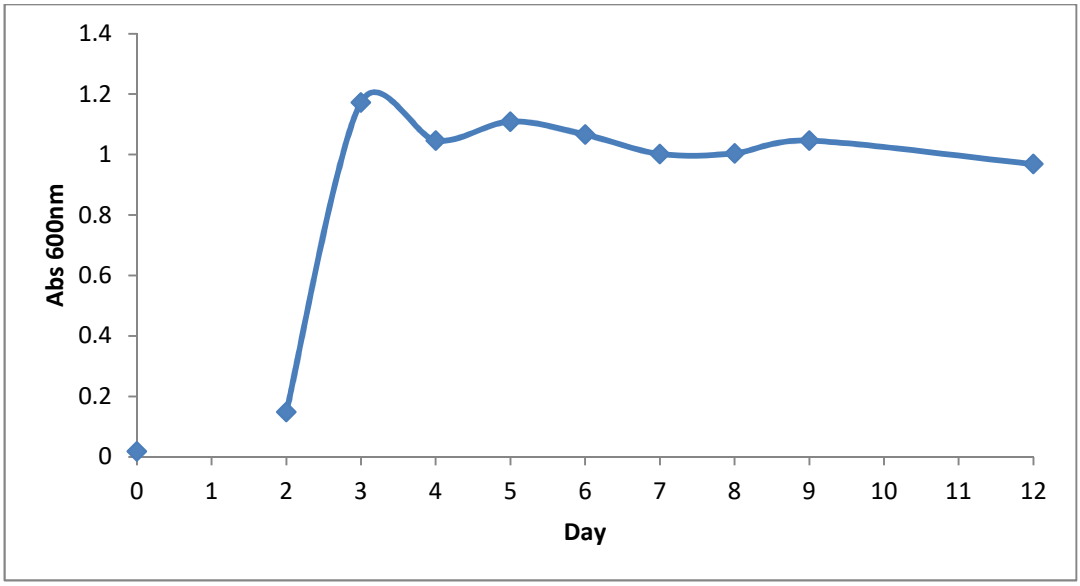

Figure 43: Growth profile of *Rhodococcus jostii* RHA045 in M9/lignocellulose media

A 10 mL sample (from 12-days culture, harvested at the end of fermentation) for was extracted with ethyl acetate, and upon complete evaporation, was resuspended in the same solvent. It was then purified by column chromatography on silica gel using ethyl acetate/hexane mixture (20/80) to give a product yield of 3 mg. Thin layer chromatography was run in 6:4 hexane/ethyl acetate as eluent. After viewing of spot under UV, R_f value of 0.89 was recorded for purified extract (by flash chromatography). This was qualitatively comparable to the enzymatically generated 4-vinylguaiacol (4VG) ran alongside, while the unpurified culture supernatant showed an R_f of 0.95. When the TLC plate was stained in vanillin and dried, spots developed from the staining matched those of the UV reflection tested beforehand.

For HPLC analysis, samples were prepared from day 2, 4, 6 and 8 of the fermentation and resuspended in methanol. HPLC was performed using Agilent reversed-phase Zorbax Eclipse XDB-C18 column on Agilent Series 1200 system with methanol and water for gradient (as described previously in Section 3.1).

Results are displayed as the retention time versus intensity of absorbance at 260 nm in Figure 44. Retention time of 33.9 mins was recorded for the culture extract, indicating the presence of ferulic acid similar to that for overexpression in *R.jostii* RHA1 reported before (Section 3.1). However, no peak corresponding to the authentic (Sigma) or the enzymatically generated 4VG (at retention time 38 min in Figure 38 b and c) was observed.

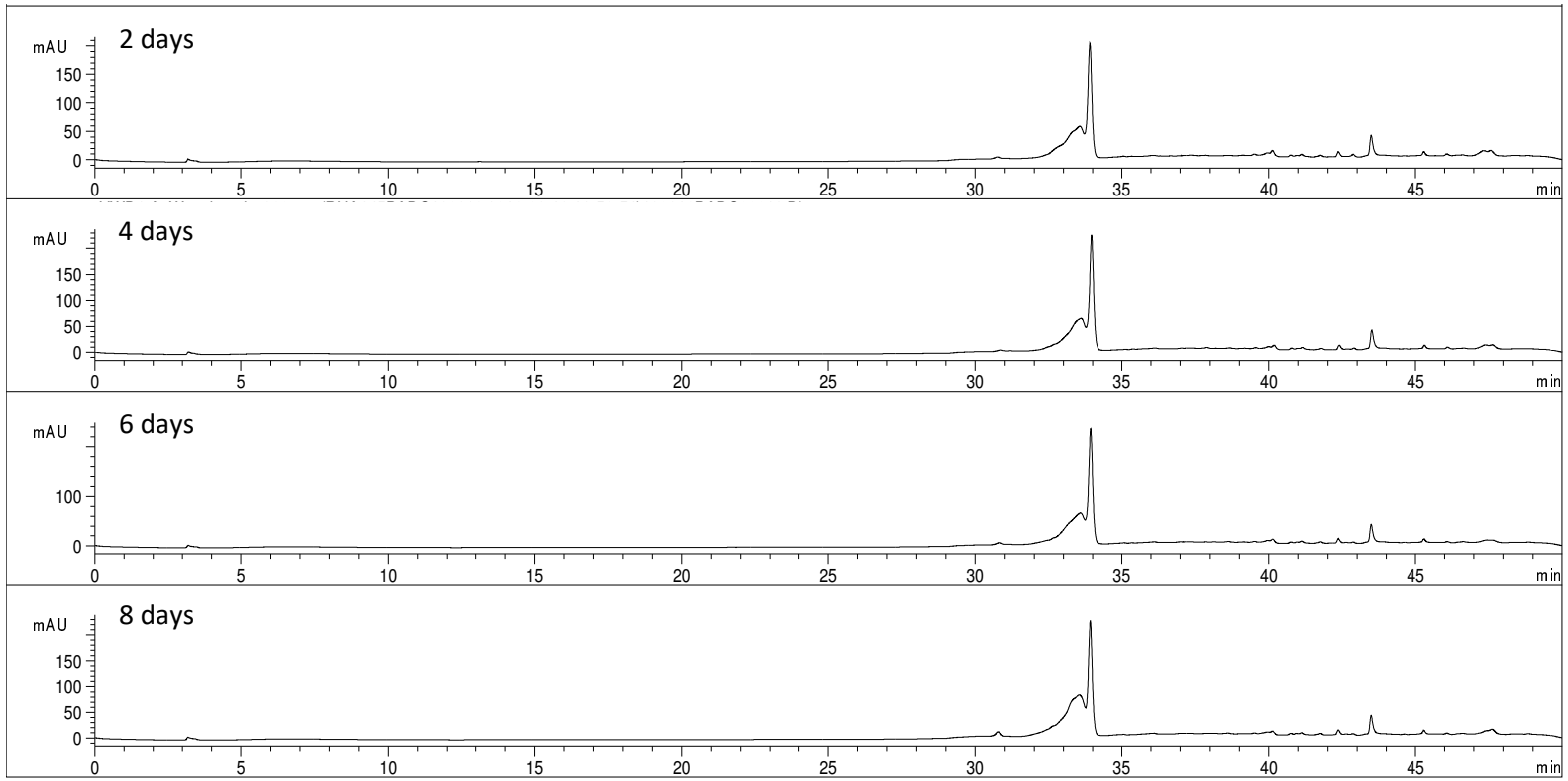

Figure 44: HPLC chromatogram at 260 nm of the time course RHA045 culture expressing PAD in M9 minimal media supplemented with milled wheat straw

Calibration with authentic standard revealed the concentration of ferulic acid, as shown in the bar chart herewith.

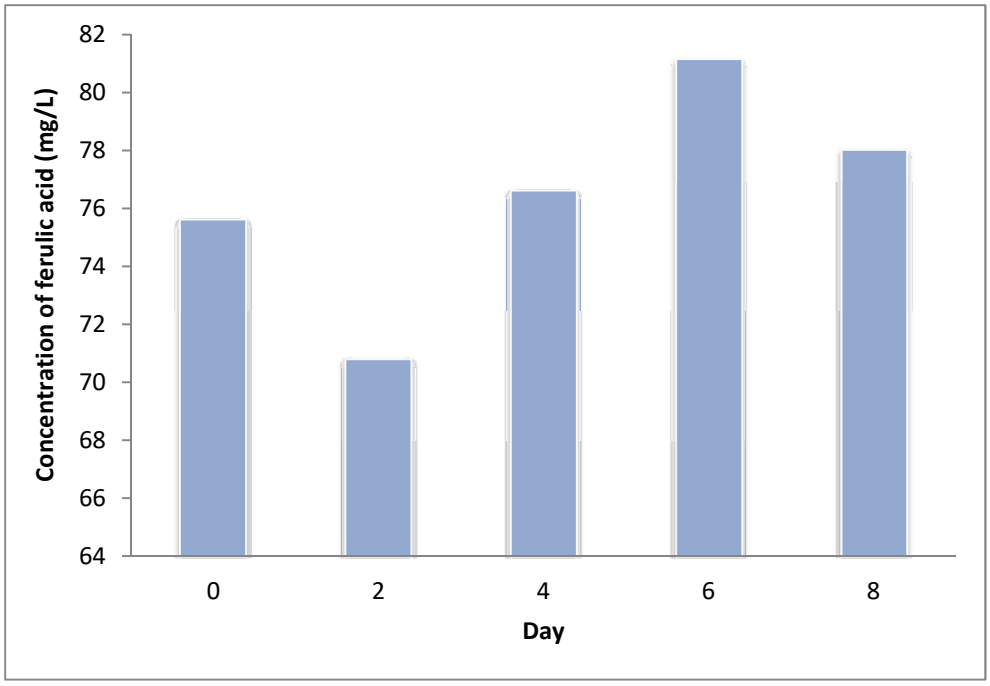

Figure 45: Concentration of ferulic acid in culture supernatant of *R.jostii* RHA45 with the *padC* gene insertion

The highest ferulic acid concentration was released on the 6th day of fermentation with 81 mg/L (0.42 mM) extracted. Just like the initial experiment in Section 3.1, the control culture containing no bacteria showed presence of ferulic acid, at an even higher amount compared to the 2nd day culture supernatant. From day 2 to 6, there was a steady increase of ferulic acid concentration, and a decline on the 8th day.

These data suggest that ferulic acid is initially released non-enzymatically, but that additional ferulic acid is generated during the fermentation by *R.jostii* RHA045. However, the amount was still too low, at merely 0.42 mM when compared to the K_m value of 1.68 mM (see Table 3) to drive PAD reaction successfully. In contrast, when grown in medium containing 0.1% (w/v) ferulic acid, which gave a total of 5.15 mM substrate, 4-vinylguaiacol was successfully accumulated (see Section 3.2).

3.4 Pre-treatment of wheat straw lignocellulose with NaOH as substrate for PAD overexpression in *Rhodococcus jostii*

The fact that wheat straw lignocellulose contain alkali-labile bonds have long been established, and discussed (see Section 1.1.4). Therefore, pre-treatment with alkaline confers many advantages in terms of scalability and cost since it produce a rich stream of lignin readily separated from the rigid lignocellulosic biomass [36], [43], [185], [186]. Based on this argument, an experiment was devised to see the effect of NaOH pre-treatment to generate ferulic acid as substrate for PAD.

Initially, ground wheat straw was left immersed in 0.125 M NaOH for 1, 1.5 and 2 hours in room temperature (23°C), after which, an equivalent concentration and amount of HCl was added to neutralise the sample to pH 7. The mixture was centrifuged to separate the supernatant from wheat straw, and later extracted with ethyl acetate to prepare for HPLC analysis to determine the phenolic acids released from the chemical treatment.

Figure 46 shows the HPLC trace of the three samples, where substantial increase of peaks at RT 31.9 and 32.6 minutes were observed with the increase of incubation time in the NaOH solution. The control in deionised water, with no NaOH added did not show any change at all. When compared to the authentic compounds of the possible hydroxycinnamic constituents of lignocellulose in Figure 47, the observed peaks show similar retention times to *p*-coumaric acid (RT 32.5 min) and ferulic acid (RT 33.1 min).

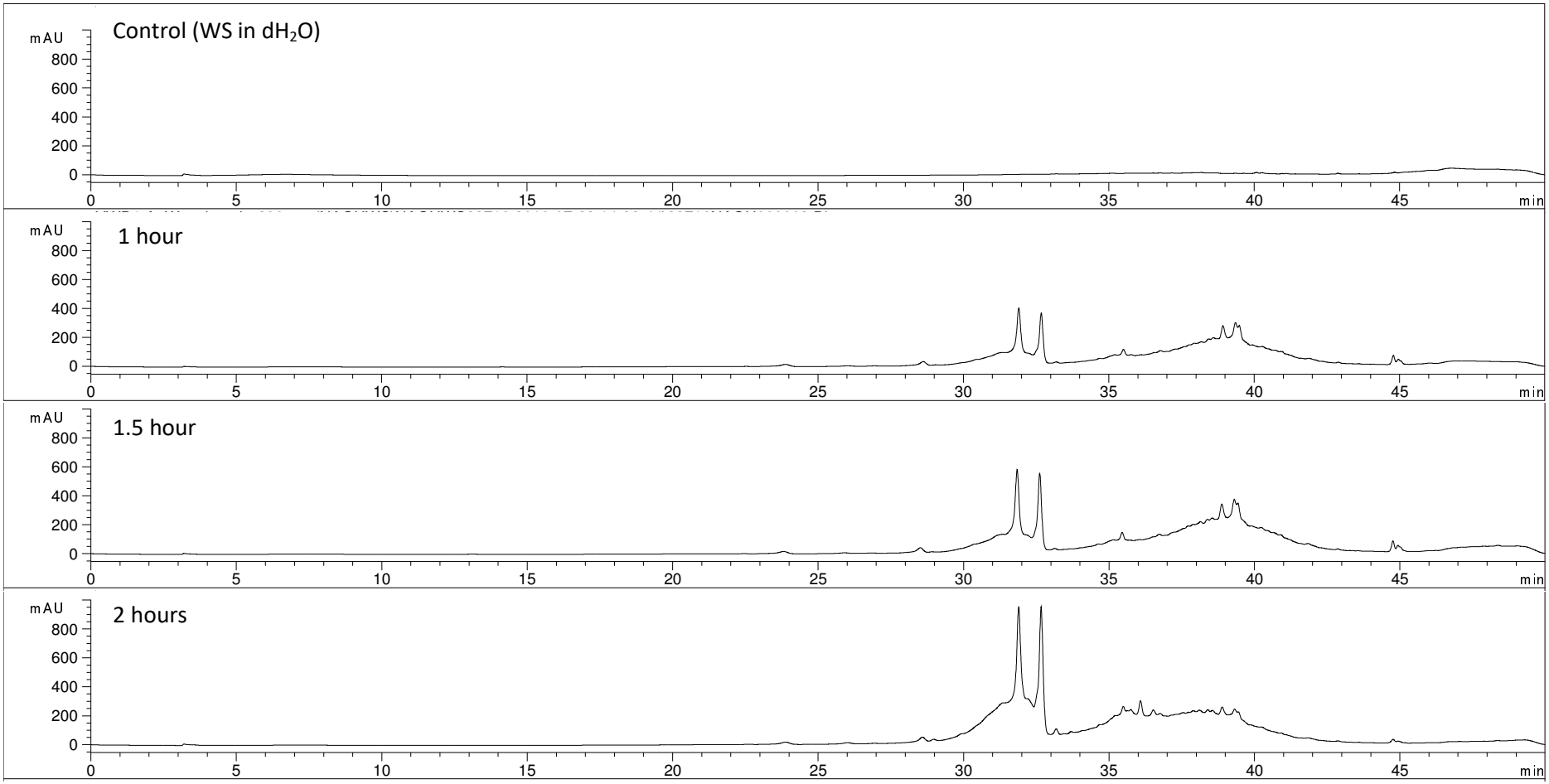

Figure 46: HPLC trace (at 280 nm) for the time course incubation of wheat straw in NaOH

(a) Ferulic acid

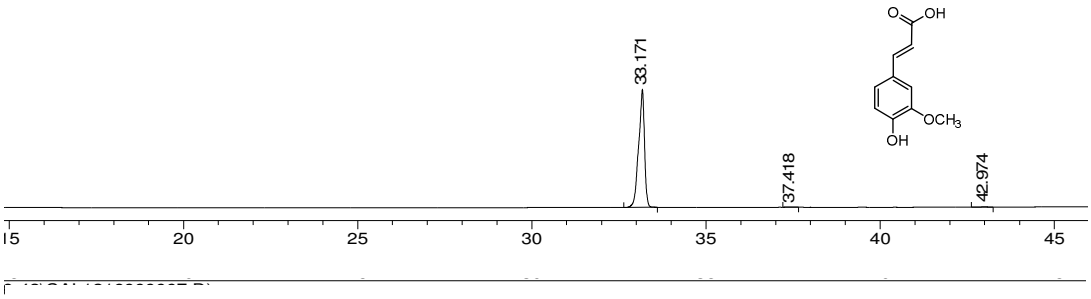

(b) Caffeic acid

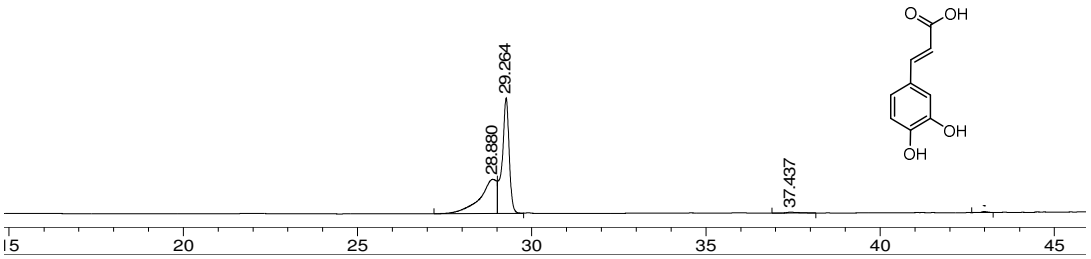

(c) Sinapic acid

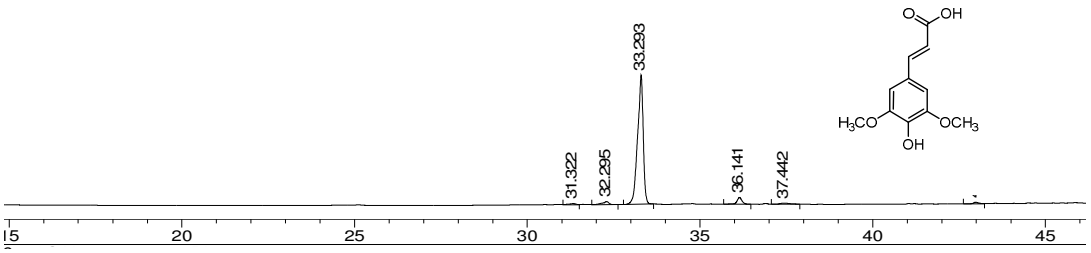

(d) *p*-coumaric acid

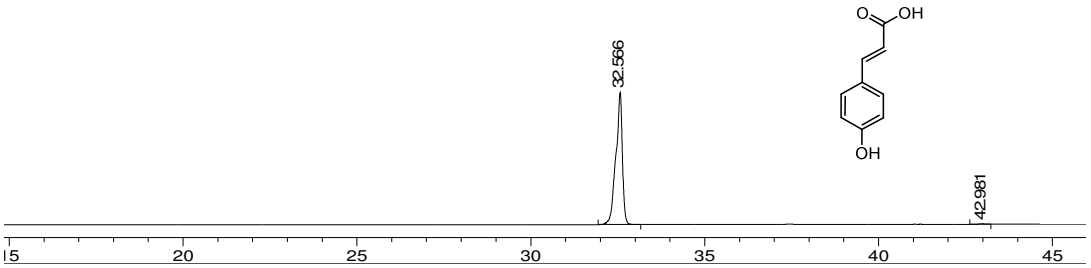

Figure 47: Major peaks detected by HPLC for hydroxycinnamic acids authentic standards at 280 nm

The 1 hour reaction component was also analysed by LCMS in positive mode and monitored at 280 nm. The result in Figure 48 shows the extracted ion chromatogram (EIC) as entities for m/z of 165 and 195 at retention time (RT) of 32.7 and 33.2 min

each, which corresponds to a positively charged ion (MH^+) of *p*-coumaric acid and ferulic acid respectively. Another two peaks were also observed for m/z 225 (RT= 33.3 and 39.7 min) relating to a proton adduct of sinapic acid. The EIC for the proton adduct of caffeic acid at m/z 181 however did not show clear, sharp peak, instead scattering peaks were observed from after 30 mins until just before the end of the chromatography run.

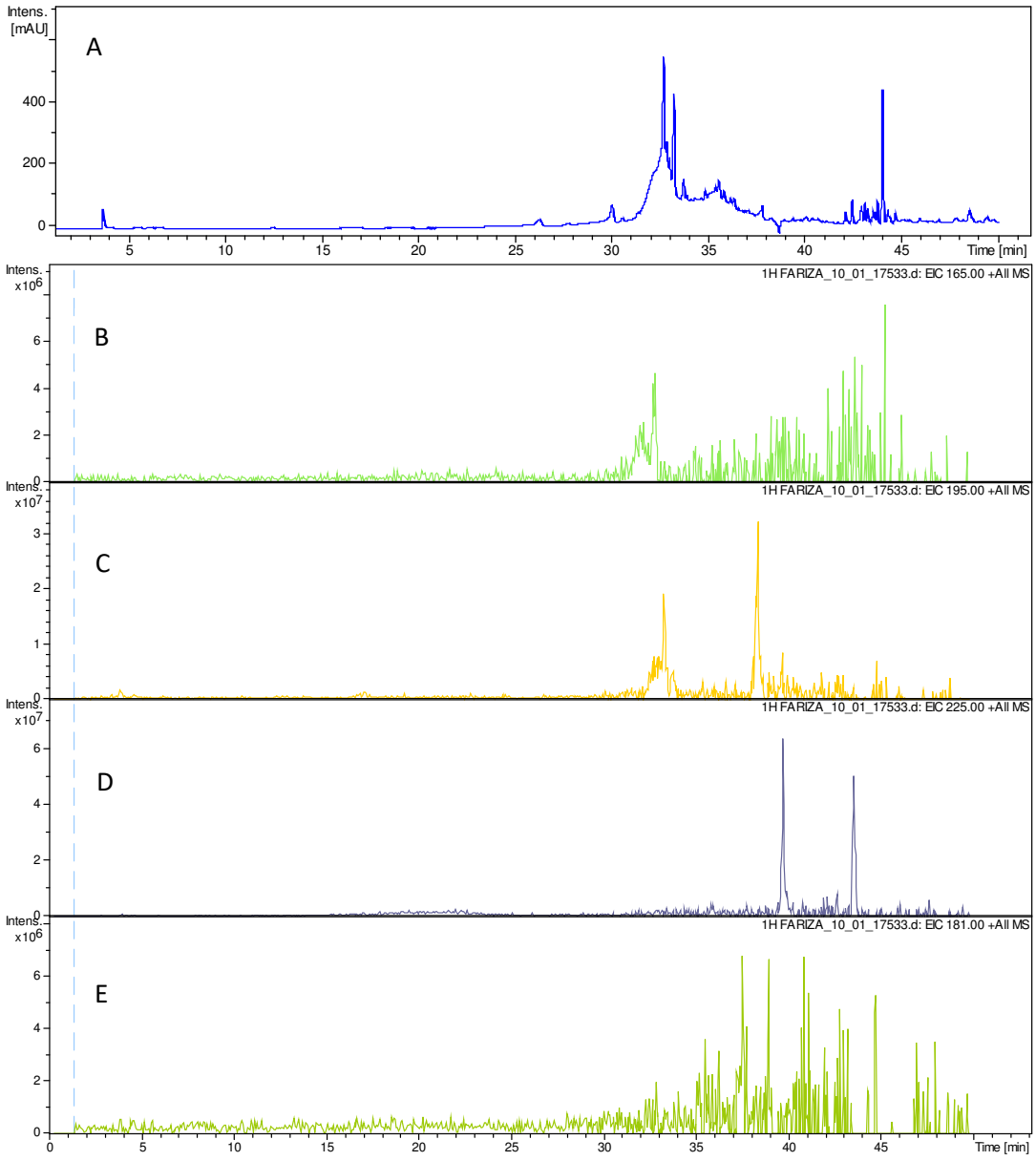

Figure 48: UV (at 280 nm) and extracted ion chromatograms from LCMS for the possible hydroxycinnamic acids released from NaOH pretreatment.

A, total absorbance at 280 nm; B, EIC at m/z 165 (p-coumaric acid); C, EIC at m/z 195 (ferulic acid); D, EIC at m/z 225 (sinapic acid); E, EIC at m/z 181 (caffeic acid).

According to Buranov and Mazza, alkali-labile ester linkages involving arabinose predominate in the Gramineae family, which are monocotyledonous flowering plants, including cereal producing grasses [9]. Due to this, 50% of the total phenolics in the aforementioned plant tissues can be easily detached with NaOH even at ambient temperature.

Following the pre-treatment of milled wheat straw with NaOH, approximately 2 mL of the slurry was separated by centrifugation at 10000 rpm for 5 minutes to obtain the clarified supernatant. A UV-Vis scan for wavelength 200-400 nm was done using Cary 50 spectrophotometer to observe any possible reaction of the aliquot before and after the addition of phenolic acid decarboxylase (PAD).

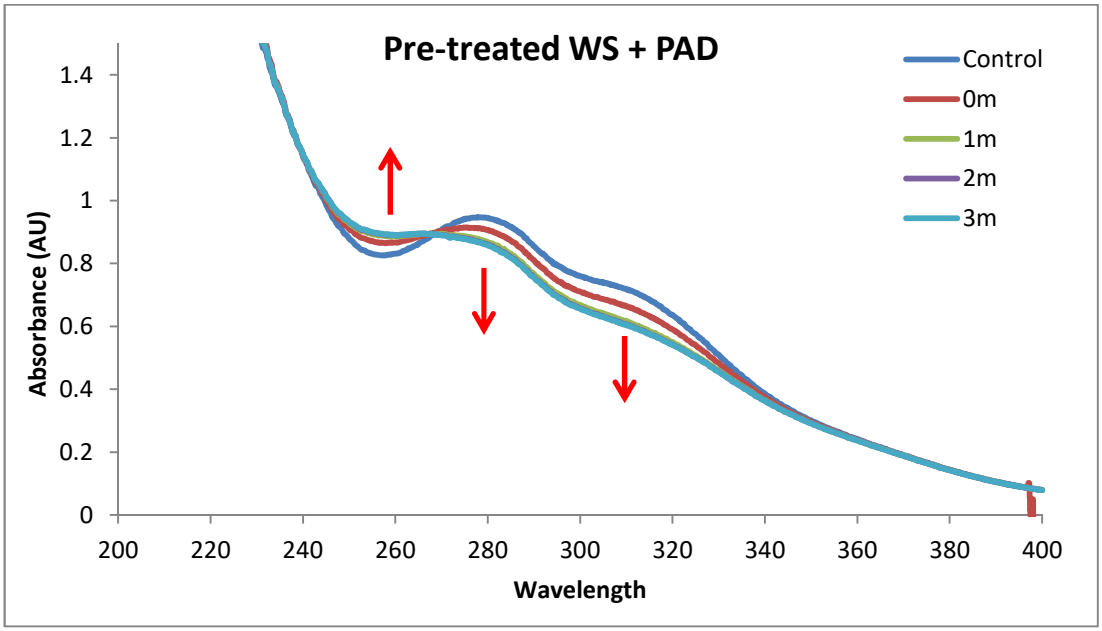

Figure 49: Reaction of purified phenolic acid decarboxylase with NaOH pre-treated wheat straw slurry

Figure 49 above illustrates the reaction spectrum of which 'control' was the NaOH treated supernatant showing the maximum absorption at 280 nm, with a shoulder at 310 nm, similar to earlier UV-Vis spectra of hydroxycinnamic acids (see Chapter 2).

Upon addition of the enzyme (0 m), the peak at 280 nm gradually declines by 1 min interval, followed by a slight increase of absorbance close to 260 nm region consistent with a reaction catalysed by PAD.

To further investigate, several strains of *R.jostii* (RHA1 wild type, RHA1 and RHA45 with *padC* insert), have been cultured in 50 mL M9 minimal media containing 1 g wheat straw, pre-treated with 0.125 M NaOH for 1 hour (then neautralised with HCl), supplemented with 0.2% (w/v) glucose. For both RHA1 and RHA045 cultures that carried plasmid construct, 35 µg/mL chloramphenicol and 1 µg/mL thiostrepton were added as resistance marker and inducer. Incubation was at 30°C in orbital shaker. Aliquots sampled on daily basis starting from 24 hours after the inoculation were used to monitor cell growth, as well as for analysis by reversed phase HPLC to check the metabolites produced.

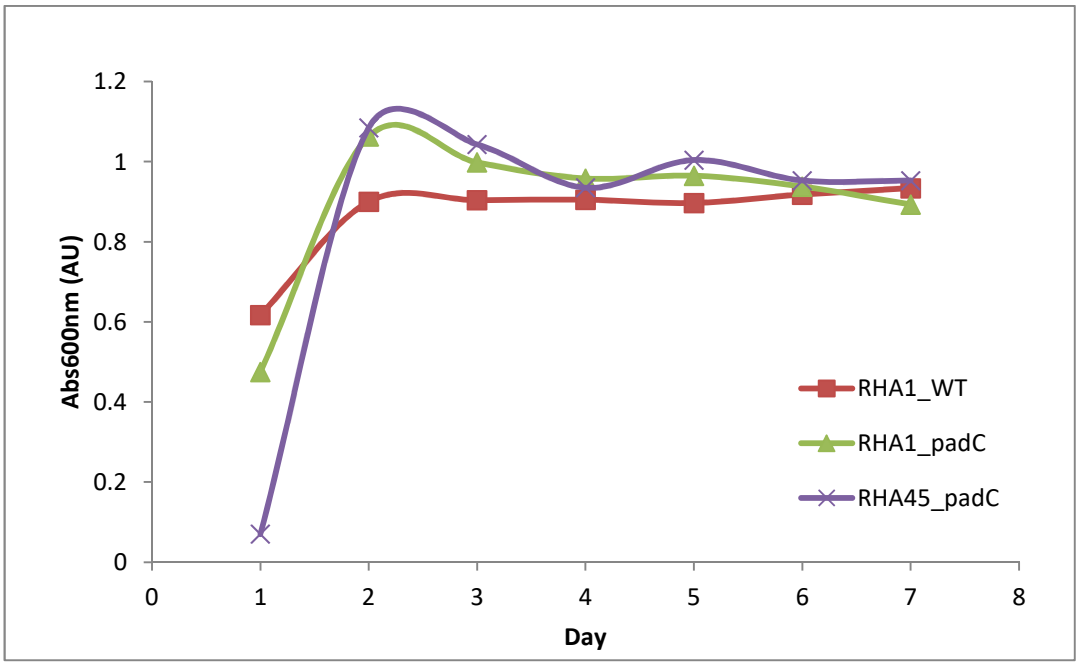

Figure 50: Growth profile of *Rhodococcus jostii* with and without *padC* construct in NaOH treated wheat straw media measured at 600 nm

As depicted in Figure 50, all three variants of *R.jostii* grew well in the pre-treated M9/wheat straw media, surpassing the initial log phase on the second day of fermentation. After that, due to glucose exhaustion, stationary absorbance at 600 nm was seen for the wild type variant until the end of fermentation. However for those that contained *padC* plasmid construct, a drop in A_{600nm} was observed between the second and fourth day, followed by stationary A_{600nm} afterwards.

For each culture, samples taken from day 1, 3, 5 and 8 of the fermentation were analysed. Extraction was done with ethyl acetate and then reconstituted with methanol. RP-HPLC was carried out with 100 µL sample injected, using the same gradient as described earlier (in Section 3.1) and monitored at 260 nm. Analyses of the resulting metabolites were compared against the retention time of authentic compounds of the hydroxycinnamic acids, and 4-vinylguaiacol.

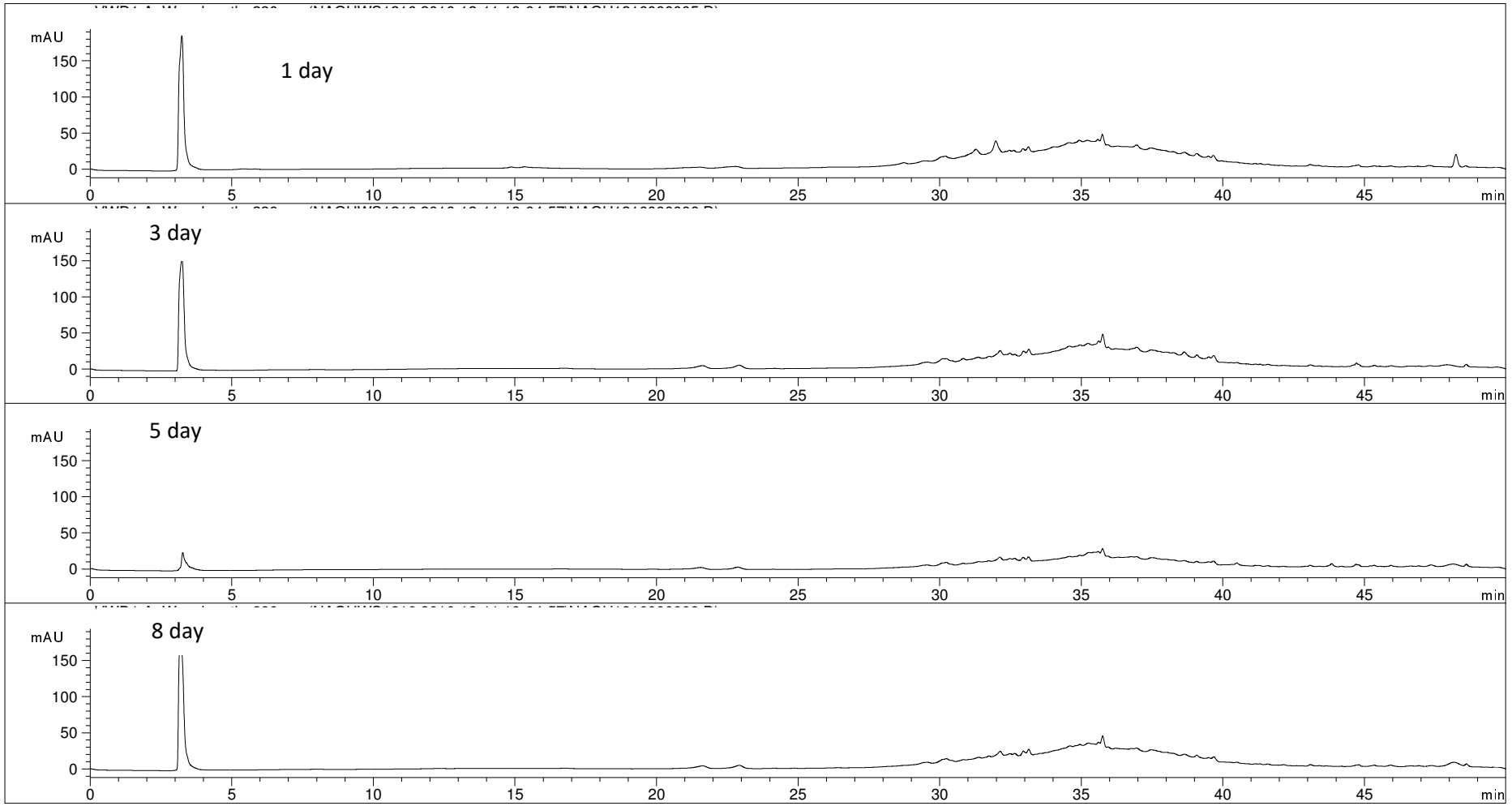

Figure 51: HPLC trace for incubation of *R.jostii* RHA1 wild type in pre-treated wheat straw medium

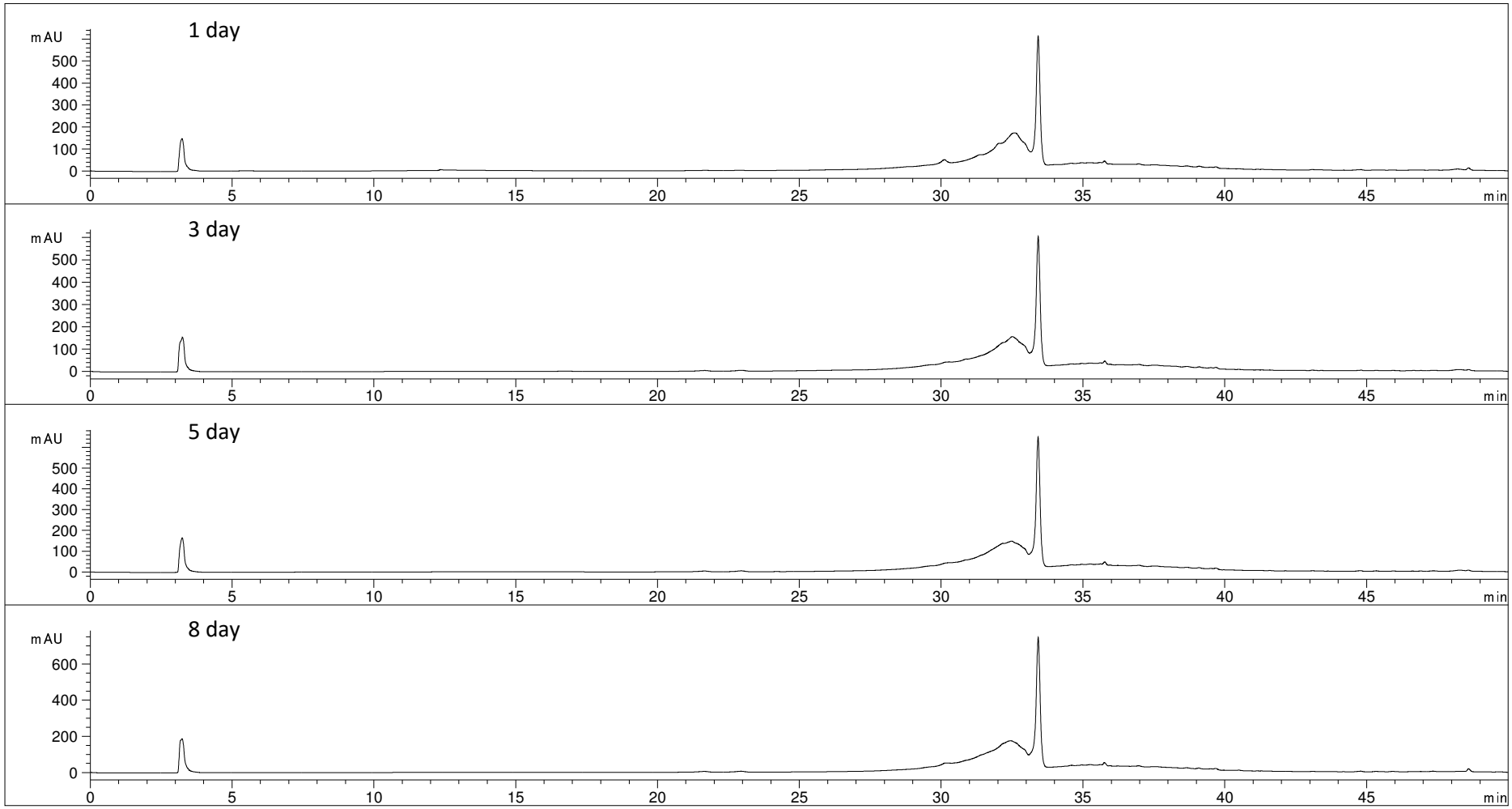

Figure 52: HPLC trace for incubation of *R.jostii* RHA1 (pTipQC2_*padC*) construct in pre-treated wheat straw medium

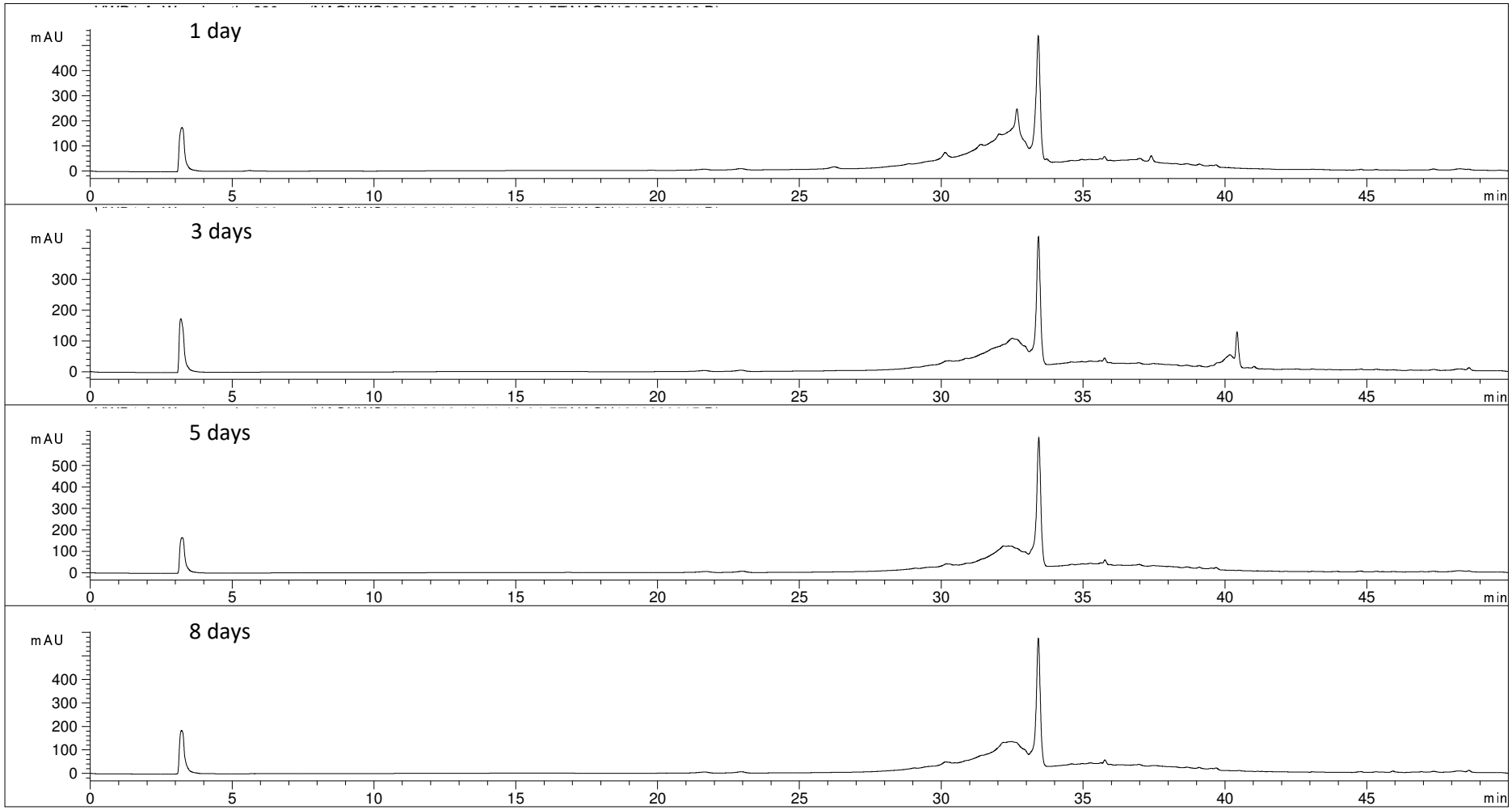

Figure 53: HPLC trace for incubation of *R.jostii* RHA045 (pTipQC2_*padC*) construct in pre-treated wheat straw medium

Although *R.jostii* RHA1 was known to degrade lignin through the action of extracellular esterases and Dyp type peroxidases [187], no clear peak was observed from the wild type bacterium fermentation with the pre-treated slurry. Only a broad peak was observed from minute 30 to 40 of the chromatogram (see Figure 51) signifying a various mixture of many nearly hydrophobic compounds.

Both the RHA1 and RHA045 bacteria that contain the PadC construct however, showed a sharp peak at RT 33.4 min (Figure 52 and 53 respectively), consistent with the presence of ferulic acid. Unfortunately, they were not anywhere near to that of any substituted mono-styrene product at all (RT 37 min). The 3 day sample for RHA045 showed a small peak at RT 40.4 min which could perhaps be mono-styrene product. However, after 3 days, this peak was no longer observed. A similar phenomenon has been reported before by Kang *et al*., with a similar *padC* gene construct overexpressed in *E.coli* [138]. The peak that they have initially detected in the early fermentation period matching the 4-vinylguaiacol standard disappeared towards the end of fermentation period. The reason was not explained, but the possibility of a further reaction within the culture media with the live cells is endless.

To summarise, the overexpression of phenolic acid decarboxylase in *R.jostii* host was unable to accumulate the desired substituted mono-styrene 4-vinylguaiacol when cultured in lignocellulose medium (wheat straw). The bioconversion showed some accumulation of ferulic acid; however, it was not high enough concentration to produce 4-vinylguaiacol using PAD. This is due to PAD having high K_m value (1.68 mM) for ferulic acid (see Section 2.4). The overexpression of PAD by RHA045 mutant for example, only managed to accumulate 81 mg/L ferulic acid, which was an equivalent of 0.42 mM. Nevertheless, this aim was achievable when using pure ferulic acid in a controlled amount, as seen in Section 3.2.

Pre-treatment with NaOH was able to break up the rigidity of lignocellulose structure by hydrolysing the alkali-labile ester bonds connecting lignin to hemicellulose and linkages. This provides accessibility for extracellular enzymes to act on them and allow its valorisation into value added products. Milling the wheat straw is already considered as an initial mechanical pre-treatment since it breaks the original structure to increase surface area of further reaction. A combination of these mechanical, thermal (autoclave) and chemical (NaOH) pre-treatment were, however, not able to accumulate enough hydroxycinnamic acid to generate the substituted styrene bioproduct from wheat straw using phenolic acid decarboxylase.

CHAPTER 4 ENZYMATIC POLYMERISATION OF 4-VINYLGUAIACOL

4.1 Introduction

The conventional production of polystyrene begins with the addition of initiator such as AIBN (2,2′-Azobis(2-methylpropionitrile)) into styrene monomer in the absence of oxygen to undergo radical polymerisation.

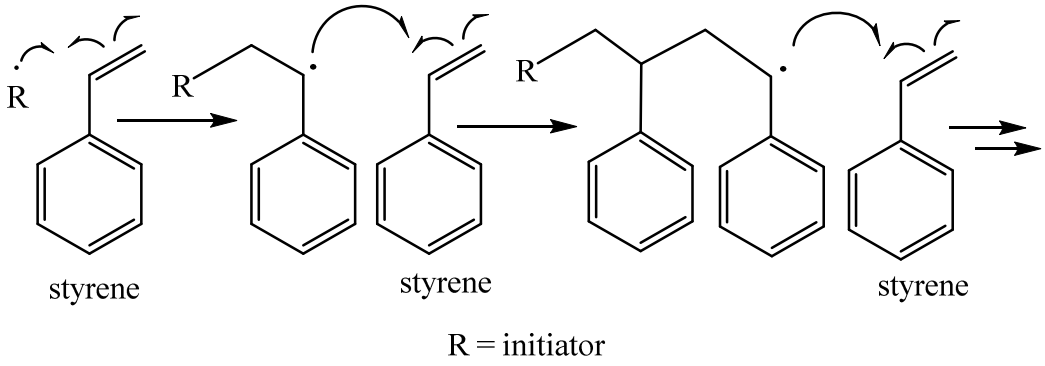

Figure 54: Radical polymerisation of styrene

This process is mostly based on the use of petrochemical and some reactions could release massive amount of heat. Since usage of crop residues is able to provide a renewable alternative, the potential to convert lignin based phenolic molecules into substituted polystyrene has been investigated. For example, polystyrene mimics such as polyethylene ferulate and poly[(caffeic acid)-co-(4-coumaric acid)]. They have been successfully synthesised chemically from ferulic acid, caffeic acid and p-coumaric acid at temperature ranging from 150 to 250 °C in the absence of oxygen [82], [102], [188], [189]. Alternatively, this process can actually be done

enzymatically with the use of phenolic acid decarboxylase (PAD), thus, eliminating the requirement of high temperature and is energy efficient.

Among the proposed use of this phenolate based substituted styrene is to serve as a formaldehyde-free adhesive. This is based on the adhesive ability of a catechol pendant group, mimicking the mussel foot protein that allows attachment on any surface [167], [174], [190]–[194]. Since PAD accepts both ferulic acid and caffeic acid as substrates, both 4-vinylguaiacol and 4-vinylcatechol could potentially be generated, and used as substrates for polymerisation. Incorporation of 4-vinylguaiacol, as well as 4-vinylcatechol may lessen the cross-linking reaction and prevent insolubility [191]. In order to complement the enzymatic decarboxylation of ferulic acid, we wished to find an enzymatic method for polymerisation as suggested in Figure 55.

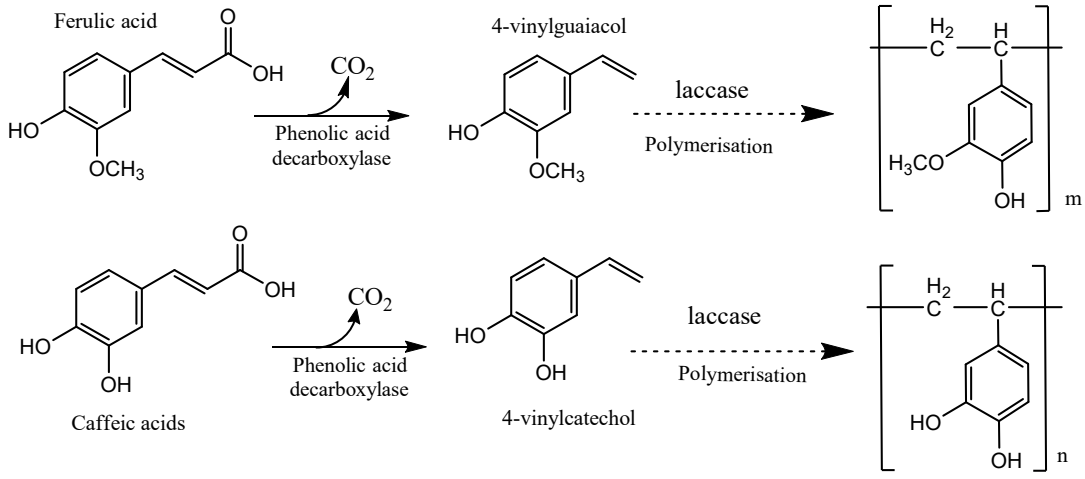

Figure 55: Bioconversion of ferulic acid and caffeic acid into substituted polystyrene

Two enzyme classes dominate the field of biocatalytic radical polymerisation: peroxidases (EC 1.11.1) and laccases (EC 1.10.3.2). Though quite different with

respect to catalytic mechanism and active site structure, both enzyme classes predominantly catalyse hydrogen abstraction reactions yielding radical species to initiate the polymerisation reaction [148]. For instance, a laccase-catalysed reaction was used for the polymerisation of catechol monomers for poly-catechol synthesis [151] with application in wood composites, fiber bonding, laminates, coatings, and adhesives.

Laccase mediated polymerisation has been demonstrated on fractionated lignin, lignosulphonates, and lignin model compounds not long ago. According to Areskogh *et al.,* the ability of laccase to cross-link lignin molecules is through its oxidising action towards lignin model compounds (such as vanillyl alcohol and syringyl alcohol) bearing the phenolic end groups. Radical coupling predominantly formed 5-5' and 4-O-5' bonds which served as the initiation point of polymerisation, just like the naturally occurring bonds within lignin (as seen in Figure 4). Their resulting oligomers reached a molecular weight between 800 to 1250 g/mol [156]. They have also investigated the polymerisation of lignosulphonates. Higher concentration of lignosulphonates reacted with *Trametes villosa* laccase yielded in an increase of molecular weight up to 20-fold within 4 hours of reaction [146].

Besides lignosulphonates, dissolved Kraft lignin has also been used to act as substrate for laccase mediated polymerisation. Gouveia *et al*., observed a molecular weight increase by a factor of 4 to 21 with 99032 g/mol being the highest MW recorded after incubation with Novozyme's *Myceliophthora thermophile* laccase [195].

Therefore, this chapter is the continuation of the work described in Chapter 2 where the conversion of ferulic acid and caffeic acid into their respective styrenic monomers, 4-vinylguaiacol and 4-vinylcatechol has been carried out. Using laccase, a polymerisation of these styrene monomers are evaluated and compared against references with similar polymer type.

4.2 Enzyme catalysed polymerisation

Following the experiment described in Section 2.2, enzymatic reaction of 0.1 mM ferulic acid or caffeic acid with phenolic acid decarboxylase was carried out until their products; 4-vinylguaiacol and 4-vinylcatechol reached their respective maximum absorbance for about 15 minutes. To that 1 mL reaction mixture, 7.2 μg (0.15 U) of *Trametes versicolor* laccase (Sigma) was added to the cuvette to initiate the radical polymerisation.

The graph in Figure 56 (a) and (b) shows the gradual decrease of absorbance 1-10 minutes after the addition of laccase. It was observed that the 4-vinylguaiacol peak at 260 nm slowly diminished for the first 3 min, and then started shifting to form a broad new peak, with a shoulder at 283 nm. While for the reaction of laccase with the decarboxylation product of caffeic acid, namely 4-vinylcatechol, a steady decrease of peak absorbance around the 280 nm region was simultaneously joined by the increase of a broad, less intense peak in the visible region between 380 – 450 nm.

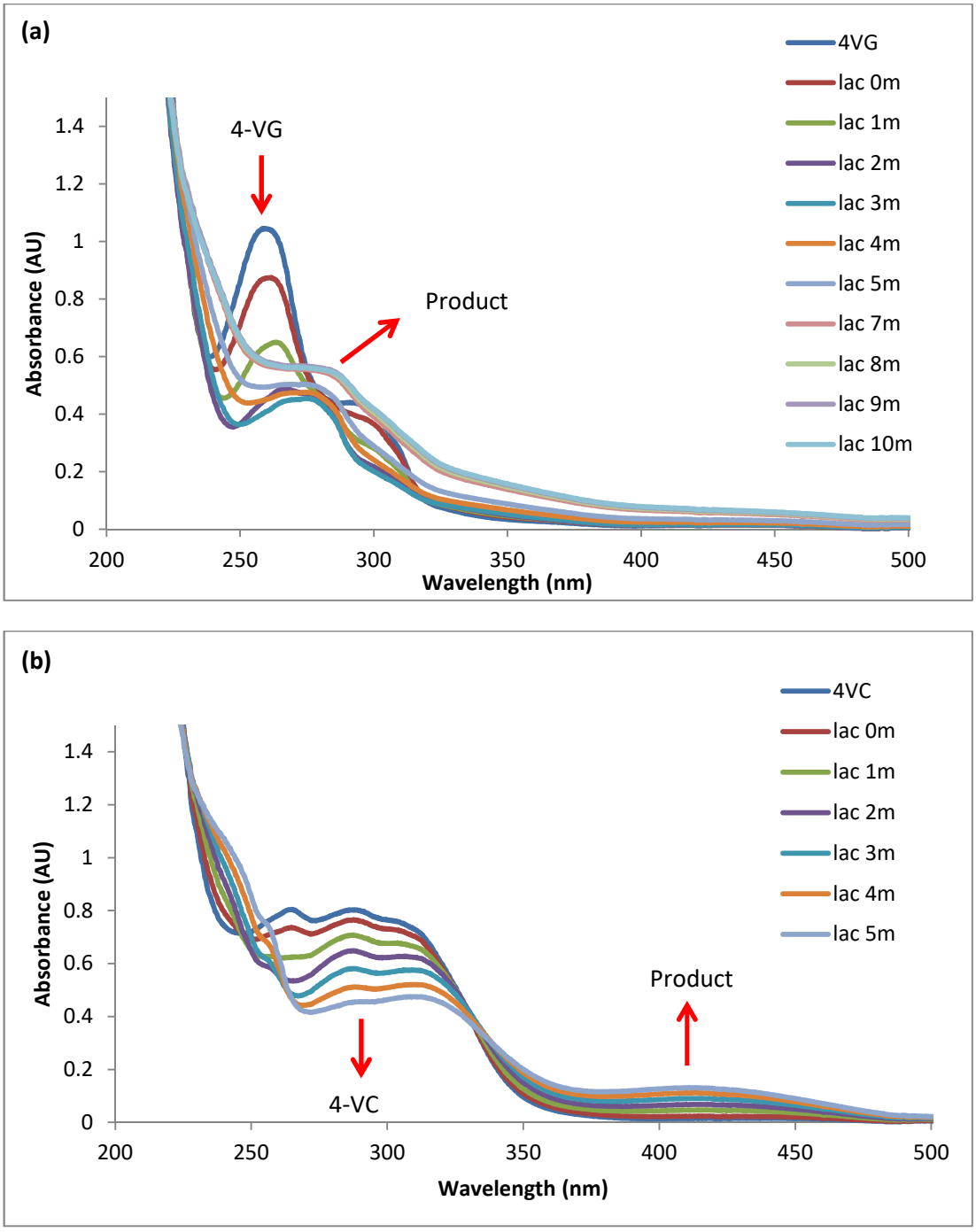

Figure 56: Decrease of absorbance for the (a) 4-vinylguaiacol, 4VG and (b) 4-vinylcatechol, 4VC peaks at 1 – 10 (or 5) min after addition of *T.versicolor* laccase

According to Pollegioni *et al.*, laccase activity is pH dependent and especially for phenolic substrates, the optimal pH follows a bell-curve with peak at acidic region

[59]. Based on this, the whole reaction was maintained in a mildly acidic environment in pH 5.0 of 50 mM sodium acetate buffer to optimise laccase reaction.

To scale up, a total of 50 mL reaction with each enzyme-substrate mixture was made up in amber vials. Each contained 10 mM substrate in 50 mM sodium acetate buffer at pH 5.0, added with a total of 1.1 mg PAD which was then left standing with occasional inversion at room temperature for 24 hours. After that, 100 μL of 11.52 U/mL laccase (Sigma) was added and the mixture was further incubated for 2 days at room temperature. From initial colourless and homogenous solutions, both reaction mixtures were found to form precipitates, orange-yellow for 4-vinylguaiacol and black for 4-vinylcatechol, as represented by Figure 57.

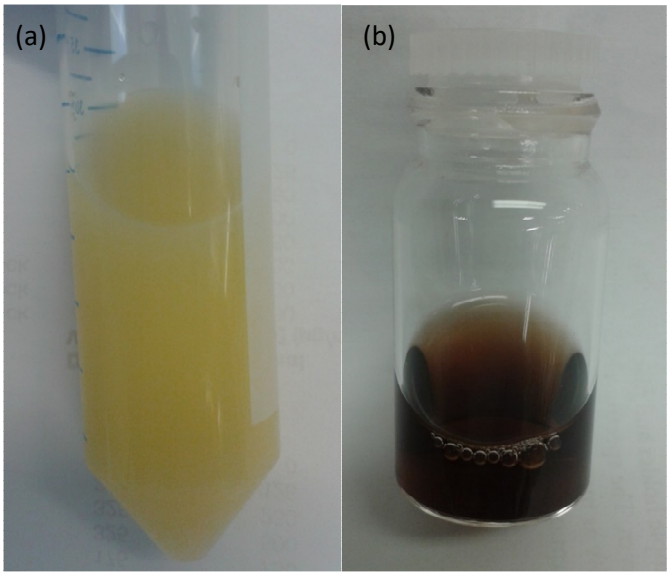

Figure 57: the formation of precipitates for polymerisation reaction of laccase with the enzymatically generated (a) 4-vinylguaiacol and (b) 4-vinylcatechol

Each mixture were then transferred into centrifuge tube and spun down at 5000 rpm for 30 minutes. The retained pellet was lyophilised to give a powder of 60 mg

weight. It was observed that the resulting poly(4-vinylguaiacol) precipitate did not dissolve in water or methanol. The polymerisation product from 4-vinylcatechol was also absolutely insoluble in water, as well as in many other organic solvents including methanol, THF, DMF and DMSO, even with sonication.

To determine the molecular weight of the polymerised material, the poly(4-vinylguaiacol) precipitate was solubilised in THF, followed by a filtration through 0.2 µm membrane prior to analysis by gel permeation chromatography (GPC), carried out using Agilent 390-MDS system, and eluted with THF over 30 min run. Calibration was set against narrow polystyrene molecular weight standard in a range of 157 to 3.0×10^6 g/mol.

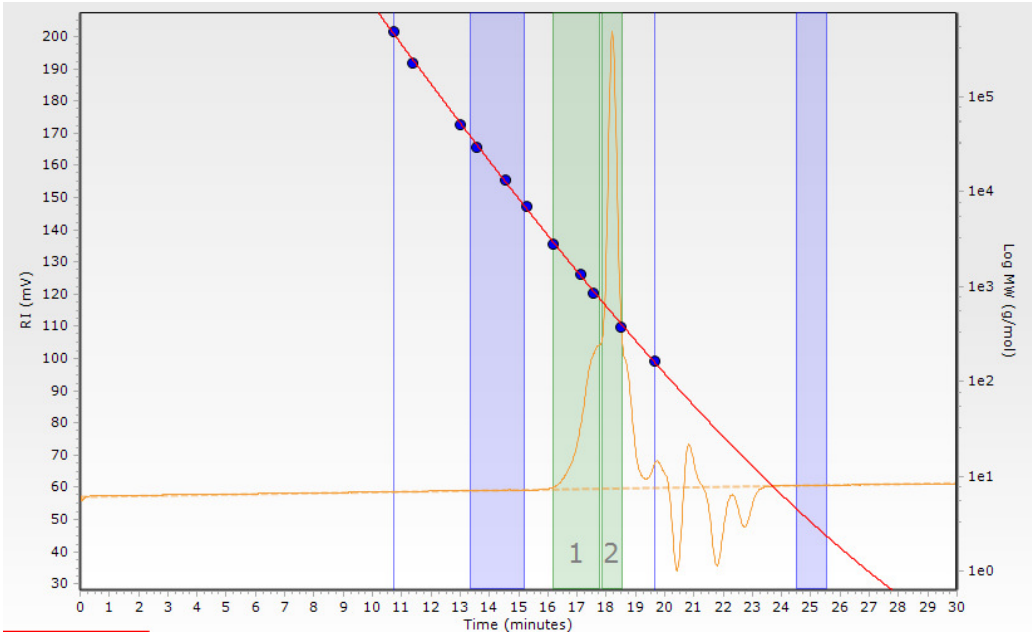

Figure 58: GPC trace of enzymatically generated 4-vinylguaiacol after reaction with laccase

Figure 58 depicts the chromatogram of the poly(4-vinylguaiacol) which is shown against the polystyrene calibration curve. The major peak is at a retention time of 18 min (peak 2) with MW 515 g/mol (PD 1.02) which is probably a trimer. A smaller

peak 1 was observed with MW 1075 g/mol, corresponding to 6 monomer units. This is very low MW compared with the chemically synthesised poly(4-vinylguaiacol), MW 451000 g/mol and poly(4-vinylphenol), MW 704000 g/mol reported by Hatakeyama in 2009 [196]. Since there was some insoluble residue recovered from the filtration membrane, the GPC chromatogram actually represents the soluble fraction of the polymer that managed to pass through the 0.2 µm filter pore.

To further investigate, a similar reaction component was repeated, under a balloon containing 100% oxygen. It is known that laccase uses molecular oxygen for catalysis, so, the effect of this towards the polymerisation would be tested.

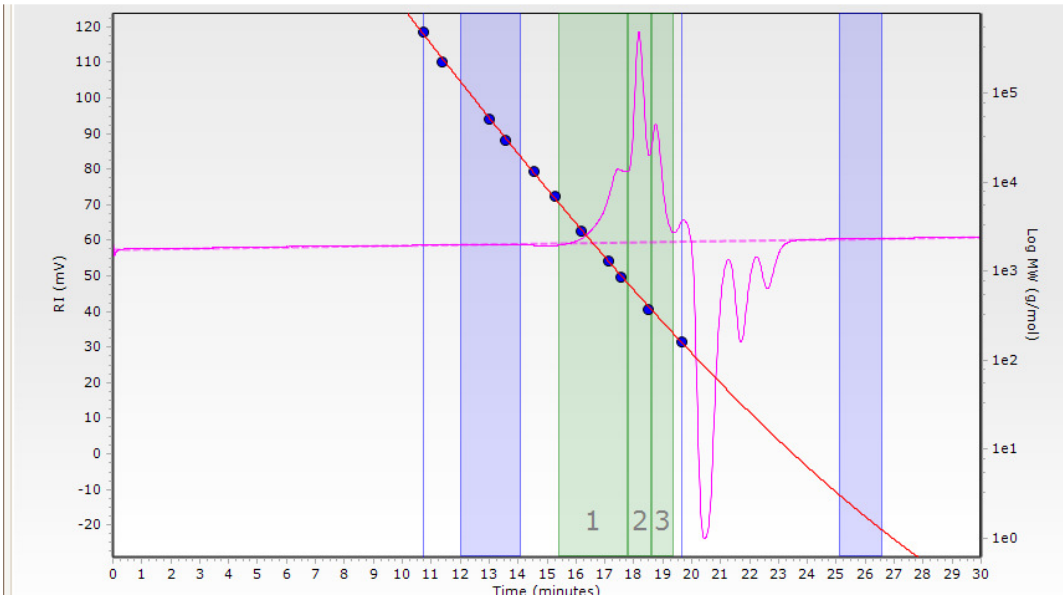

Figure 59: GPC trace for polymerised of 4-vinylguaiacol with laccase supplied with oxygen

The GPC trace of the product, shown in Figure 59, is similar to that obtained previously. The major peak 2 at 18 min corresponds to MW 515 g/mol (PDI 1.02). The highest molecular weight peak (peak 1) corresponds to 1190 g/mol and the amount generated was 50 mg. A similar polymerisation experiment with laccase

duplicated with the commercially available 4-vinylguaiacol (Sigma) also showed a very similar molecular weight. Therefore, we can say that the product in these cases was actually an oligomer, of molecular weight 500 – 1200 g/mol.

For the poly(4-vinylcatechol), it was not possible to determine the molecular weight due to insolubility in THF. Isakova *et al*., as well as Leibig and co-workers have reported the challenges they faced to synthesise 4-vinylcatechol since the exposed OH groups are prone to cross-linking and led to undesired side reactions and insolubility [175], [197]. They had to protect the hydroxyl groups in order to allow polymerisation to occur.

The experiment was repeated with 500 mL total volume of 10 mM ferulic acid starting material. All other aspects were scaled up accordingly except, to maximise the precipitation, the resulting 4-vinylguaiacol mixture was placed into ten 50 mL amber vials, and reacted with laccase in a 30°C shaking incubator. After 2 days, precipitate was collected and freeze-dried. When applied to GPC, a similar result was obtained. However, a cloudy and sticky layer coating the inside of the vial was found in 2 of out of the 10 reaction vessel as shown in Figure 60.

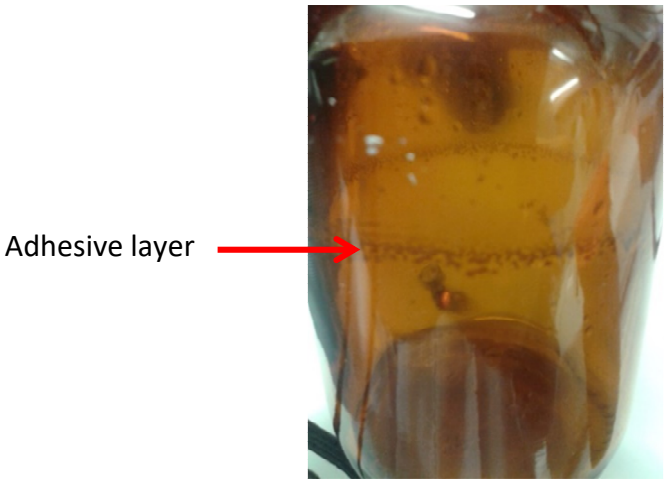

Figure 60: Adhesive layer found inside 50 mL reaction vial of poly(4-vinylguaiacol)

Since it was difficult to remove, the layer was solubilised in THF and tested with GPC, where it showed a broad peak with a higher molecular weight entity at 48496 g/mol (PD 3.0) as depicted by peak 1 in Figure 61. The amount of this adhesive layer was small compared to the precipitate recovered, however, it was interesting that an adhesive polymer of poly(4-vinylguaiacol) appeared to have been formed.

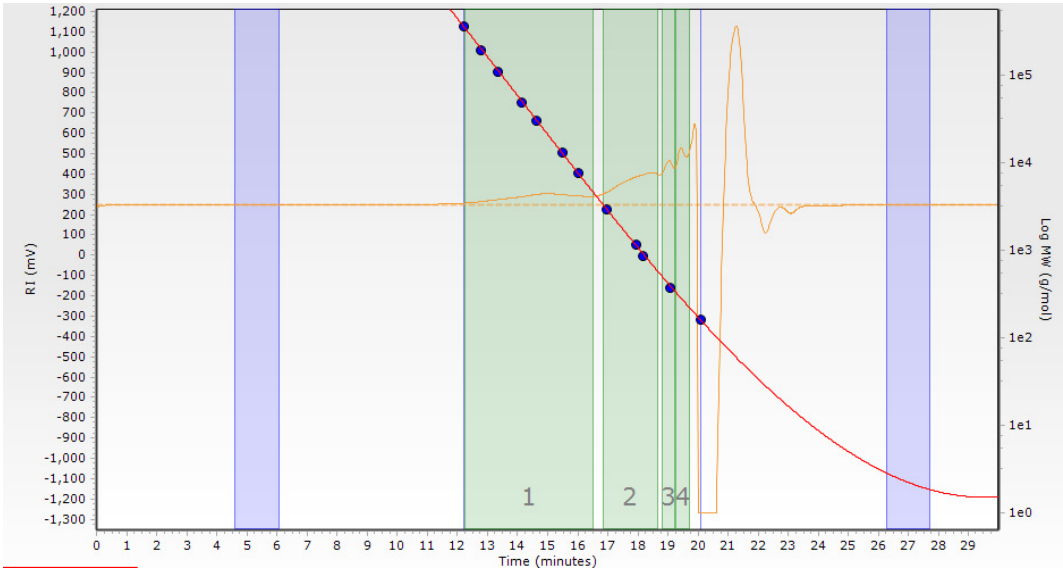

Figure 61: GPC trace for polymerised 4-vinylguaiacol adhesive layer formed inside the reaction vial

Besides laccase, polymerisation of 4-vinylguaiacol was also tested using 0.2 mg/mL horseradish peroxidase type IV (Sigma) in the presence of 0.5 mM H_2O_2 and 0.72 mg/mL DypB peroxidase from *Pseudomonas fluorescence* PF5 (referred to as Dyp324, courtesy of Dr Rahman Rahmanpour) at room temperature. No product precipitation was observed when these enzymes were used. Therefore, extraction with ethyl acetate was performed to recover the organic material from the aqueous mixture, evaporated, and reconstituted in THF prior to GPC. The poly(4-vinylguaiacol) generated showed similar molecular weight pattern, i.e: an oligomer with 4 to 7 repeated units.

4.3 Co-polymerisation

Since polymerising 4-vinylcatechol resulted in an insoluble mass, an experiment was set up to co-polymerise 4-vinylcatechol with 4-vinylguaiacol.

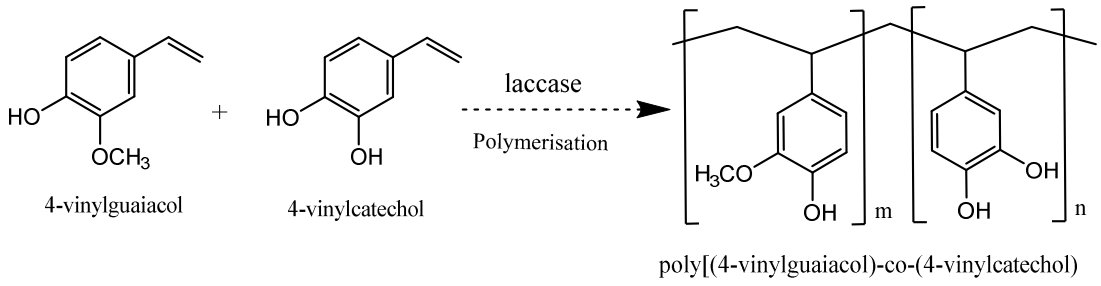

Figure 62: Co-polymerisation 4-vinylcatechol with 4-vinylguaiacol

Co-polymerisation was carried out by varying the molar ratio of caffeic acid and ferulic acid reaction with phenolic acid decarboxylase. The concentration of the starting materials and the molecular weight of the resulting polymers are listed in Table 4.

Table 4: Monomer concentration and the molecular weight of the resulting co-polymer, measured by GPC

Total volume (ml)	Monomer's concentration (mM)		Molar ratio	Temperature (°C)	Yield (mg)	MW (g/mol)	PD
	Ferulic acid	Caffeic acid					
20	5	5	1:1	RT (23)	27*	ND	-
20	7.5	2.5	3:1	RT	33	712	1.11
50	10	1	10:1	30	20	1352	1.04
50	10	2	5:1	30	20	703	1.16
50	10	5	2:1	30	40	583	1.07
500	10	5	2:1	30	291	543	1.06

ND Not determined due to polymer insolubility
*obtained by extraction with ethyl acetate

It was observed that the molecular weight of the co-polymers were still mostly below 1000 g/mol. A higher concentration of 4-vinylguaiacol (from the initial higher concentration of ferulic acid) was showed to produce slightly higher molecular weight of co-polymer. At the same time, co-polymers with a higher content of 4-vinylcatechol always resulted in insoluble residues. Synthetic polymerisation with monomer containing catechol pendant group [197], [198], found that the polymer product were very prone to cross-linking making it insoluble in organic solvent, causing difficulty for analysis. Only reactions carried out in -20°C, with protection of both hydroxyl groups were able to produce a soluble polymer after deprotection.

4.4 Scanning electron microscopy (SEM)

To physically characterise the polymer, scanning electron miscroscopy method was employed. The morphology of the polymer was observed by the field emission scanning electron microscope (Zeiss SUPRA 55-VP). The freeze-dried samples of poly(4-vinylguaiacol) and the 2:1 poly[(4-vinylguaiacol)-co-(4-vinylcatechol)] were each mounted on a conducting double-sided carbon tape and inserted into a vacuumed chamber inside the scanning electron microscope (SEM). The images in Figure 63 show that the resulting polymer particles have a variety of sizes and shapes, which mostly are spherical in shape, and the grain structure is comparable to the synthetic polystyrene particles reported by Hornig *et al*., [199].

Since the size were not uniform, some particles even reach 1 μm in diameter, and were clustered together especially for the co-polymer, as shown in Figure 63 (b). Larger particle size also meant that the insoluble polymer in THF prior to GPC was unable to pass through the filter membrane with 0.2 μm pore. This explains why the MW distribution was not exactly representing all the polymer samples.

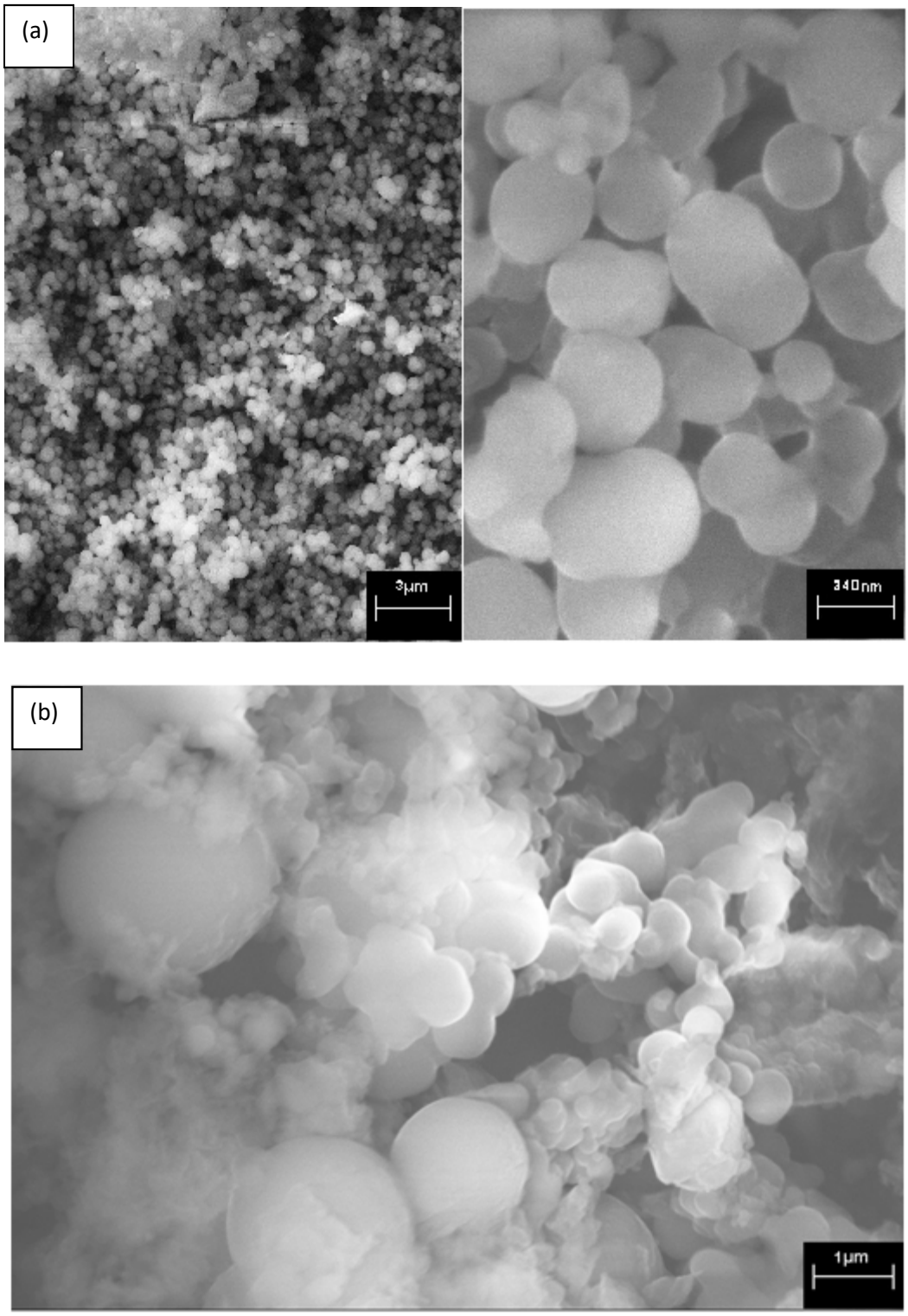

Figure 63: SEM images of (a) poly(4-vinylguaiacol) and (b) 2:1 poly[(4VG)-co-(4VC)] co-polymer

4.5 Determination of adhesives tensile lap-shear strength

We wished to determine the capability of the polymer to act as potential adhesive, by testing it against aluminium substrates. Meredith and co-workers have optimised the method to perform lap shear test for a biomimetic polymer poly[(3,4-dihydroxystyrene)-co-styrene] that they chemically synthesised and the best adhesion obtained was 11 MPa, surprisingly superior than Loctite™ cyanoacrylate glue (at 5 MPa) [191]. Their experimental method were partly developed from Cha *et al*., and Yang *et al*., in which they tested a recombinant mussel adhesive protein using aluminium adherends mixed with periodate as cross-linking agent [194], [200]. The minimum amount of material needed for testing was 0.3 mg/mL solution. Therefore, the testing was performed only on reactions that were scaled up, which were the poly(4-vinylguaiacol) and the 2:1 ratio of poly[(4-vinylguaiacol)-co-(4-vinylcatechol)]. Combining these methods, a protocol for the lap shear experiment is as follows.

Aluminium plates were cut into 100 mm (L) x 25 mm (W) dimension with each plate having a 0.8 mm thickness. It was soaked for 15 min each in hexane, acetone and ethanol and allowed to air dry under the flow hood at room temperature. Then, each polymer sample was mixed with 1:1 DCM/acetone to form 0.3 mg/mL paste and applied onto each aluminium plate (67.5 μL each side), to equally covering an area of 25 mm x 25 mm which became the shear area. Straight afterwards, 15 μL (50 mM final concentration) of freshly prepared 500 mM $Na(IO)_4$ solution was dropped onto each adherend, and the shear area was joined together immediately, supported by a 51 mm (L) binder clip (see Figure 64 (a)). They were allowed to cure 30 min at room temperature before incubation in a 37°C oven for 24 hours. The bonding was

initially observed by clipping one end of the adherend with a retort stand, and the poly(4-vinylguaiacol) showed a successful attachment between the two bonded assemblies as shown in Figure 64 (b).

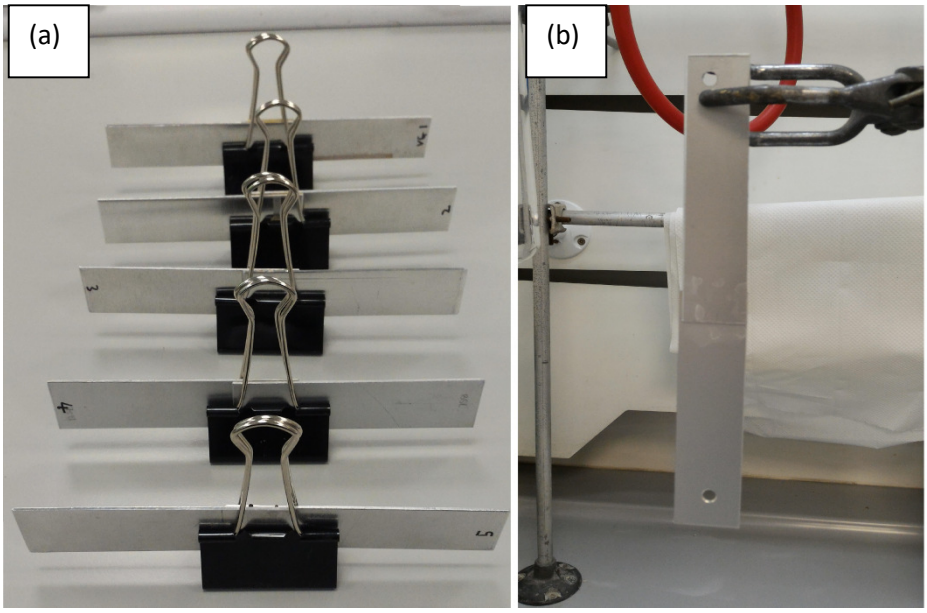

Figure 64: Single lap shear assembly performed on aluminium using the enzymatically synthesised polymers.
(a) Assembled aluminium plates bound with binder clips; (b) assembly using poly(4-vinylguaiacol)

To follow up, a lap shear adhesion test was carried out using a tensile testing machine (Instron 3367; Instron, USA) with a 5000 N load cell. The bonded samples were held by two grips near the midpoint of the sample and pulled in opposite directions at a displacement rate of 0.25 mm/min. Figure 65 illustrates the schematic of sample arrangement for the lap shear test.

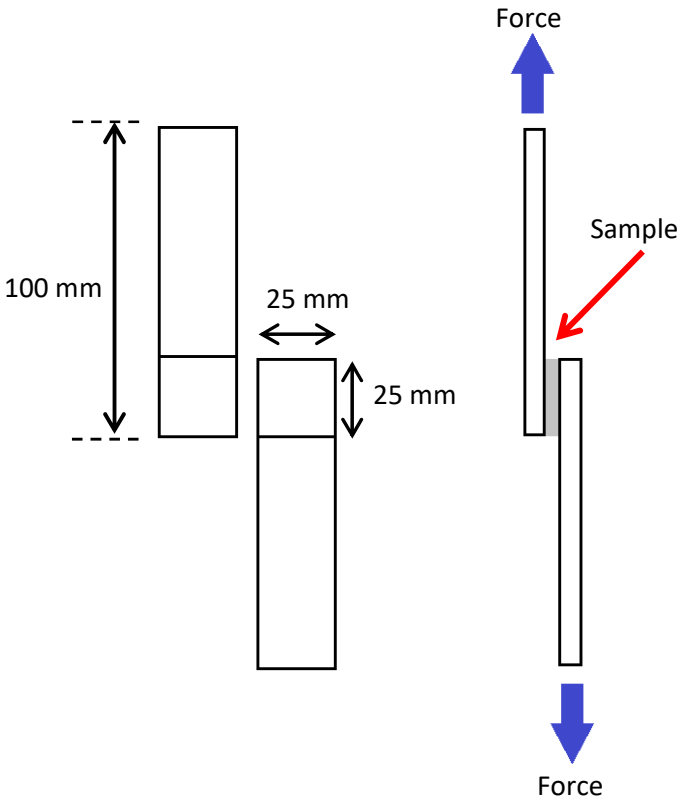

Figure 65: Schematic of sample for the adhesion strength test

The force and the displacement of the fixture were simultaneously monitored by the Instron Bluehill software connected to the machine. The shear strength in Newton (N) was obtained by plotting the maximum point of the extension (in mm) versus force, just prior to the joint's breaking point (see Figure 66). The adhesion force in Pascals (Pa) was calculated from the shear strength (N) divided by the overlap area (in m^2).

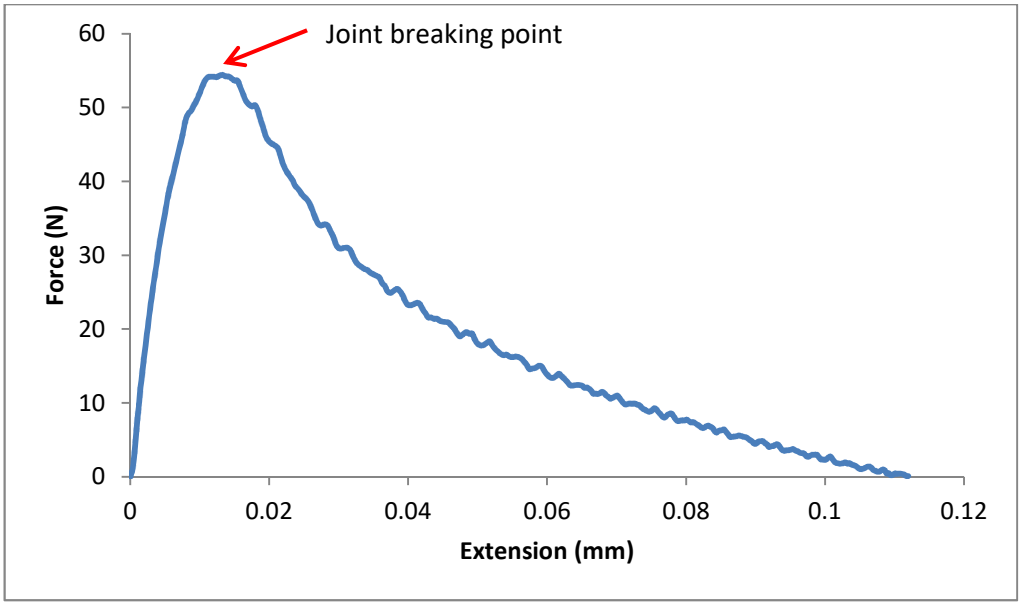

Figure 66: Force-extension curve of adhesion measurement for poly(4-vinylguaiacol). Peak of the curve shows the breaking point of the adhesive joint

Based on Figure 66, poly(4-vinylguaiacol) showed apparent adhesion towards the aluminium substrates as seen from the positive slope generated while the shearing force was increased gradually. The sudden drop of the curve indicated the breaking point due to fracture of bonded joints and its failure to carry out more loads.

Its co-polymer on the other hand, showed bonding failure since they were not sticking at all upon removal of the binder clip from the assembled adherends (see Figure 67). All the five replicates of poly[(4-vinylguaiacol)-co-(4-vinylcatechol)] and poly(4-vinylguaiacol) showed a mixture of adhesive and cohesive failure pattern towards the adherends.

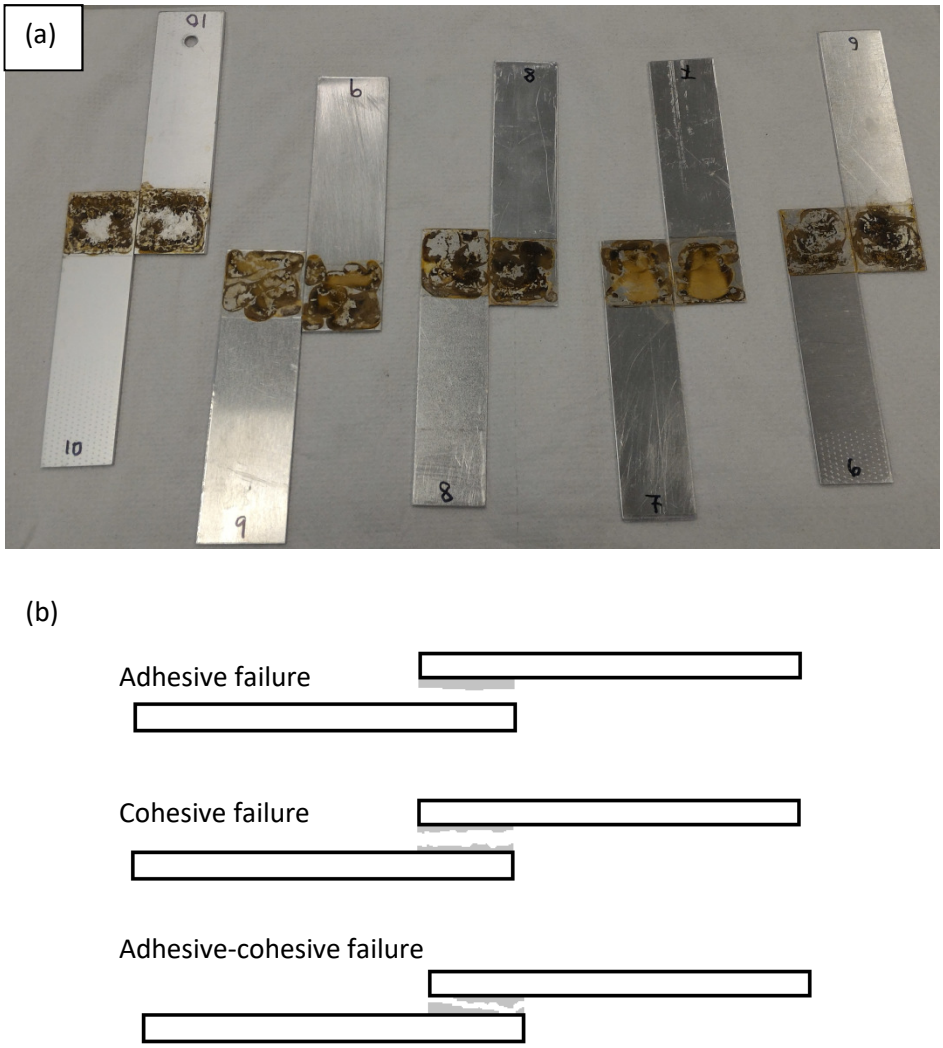

Figure 67: (a) Bonding failure poly[(4-vinylguaiacol)-co-(4-vinylcatechol)]; (b) Identification of bonding failure observed from pattern of adhesive breakage.

Table 5 listed the adhesion strength the polymer from the lap shear test, in comparison to other reported catechol-containing polymers as well as commercial glue. Adhesion strength of 0.09 MPa was recorded for poly(4-vinylguaiacol), and it was not determined for poly[(4-vinylguaiacol)-co-(4-vinylcatechol)] due to bonding failure prior to testing.

Table 5: Adhesion strength for selected polymers and commercial glue

Polymer	**Concentration (g/mL)**	**Curing temperature (°C)**	**Cross-linker**	**Adhesion strength (MPa)**	**Reference**
Poly(4-vinylguaiacol)	0.3	37	50 mM $NaIO_4$	0.09	This research
Poly[(4-vinylguaiacol)-co-(4-vinylcatechol)]	0.3	37	50 mM $NaIO_4$	ND	This research
Poly[(3,4-dihydroxymandelic acid)-co-(lactic acid)]	0.3	37	$[N(C_4H_9)_4](IO_4)$	2.6	[190]
Poly(lactic acid)	0.3	37	$[N(C_4H_9)_4](IO_4)$	0.21	[190]
Gorilla Glue (polyurethane)	0.3	37	$[N(C_4H_9)_4](IO_4)$	2.8	[190]
Poly[(4-vinylcatechol)-co-styrene][a]	0.3	37	$[N(C_4H_9)_4](IO_4)$	4.0	[191]
Poly[(4-vinylcatechol)-co-styrene][a]	1.2	55	-	11.0	[191]
Loctite Super Glue (ethylcyanoacrylate)	1.2	55	-	5.0	[191]
Modified fp-151[b]	0.26	45	500 mM $NaIO_4$	0.07	[194]
Modified fp-151[b]	0.26	45	50 mM $NaIO_4$	0.86	[194]

[a] Originally reported as poly[(3,4-dihydroxystyrene)-co-styrene]; contained 10% (w/w) $CaCO_3$ filler as reinforcing material and 1:3 cross-linker/catechol ratio
[b] Recombinant mussel adhesive protein, modified by converting tyrosine residues into *L*-3,4-dihydroxyphenylalanine groups
ND not determined

Kaneko *et al.*, explained that their synthetic co-polymerisation of caffeic acid with *p*-coumaric acid has created a high-performance and biodegradable plastic resins with high heat resistance (over 150°C) [188]. Besides that, they have also discovered the hyper-branched properties of the co-polymer due to the catechol groups at its chain-ends. An advantage of this is that this end group could produce strong interactions with the surfaces of various materials. For example, shear test on steel (100 mm (L) X 25 mm (W); 10 mm X 25 mm shear area) and glass (50 mm (L) X 50 mm (W); 10 mm X 50 mm shear area) substrates with the resin produced more than 9 MPa adhesion strength. However, in their case, the synthesis of the polymer and substrate binding prior to shear test were both done at 200°C temperature, which would be unsuitable for enzymatic polymerisation.

To summarise, polymerisation of 4-vinylguaiacol and 4-vinylcatechol generated from ferulic acid and caffeic acid have been carried out using *Trametes versicolor* laccase. Some of the resulting poly(4-vinylguaiacol) and its co-polymer were quite insoluble, leading to difficulty in determining the actual molecular weight. Some of the insoluble fraction that did not pass through the filtration membrane could be larger than 0.2 μm and this was proven by the SEM of the polymers. Poly(4-vinylguaiacol) showed adhesive property, and has been verified using single lap shear test. The co-polymers however, did not show adhesiveness, and were mostly insoluble.

CHAPTER 5 CONCLUSIONS

Research for renewable resource and alternative materials have been highly active these recent decades to decrease dependency towards fossil-based hydrocarbons. Among them is the work on conversion of waste products into value-added materials since it can reach two goals at the same time, 1) increase production of renewable material, 2) reduce build-up of waste, especially from agriculture industry. At the same time, consumers being more conscious on the Earth's wellbeing and maintaining sustainability has put mounting pressure on industries to produce more green alternatives for existing products.

Lignin is the most abundant natural aromatic resource in this biosphere. After harvesting agricultural crops, many of the residues remain underutilised. Wheat straw is known to contain ferulic acid. Previous research within the group has shown that *Rhodococcus jostii* RHA1 grown in minimal media containing milled wheat straw have been able to accumulate ferulic acid.

In this work, an enzymatic conversion of ferulic acid into 4-vinylguaiacol, a substituted styrene was explored using phenolic acid decarboxylase. Kinetic characterisations showed that the enzyme has a preference only for substrates bearing a *para*-hydroxyl group, a K_m value of more than 1 mM, and has wide range of optimum pH (3.5 – 6).

Overexpression of PAD in *R.jostii* RHA1 and RHA045, in minimal media containing 1% wheat straw did not manage to accumulate any monostyrene product.

However, growth in minimal media containing 0.1% (w/v) pure ferulic acid has accumulated up to 3.28 g/L in 4 days.

To overcome the limitation of lignocellulose conversion into biostyrene, site-directed mutagenesis can be carried out in the future to design the PAD with lower K_m that can directly convert ferulic acid into 4-vinylguaiacol as they are formed within the lignocellulose – lignin degrading bacteria culture.

The research on bio-based polymer has been actively ongoing in this decade. Taking the inspiration from mussel adhesive protein, many synthetic biomimetic polymers have been produced from hydroxycinnamic acids as starting material. In this PhD, an enzymatic approach to polymerise 4-vinylguaiacol and 4-vinylcatechol as well as their co-polymerisation has been studied. With scanning electron microscopy, the polymer was shown to have similar morphology with synthetic polystyrene. The poly(4-vinylguaiacol) was also proven to have adhesive properties, as observed and tested with aluminium lap-shear test.

Ultimately, further research can be done to accumulate the substituted styrene in lignocellulose media by overexpressing PAD in other lignin degrading bacteria. The enzymatic polymerisation of this bio-based styrene can open a new possibility of producing an environmental friendly material that is renewable and biodegradable, in ambient conditions.

CHAPTER 6 EXPERIMENTAL

6.1 General materials and methods

6.1.1 Chemicals and reagents

All chemicals used in the experiments were purchased from Sigma-Aldrich, UK, Fischer Scientific, UK, Bio-Rad, UK and Difco Laboratories, UK, unless otherwise stated and were used as received. HPLC and LCMS were carried out using HPLC grade water and methanol from Fischer Scientific pre-filtered through a 0.2 μm membrane prior to use. The source of lignocellulose in experiments was wheat straw milled in a Retsch grinding mill (model RM 200) and sieved through a 1.0 mm mesh.

6.1.2 Instruments and equipments

High-performance liquid chromatography (HPLC) was performed with an Agilent 1200 Series liquid chromatograph (Agilent Technologies, UK) equipped with a G1311A quaternary pump and a variable-wavelength UV detector. Separations were carried out using an Agilent reversed-phase Zorbax Eclipse XDB-C18 column (250 X 4.6 mm, 50 μm particle size).

Liquid chromatography mass spectrometry (LCMS) analysis was done using Agilent 1200 Series system, equipped with a DAD photodiode detector (G1315B), linked to Bruker HTC-Ultra ESI mass spectrometer (Coventry, UK) both coupled to an Agilent ChemStation (Version B.01.03) for data processing.

Thin layer chromatography (TLC) was performed on 0.25 mm thick TLC F254 aluminium plates coated with silica gel (Merck, Germany) and visualised under a low-frequency UV lamp.

Growth of bacterial cultures and Bradford assay was measured using a Thermo BioMate3 spectrophotometer. Bio-Rad Mini-PROTEAN electrophoresis system was used to perform SDS-PAGE. The centrifuges used were Eppendorf models 5424 and a Fisher Scientific AccuSpin Microcentrifuges and a free-standing Sorvall with SLA-3000 rotor. A Varian Cary 50 Bio UV-Visible Spectrophotometer was used to monitor the enzyme assays and measurements taken using a 1 mL quartz cuvette. A pneumatic cell disrupter (Constant Systems, UK) was used to lyse cells (at ~20 Psi).

6.1.3 Solutions and buffers

All water used to prepare the solutions and buffers were deionised and prepared at room temperature (23°C).

6.1.4 Media

All media were prepared in deionised water and either autoclaved or filter-sterilised prior to use. When required, filter-sterilised Kanamycin (dissolved in water) or Chloramphenicol (dissolved in ethanol) was added to the media at a final concentration of 35 µg/mL.

6.1.4.1 LB

Tryptone 10g/L, yeast Extract 5 g/L, NaCl 10 g/L, all added into deionised water. (For LB plates, 15 g/L agar was added prior to autoclaving).

6.1.4.2 M9 Minimal medium (M9)

The recipe for 1 L medium contains: 0.85 g $Na_2HPO_4.12H_2O$, 1.0 g NH_4Cl, 3.0 g KH_2PO_4, and 0.5 g NaCl. They were dissolved in deionised water and autoclaved. Prior to incoculation, 1 mL of 1 M $MgSO_4$ (final concentration 1 mM) and 20 mL of 20% (w/v) glucose (final concentration 0.4% (w/v) glucose) were added.

6.1.5 Bacterial strains

Unless otherwise stated, all bacterial strains were the property of the Chemical Biology Research Facility, Department of Chemistry, University of Warwick.

The following *Rhodococcus* strains were used:

- *R. jostii* RHA1 wild type
- *R. jostii* RHA045, a Δ*vdh* knockout mutant of RHA1 (ro02986) provided by Prof. Lindsay Eltis (University of British Columbia)

The following *Escherichia coli* were used:

- *E. coli* DH5α
- *E. coli* BL21 (DE3)

6.2 Expression in *Escherichia coli* and purification of phenolic acid decarboxylase

Plasmid construct of phenolic acid decarboxylase was prepared by Dr Elizabeth Hardiman in 2012 as indicated herewith (Figure 68).

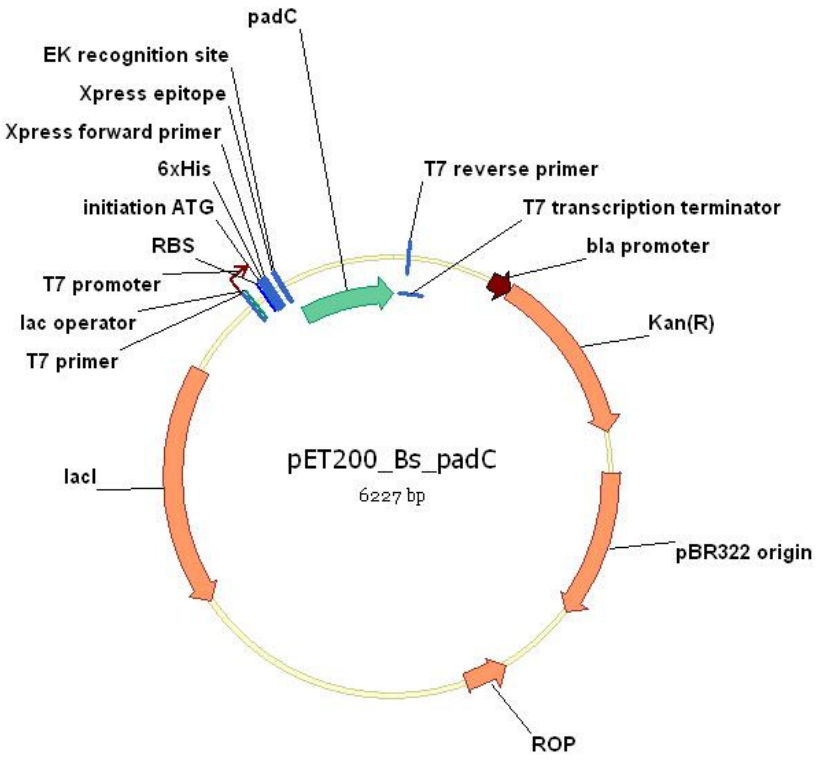

Figure 68: Plasmid map of pET200_*BspadC*

It was made using pET200/D-TOPO (Invitrogen) and contained the phenolic acid decarboxylase gene from *Bacillus subtilis* as well as the His_6 tag and kanamycin resistance marker. The plasmid was transformed into *Escherichia coli* BL21 Star (Invitrogen) by heat shocking the cell at 42°C. Production of the enzyme by *E. coli* BL21 pET200_*padC* was done by inoculating an overnight starter culture in 1 L LB broth at an initial temperature of 37°C in the presence of 35 µg/mL kanamycin. Once the absorbance at 600 nm reached about 0.8, the culture was induced by the addition

of IPTG (0.8 mM final concentration). Then, it was further incubated at 16°C overnight for enzyme expression.

The cells were harvested by centrifugation for 20 min at 5000 rpm at 4°C. The supernatant was decanted and pellets resuspended in a pH 8.0 lysis buffer containing 50 mM NaH_2PO_4, 300 mM NaCl and 10 mM imidazole. The cells were broken down by OneShot cell disruptor (Constant Systems Ltd, UK) at 20 Psi and centrifuged again at 10000 rpm for 30 minutes at 4°C to remove cell debris.

The supernatant was later filtered through 0.2 µm syringe-filter to further remove particulate matters and collected in 50 mL Falcon tube. Nickel-nitriloacetate agarose (Ni-NTA) affinity chromatography resin (Qiagen) was added to the cleared lysate and the two were mixed by inversion for one hour in the cold room to allow binding with the enzyme. Once the matrix-lysate mixture was packed in a 10 mL-sized column, the unbound fraction was collected by elution with wash buffer (50 mM NaH_2PO_4, 300 mM NaCl and 20 mM imidazole) at pH 8.0. Then, the His-tagged protein was eluted in three fractions of 5 mL each by the elution buffer made up of 50 mM NaH_2PO_4, 300 mM NaCl and 250 mM imidazole also at pH 8.0.

All the bound fractions were transferred into a 50 mL Millipore 10 kDa molecular-weight cut-off diafiltration tube and then centrifuged at 5000 rpm for 15 minutes. Fresh 50 mM sodium phosphate buffer (pH 7.4) was added to dialyse the bound fractions of the purified enzyme. Molecular weight of the enzyme was determined by SDS-PAGE of 12% polyacrylamide gel using Bio-Rad PAGE system at 200V.

6.2.1 Sodium dodecyl sulphate polyacrylamide gel electrophoresis (SDS-PAGE)

To estimate the molecular weight of the purified phenolic acid decarboxylase, SDS-PAGE was done using a 12% polyacrylamide for the resolving gel and a 5% stacking gel. The recipe for 2 gel slabs with 10 wells each was as follows:

	Resolving gel	Stacking gel
dH_2O	3.77 mL	3.25 mL
1.5 M Tris-HCl pH 8.8	2.82 mL	-
0.5 M Tris-HCl pH 6.8	-	1.25 mL
30% (w/v) acrylamide/bis-acrylamide	4.55 mL	0.5 mL
10% (w/v) sodium dodecyl sulphate (SDS)	115 µL	50 µL
10% (w/v) ammonium persulphate	115 µL	50 µL
TEMED (Tetramethylethylenediamine)	10 µL	7.5 µL

Protein samples were diluted with an equal volume of 2x loading buffer (0.1 M Tris-HCl, pH 6.8, 20 % (v/v) glycerol, 200 mM DTT, 4% (w/v) SDS, 0.2 % (w/v) bromophenol blue) and incubated at 95°C for 10 min. Each sample were loaded into wells alongside a protein molecular weight ladder (PageRuler Plus Prestained Protein Ladder (ThermoScientific, UK) and the gel was run in SDS-PAGE running buffer (25 mM Tris, 192 mM glycine, 0.1 % SDS, pH 8.3) at 200 V until the dye front reached the bottom of the gel.

To visualise proteins resolved by SDS-PAGE, the gel was initially immersed in fixing solution (50% methanol, 10% acetic acid) for 1 hour, followed by 1 hour staining with Coomassie Brilliant Blue reagent (0.1 % w/v Coomassie Brilliant Blue R-250, 50 % methanol, 10% acetic acid). Finally, the dyeing reagent was removed in

de-staining solution (40% methanol, 10% acetic acid) until the bands were visible. The protein sizes were determined by comparing the migration of the protein band to a molecular weight ladder.

6.2.2 Bradford assay to determine protein concentration

Protein concentrations were determined by the Bio-Rad's Bradford method, following the manufacturer's instruction. Bovine serum albumin (BSA) of a 2 mg/mL stock diluted to a series of concentration at 1.4, 1.0, 0.5, 0.25, 0.125 mg/mL was used to plot a calibration plot. 1.0 mL of the Bradford reagent was pipetted into disposable 1.5 mL plastic cuvettes, followed by the addition of 20 µL of each standard dilution and the purified enzyme. Each sample was mixed immediately by inversion and incubated at room temperature for approximately 5 minutes. The absorbance of each sample was measured with spectrophotometer at 595 nm with a mixture of 20 µL water and 1.5 mL reagent serving as blank. The enzyme concentration was calculated from the calibration curve of the BSA standard.

6.3 Assays and kinetic characterisation of phenolic acid decarboxylase

UV-Vis scan for 200-400nm for 15 minutes was performed to estimate the activity of phenolic acid decarboxylase. Assays were carried out using Cary 50 UV-Vis spectrophotometer. The 1 mL assay mixture consists of 50 mM sodium acetate buffer pH 5.0 containing 0.1 mM ferulic acid to which 10 µL of 0.8 mg/mL enzyme

was added to initiate the reaction. All assays were carried out at room temperature with the enzyme stored on ice prior to mixing with other assay substances.

For determining the activity, a calibration curve of ferulic acid was done using a commercial standard procured from Sigma, dissolved in the assay buffer ranging between 0.00625-0.125 mM. Extinction coefficient was obtained from the curve and used to calculate the rate of reaction following the Beer-Lambert law.

The effect on enzyme activity of varying pH was examined. To determine the optimum pH, assays were performed at 23°C for 20 min in a series of sodium acetate and sodium phosphate buffers covering the pH range 3.0–8.0 with 0.5 pH interval. Kinetic parameters were obtained by Michaelis–Menten equation and the double reciprocal Lineweaver-Burk plot using Microsoft Excel 2010 software. The experiments were carried out with a variety of substrate concentrations under optimal reaction conditions for 5 min.

6.4 Substrate specificity of phenolic acid decarboxylase

Several substrate analogues were tested for assay with phenolic acid decarboxylase besides ferulic acid. UV-vis assay was done as previously described with similar conditions, except that ferulic acid was replaced by each substrate analogues of 0.1 mM concentration.

Table 6: Cinnamic acids used for the substrate specificity assay

3-hydroxycinnamic acid 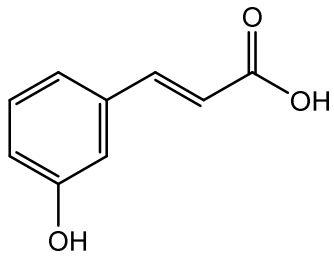	4-hydroxycinnamic acid (*p*-coumaric acid) 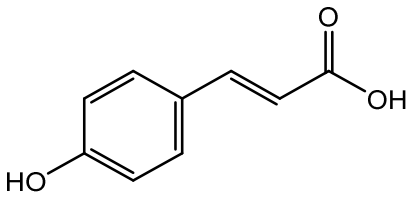
3,4-dihydroxycinnamic acid (Caffeic acid) 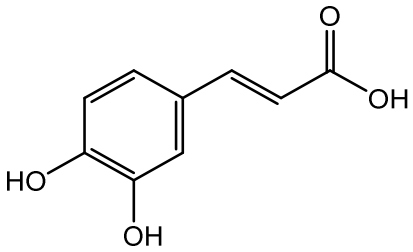	4-hydroxy-3-methoxycinnamic acid (Ferulic acid) 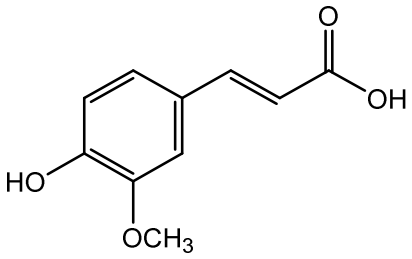
4-hydroxy-3,5-dimethoxycinnamic acid (Sinapic acid) 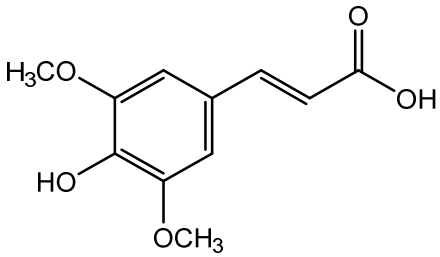	2-methoxycinnamic acid 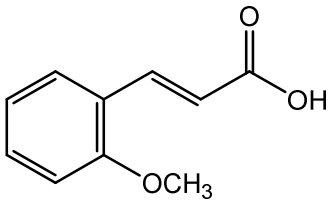
3-methoxycinnamic acid 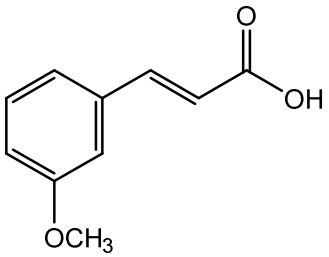	4-methoxycinnamic acid 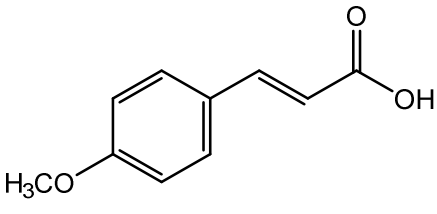

6.5 Whole cell bioconversion of ferulic acid into 4-vinylguaiacol

A culture of *E.coli* BL21 bearing the plasmid pET200_*padC* for protein expression was prepared in 100 mL LB containing 35 µg/mL kanamycin. Upon reaching the OD_{600nm} of 0.8, the culture was centrifuged for 20 min at 5000 rpm to remove the LB. Whole cell suspension was prepared by resuspending the cell pellet in M9 minimal media, supplemented with 0.2% (w/v) glucose, 35 µg/mL kanamycin and 0.8 mM IPTG prior to further incubation at 16°C. All the process were done while maintaining the sterile condition of the culture. After 15 hours, ferulic acid was added to the medium to a final concentration of 2 mM and further incubated for 30 hours. One millilitre sample was taken out at various time points for metabolite analysis.

The samples were extracted with ethyl acetate, and upon complete evaporation, resuspended in methanol. They were subjected to reversed phase high performance liquid chromatography (HPLC) with variable wavelength ultraviolet (UV) detection on Agilent Series 1200 system was carried out using Agilent reversed-phase Zorbax Eclipse XDB-C18 column (130 Å, 250 mm x 4.6 mm) at a flow rate of 0.8 mL/min, with monitoring at 260 nm. The HPLC solvents were water/0.1% trifluoroacetic acid (solvent A) and methanol/0.1% trifluoroacetic acid (solvent B). The applied gradient was 10% B for 5 min; 10–15% B over 10 min; 15–25% B for 8 min; and 25–100% B for 19 min, at a flow rate of 0.8 mL/min. Commercial analytical grade ferulic acid and 4-vinylguaiacol were used as internal standard to compare the metabolites with.

6.6 Overexpression in *Rhodococcus jostii* RHA1

Lignin degrading bacteria *Rhodococcus jostii* RHA1 was used as a host for overexpression of phenolic acid decarboxylase from *Bacillus subtilis* using the padC gene inserted within the pTipQC2 vector. The construct was kindly provided by Dr E. Hardiman.

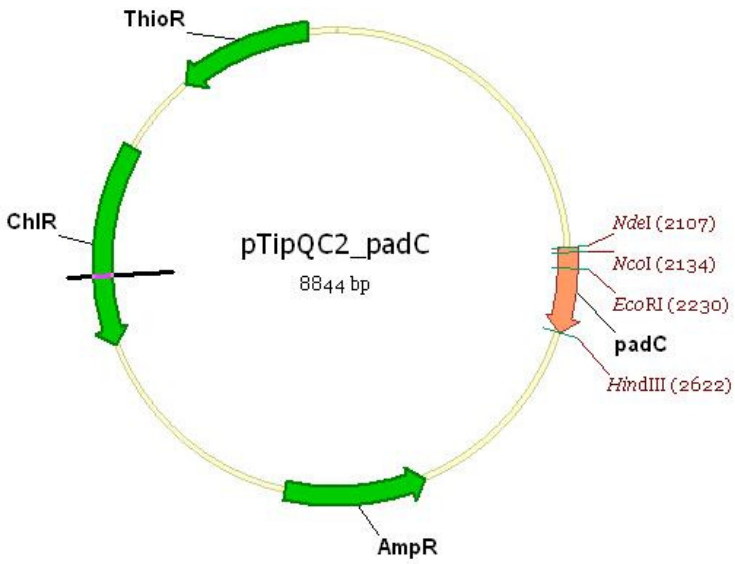

Figure 69: Plasmid map of pTipQC2_*padC*

Starter culture of *R.jostii* RHA1 pTipQC2_*padC* was grown in LB broth containing 35 µg/mL chloramphenicol at 30°C inside 180 rpm orbital shaker. Once it reached an absorbance of around 0.8 at 600 nm, 1 mL of the culture was inoculated into 50 mL M9 minimal media containing 0.2% (w/v) glucose, 35 µg/mL chloramphenicol and 1% w/v milled wheat straw.

On the second day, 1 µg/mL thiostrepton was added to the culture to induce enzyme expression. Sampling was done on daily interval by taking 1 mL sample for 10 days and absorbance reading at 600 nm was recorded to plot growth profile. After that, it was spun down at 10000 rpm for 5 minutes in a microcentrifuge tube and stored in the -20°C freezer for metabolite analyses.

Once the fermentation reached 10 days, a similar volume of ethyl acetate was added to all the collected samples. The organic layer was taken and transferred into new tube and left to evaporate overnight. Once all the extracts were completely dried, methanol was added to each of them and then filtered through cotton wool into the snap-top vials for the LC run (HPLC or LCMS).

HPLC analysis was conducted using Agilent Zorbax Eclipse XDB-C18 reverse phase column (130 Å, 250 mm x 4.6 mm) on Agilent Series 1200 analyser, at a flow rate of 0.8 mL/min, with monitoring at 260 nm. Eluents were HPLC grade methanol and water supplemented with 0.1% (v/v) trifluoroacetic acid. The HPLC gradient was: 10% MeOH over 5 min; 10–15% MeOH over 5–15 min; 15–25% MeOH over 15–23 min, 25-100% MeOH over 23-42 min, 100% MeOH over 42-45 min and from 45-49 min back from 100% MeOH to 10% MeOH with 10% MeOH for the 50th minute.

LCMS was carried out with Agilent 1200 Series system connected to Bruker HTC-Ultra ESI mass spectrometer, at a flow rate of 0.8 mL/min with similar gradient system as HPLC described above. Methanol and water used for the gradient were of HPLC grade, and commercial 4-vinylguaiacol and *trans*-ferulic acid (Sigma) were used as authentic standard.

The identification of reaction products was carried out by comparing the retention times and spectral data for each peak with those of authentic standards obtained from commercial suppliers.

Similar experiment was repeated with M9 minimal media containing 0.1% w/v each of the ferulic acid (Fluka) and *trans*-ferulic acid (Sigma). After 9 hours of incubation at 30°C, 1 µg/mL thiostrepton was added to the culture to induce enzyme expression. Fermentation for a total of 4 days was done to investigate the production of 4-vinylguaiacol in pure ferulic acid media.

6.7 Overexpression in *Rhodococcus jostii* RHA045

The vanillin dehydrogenase (*Δvdh*) knockout mutant *Rhodococcus jostii* RHA045 was used as a host for overexpression of pTipQC2*_padC*. Competent cells of *R.jostii* RHA045 were made by growing the cell in 500 mL LB until it reached an Abs_{600nm} of 0.8. Cells were then harvested in sterile condition by centrifugation at 5000 rpm for 20 minutes. Supernatant was discarded and the pellet was resuspended and washed 4-5 rounds with 10% sterile glycerol solution. After the final wash, the cell was resuspended in 1 mL wash solution, and aliquoted into 100 µL volume in microcentrifuge tubes.

For transformation, Gene Pulser cuvette (Bio-Rad, UK) was used to insert 200 ng pTipQC2*_padC* plasmid into the aliquot of competent cells. The voltage was set to 1.8 kV, and electroporation was done for 2-3 seconds. The transformants were transferred into 200 µL LB and incubated at 30°C in the microcentrifuge tube while

shaking at 180 rpm. After 4 hours, the entire suspension was spread on LB containing chloramphenicol (35 µg/mL) plates and incubated at 30°C for 2 days.

Starter culture of *R.jostii* RHA045 pTipQC2_*padC* was grown in LB broth containing 35 µg/mL chloramphenicol at 30°C inside 180 rpm shaker. Once it reached an absorbance of around 0.8 at 600 nm, 1 mL of the culture was inoculated into 50 mL M9 minimal media containing 0.2% (w/v) glucose, 35µg/mL chloramphenicol and 1% w/v milled wheat straw. The expression of PAD was induced with 1 µg/mL thiostrepton on the second day, with sampling at 1 day interval for metabolite analysis with methods described in Section 6.6 previously.

6.8 Enzyme catalysed polymerisation

For 50 mL reaction volume, the mixture contained 10 mM final concentration of ferulic acid in 50 mM, pH 5.0 sodium acetate buffer with the addition of 0.5 mL (2.22 mg/mL) phenolic acid decarboxylase (PAD). An overnight incubation in room temperature was done to ensure the complete conversion of all ferulic acid into 4-vinylguaiacol. Similar procedure was carried out by replacing ferulic acid with caffeic acid to generate 4-vinylcatechol. Amber bottles were used since the products generated are light-sensitive.

Then, 100 µL (11.52 U/mL) laccase from *Trametes versicolor*, procured from Sigma was added to the mixture to initiate polymerisation into the substituted polystyrene. For co-polymerisation, 10 mM ferulic acid containing various molar concentrations of caffeic acid was pre-incubated with PAD at room temperature overnight with

occasional shaking. This was followed by the addition of laccase, and then further incubated for 2 days.

The precipitate formed in each polymerisation was recovered by centrifugation at 5000 rpm for 30 min in Falcon tubes. After that, the supernatant was discarded, the solid residue was recovered, flash-frozen with liquid nitrogen and subjected to freeze-drying overnight.

6.9 Gel permeation chromatography

Molecular weight of the obtained polymeric samples was determined using gel permeation chromatography (GPC). Each polymer sample was dissolved at a final concentration of 1 mg/mL in THF (HPLC grade, contains 2% TEA and 0.01% BHT (Topanol) and clarified using syringe filter (Millipore hydrophobic PVDF membrane, 0.22 μm pore size) to remove insoluble particulate matters prior to injection into the GPC analyser.

Gel permeation chromatography samples were run on an Agilent 390-LC system equipped with a PL-AS RT autosampler, a 100 μL injection loop, a 5 μm PLgel guard column (50 mm x 7.5 mm), two 5μm PLgel Mixed D columns (50 mm x 300 mm) and a differential refractive index (DRI) detector. The system was eluted with THF at a rate of 1 mL/min and the detector was calibrated with PL narrow polystyrene (157 to 300 000 g/mol) standard easy vials. Molecular weights of the samples were calculated using the polystyrene calibration. GPC system was run under Agilent Chemstation, which had GPC add-on software.

6.10 Scanning electron microscopy (SEM)

The morphology of the polymer was observed by the field emission scanning electron microscope (Zeiss SUPRA 55-VP). The freeze-dried sample was mounted on a conducting double-sided carbon tape and inserted into a vacuumed chamber inside the scanning electron microscope (SEM). It was performed at the acceleration voltage of 5 kV. The electron microscope was kindly operated by Mrs Nur Alifah Abdul Rahman from the Department of Physics, University of Warwick.

6.11 Determination of adhesive tensile lap shear strength

Aluminium plates with thickness of 0.8 mm were cut according to the dimensions stated in the British Standard manual for '*Determination of tensile lap-shear strength of bonded assemblies*' (BS EN 1465:2009) [201]. Each plate was 100 mm (L) X 25 mm (W). Prior to use, they were polished and cleaned by soaking for 15 min each in hexane, acetone and ethanol, then left to air dry. Then, each polymer sample was mixed with 1:1 DCM/acetone to form 0.3 mg/mL paste and applied onto each aluminium plate (67.5 µL each side), to equally covering an area of 25 mm x 25 mm which became the shear area. Straight afterwards, 15 µL (50 mM final concentration) of freshly prepared 500 mM $Na(IO)_4$ solution was dropped onto each adherend, and the shear area was joined together immediately, supported by a 51 mm (L) binder clip. They were allowed to cure 30 min at room temperature before incubation in a 37°C oven for 24 hours.

The samples were then taken out of the incubator and cooled for 1 h in air at room temperature. After this cure, shear load-extension curves were obtained with a

universal material testing machine (Instron 3367, USA), kindly operated by Dr Panos Efthymiadis (WMG). The force applied to the fixture was measured with a 5000 N load cell. Samples were held in place in the testing machine by testing grips near the midpoint of the overlap area of the adherends and extended in the shear direction at a speed of 0.25 mm/min. Each measurement of adhesive strength was repeated at least four times and averaged. Force-adhesion curve was plotted for the averaged values to determine the adhesion strength of the bonded assemblies and compared with available references of similar experimental methods.

BIBLIOGRAPHY

[1] P. D. Sainsbury, E. M. Hardiman, M. Ahmad, H. Otani, N. Seghezzi, L. D. Eltis, and T. D. Bugg, "Breaking down lignin to high-value chemicals: the conversion of lignocellulose to vanillin in a gene deletion mutant of *Rhodococcus jostii* RHA1," *ACS Chem. Biol.*, vol. 8, no. 10, pp. 2151–2156, 2013.

[2] M. E. Brown and M. C. Chang, "Exploring bacterial lignin degradation," *Curr. Opin. Chem. Biol.*, vol. 19, pp. 1–7, 2014.

[3] H. Lange, S. Decina, and C. Crestini, "Oxidative upgrade of lignin: Recent routes reviewed," *Eur. Polym. J.*, vol. 49, pp. 1151–1173, 2013.

[4] DEFRA, "Farming statistics – 2015 wheat and barley production, UK," *National Statictics*, 2015 [Online]. Available: https://www.gov.uk/government/statistics/farming-statistics-2015-wheat-and-barley-production-uk. [Accessed: 03-Jan-2016]

[5] F. Xu, "Structure, ultrastructure, and chemical composition," in *Cereal straw as a resource of sustainable biomaterials and biofuels: chemistry, extractives, lignins, hemicelluloses and cellulose*, Sun, RunCang, Ed. 2010, pp. 9–47.

[6] P. Van Soest, "Rice straw, the role of silica and treatments to improve quality," *Anim. Feed Sci. Technol.*, vol. 130, no. 3, pp. 137–171, 2006.

[7] J. Vadiveloo, B. Nurfariza, and J. Fadel, "Nutritional improvement of rice husks," *Anim. Feed Sci. Technol.*, vol. 151, no. 3, pp. 299–305, 2009.

[8] S. R. Collins, N. Wellner, I. M. Bordonado, A. L. Harper, C. N. Miller, I. Bancroft, and K. W. Waldron, "Variation in the chemical composition of wheat straw: the role of tissue ratio and composition," *Biotechnol. Biofuels*, vol. 7, no. 1, p. 1, 2014.

[9] A. U. Buranov and G. Mazza, "Lignin in straw of herbaceous crops," *Ind. Crops Prod.*, vol. 28, no. 3, pp. 237–259, 2008.

[10] V. Menon and M. Rao, "Trends in bioconversion of lignocellulose: biofuels, platform chemicals & biorefinery concept," *Prog. Energy Combust. Sci.*, vol. 38, no. 4, pp. 522–550, 2012.

[11] E. M. Rubin, "Genomics of cellulosic biofuels," *Nature*, vol. 454, no. 7206, pp. 841–845, 2008.

[12] G. Brunow, K. Lundquist, and G. Gellerstedt, "Lignin," in *Analytical methods in wood chemistry, pulping, and papermaking*, Sjöström, E and Alén, R, Ed. Springer, 1999, pp. 77–124.

[13] R. Sun, J. Lawther, and W. Banks, “A tentative chemical structure of wheat straw lignin,” *Ind. Crops Prod.*, vol. 6, no. 1, pp. 1–8, 1997.

[14] J. Ralph, K. Lundquist, G. Brunow, F. Lu, H. Kim, P. F. Schatz, J. M. Marita, R. D. Hatfield, S. A. Ralph, J. H. Christensen, and W. Boerjan, “Lignins: natural polymers from oxidative coupling of 4-hydroxyphenyl-propanoids,” *Phytochem. Rev.*, vol. 3, no. 1–2, pp. 29–60, 2004.

[15] J. Barros, J. C. Serrani-Yarce, F. Chen, D. Baxter, B. J. Venables, and R. A. Dixon, “Role of bifunctional ammonia-lyase in grass cell wall biosynthesis,” *Nat. Plants*, vol. 2, p. 16050, 2016.

[16] F. Lu and J. Ralph, “Chapter 6 - Lignin ,” in *Cereal Straw as a Resource for Sustainable Biomaterials and Biofuels* , Sun, Run-Cang , Ed. Amsterdam: Elsevier, 2010, pp. 169 – 207.

[17] N. D. Bonawitz and C. Chapple, “The genetics of lignin biosynthesis: connecting genotype to phenotype,” *Annu. Rev. Genet.*, vol. 44, pp. 337–363, 2010.

[18] C. Riboulet, S. Guillaumie, V. Méchin, M. Bosio, M. Pichon, D. Goffner, C. Lapierre, B. Pollet, B. Lefevre, J. Martinant, and Y. Barrière, “Kinetics of phenylpropanoid gene expression in maize growing internodes: Relationships with cell wall deposition,” *Crop Sci.*, 2009.

[19] H. A. Maeda, “Lignin biosynthesis: Tyrosine shortcut in grasses,” *Nat. Plants*, vol. 2, p. 16080, 2016.

[20] A. Lourenço, J. Rencoret, C. Chemetova, J. Gominho, A. Gutiérrez, J. C. del Rio, and H. Pereira, “Lignin composition and structure differs between xylem, phloem and phellem in *Quercus suber L.*,” *Front. Plant Sci.*, vol. 7, 2016.

[21] J. C. Del Rio, J. Rencoret, P. Prinsen, A. T. Martinez, J. Ralph, and A. Gutiérrez, “Structural characterization of wheat straw lignin as revealed by analytical pyrolysis, 2D-NMR, and reductive cleavage methods,” *J. Agric. Food Chem.*, vol. 60, no. 23, pp. 5922–5935, 2012.

[22] F. Xu, J.-X. Sun, R. Sun, P. Fowler, and M. S. Baird, “Comparative study of organosolv lignins from wheat straw,” *Ind. Crops Prod.*, vol. 23, no. 2, pp. 180–193, 2006.

[23] R. Vanholme, B. Demedts, K. Morreel, J. Ralph, and W. Boerjan, “Lignin biosynthesis and structure,” *Plant Physiol.*, vol. 153, no. 3, pp. 895–905, 2010.

[24] H. Chung and N. R. Washburn, “Extraction and Types of Lignin,” in *Lignin in polymer composites*, William Andrew Publishing, 2015, pp. 13–25.

[25] A. B. Fisher and S. S. Fong, “Lignin biodegradation and industrial implications,” *AIMS Bioeng.*, vol. 1, no. 92–112, 2014.

[26] R. A. Pérez--Camargo, G. Saenz, S. Laurichesse, M. T. Casas, J. Puiggalí, L. Avérous, and A. J. Müller, “Nucleation, crystallization, and thermal fractionation of poly (ε-caprolactone)-grafted-lignin: Effects of grafted chains length and lignin content,” *J. Polym. Sci., Part B: Polym. Phys.*, vol. 53, no. 24, pp. 1736–1750, 2015.

[27] N. H. Bhuiyan, G. Selvaraj, Y. Wei, and J. King, “Role of lignification in plant defense,” *Plant Signaling Behav.*, vol. 4, no. 2, pp. 158–159, 2009.

[28] E. Miedes, R. Vanholme, W. Boerjan, and A. Molina, “The role of the secondary cell wall in plant resistance to pathogens.,” *Front Plant Sci*, vol. 5, p. 358, 2014.

[29] J. H. Grabber, “How do lignin composition, structure, and cross-linking affect degradability? A review of cell wall model studies,” *Crop Sci.*, vol. 45, no. 3, pp. 820–831, 2005.

[30] I. Cesarino, P. Araújo, A. P. Domingues Júnior, and P. Mazzafera, “An overview of lignin metabolism and its effect on biomass recalcitrance,” *Braz. J. Bot.*, vol. 35, no. 4, pp. 303–311, 2012.

[31] D. A. B. Martins, E. Gomes, H. F. A. do Prado, H. Ferreira, M. M. de Souza Moretti, R. da Silva, and R. S. R. Leite, *Agroindustrial wastes as substrates for microbial enzymes production and source of sugar for bioethanol production*. INTECH Open Access Publisher, 2011.

[32] R. J. A. Gosselink, “Lignin as a renewable aromatic resource for the chemical industry,” 2011.

[33] K. Olofsson, M. Bertilsson, and G. Lidén, “A short review on SSF-an interesting process option for ethanol production from lignocellulosic feedstocks,” *Biotechnol. Biofuels*, vol. 1, no. 1, p. 1, 2008.

[34] V. Chaturvedi and P. Verma, “An overview of key pretreatment processes employed for bioconversion of lignocellulosic biomass into biofuels and value added products,” *3 Biotech.*, vol. 3, no. 5, pp. 415–431, 2013.

[35] D. N. Barman, M. A. Haque, T. H. Kang, M. K. Kim, J. Kim, H. Kim, and H. D. Yun, “Alkali pretreatment of wheat straw (*Triticum aestivum*) at boiling temperature for producing a bioethanol precursor.,” *Biosci. Biotechnol. Biochem.*, vol. 76, no. 12, pp. 2201–7, 2012.

[36] F. Monlau, A. Barakat, E. Trably, C. Dumas, J.-P. Steyer, and H. Carrère, “Lignocellulosic materials into biohydrogen and biomethane: impact of structural features and pretreatment,” *Crit. Rev. Environ. Sci. Technol.*, vol. 43, no. 3, pp. 260–322, 2013.

[37] S. G. Wi, E. J. Cho, D.-S. Lee, S. J. Lee, Y. J. Lee, and H.-J. Bae, "Lignocellulose conversion for biofuel: a new pretreatment greatly improves downstream biocatalytic hydrolysis of various lignocellulosic materials," *Biotechnol. Biofuels*, vol. 8, no. 1, p. 1, 2015.

[38] K. Jaisamut, L. Paulová, P. Patáková, M. Rychtera, K. Melzoch, and others, "Optimization of alkali pretreatment of wheat straw to be used as substrate for biofuels production," *Plant, Soil Environ.*, vol. 59, pp. 537–542, 2013.

[39] N. Mosier, C. Wyman, B. Dale, R. Elander, Y. Y. Lee, M. Holtzapple, and M. Ladisch, "Features of promising technologies for pretreatment of lignocellulosic biomass.," *Bioresour. Technol.*, vol. 96, no. 6, pp. 673–86, 2005.

[40] F. H. Isikgor and C. R. Becer, "Lignocellulosic biomass: a sustainable platform for the production of bio-based chemicals and polymers," *Polym.Chem.*, vol. 6, no. 25, pp. 4497–4559, 2015.

[41] X. Zhao, K. Cheng, and D. Liu, "Organosolv pretreatment of lignocellulosic biomass for enzymatic hydrolysis.," *Appl. Microbiol. Biotechnol.*, vol. 82, no. 5, pp. 815–27, 2009.

[42] A. Hendriks and G. Zeeman, "Pretreatments to enhance the digestibility of lignocellulosic biomass," *Bioresour. Technol.*, vol. 100, no. 1, pp. 10–18, 2009.

[43] L. da Costa Sousa, S. P. Chundawat, V. Balan, and B. E. Dale, "'Cradle-to-grave' assessment of existing lignocellulose pretreatment technologies," *Curr. Opin. Biotechnol.*, vol. 20, no. 3, pp. 339–347, 2009.

[44] V. Pihlajaniemi, M. H. Sipponen, O. Pastinen, I. Lehtomäki, and S. Laakso, "Yield optimization and rational function modelling of enzymatic hydrolysis of wheat straw pretreated by NaOH-delignification, autohydrolysis and their combination," *Green Chem.*, vol. 17, no. 3, pp. 1683–1691, 2015.

[45] A. Brandt, J. Gräsvik, J. P. Hallett, and T. Welton, "Deconstruction of lignocellulosic biomass with ionic liquids," *Green Chem.*, vol. 15, no. 3, pp. 550–583, 2013.

[46] S. Yang, T.-Q. Yuan, M.-F. Li, and R.-C. Sun, "Hydrothermal degradation of lignin: products analysis for phenol formaldehyde adhesive synthesis," *Int. J. Biol. Macromol.*, vol. 72, pp. 54–62, 2015.

[47] S. E. Blumer-Schuette, S. D. Brown, K. B. Sander, E. A. Bayer, I. Kataeva, J. V. Zurawski, J. M. Conway, M. W. W. Adams, and R. M. Kelly, "Thermophilic lignocellulose deconstruction.," *FEMS Microbiol. Rev.*, vol. 38, no. 3, pp. 393–448, 2014.

[48] A. Abbas and S. Ansumali, "Global potential of rice husk as a renewable feedstock for ethanol biofuel production," *Bioenerg. Res.*, vol. 3, no. 4, pp.

328–334, 2010.

[49] P. Azadi, O. R. Inderwildi, R. Farnood, and D. a. King, “Liquid fuels, hydrogen and chemicals from lignin: A critical review,” *Renewable Sustainable Energy Rev.*, vol. 21, pp. 506–523, 2013.

[50] M. W. Zahari, A. Alimon, and H. Wong, “Utilization of oil palm co-products as feeds for livestock in Malaysia,” in *Biofuel co-products as livestock feed-Opportunities and challenges*, 2012, pp. 243–262.

[51] G. Nader, G. Cun, and P. Robinson, “Impacts of silica levels, and location in the detergent fiber matrix, on *in vitro* gas production of rice straw,” *Anim. Feed Sci. Technol.*, vol. 174, no. 3, pp. 140–147, 2012.

[52] A. Raj, M. K. Reddy, R. Chandra, H. J. Purohit, and A. Kapley, “Biodegradation of kraft-lignin by *Bacillus sp*. isolated from sludge of pulp and paper mill,” *Biodegradation*, vol. 18, no. 6, pp. 783–792, 2007.

[53] R. Chandra, S. Singh, M. Krishna Reddy, D. Patel, H. J. Purohit, and A. Kapley, “Isolation and characterization of bacterial strains *Paenibacillus sp*. and *Bacillus sp*. for kraft lignin decolorization from pulp paper mill waste,” *J. Gen. Appl. Microbiol.*, vol. 54, no. 6, pp. 399–407, 2008.

[54] S. R. Couto and J. L. T. Herrera, “Industrial and biotechnological applications of laccases: a review,” *Biotechnol. Adv.*, vol. 24, no. 5, pp. 500–513, 2006.

[55] A. Bholay, B. V. Borkhataria, P. U. Jadhav, K. S. Palekar, M. V. Dhalkari, and P. Nalawade, “Bacterial lignin peroxidase: A tool for biobleaching and biodegradation of industrial effluents,” *Univers. J. Environ. Res. Technol.*, vol. 2, no. 1, pp. 58–64, 2012.

[56] R. Vicuña, “Bacterial degradation of lignin,” *Enzyme Microb. Technol.*, vol. 10, no. 11, pp. 646–655, 1988.

[57] M. Hofrichter, “Review: lignin conversion by manganese peroxidase (MnP),” *Enzyme Microb. Technol.*, vol. 30, no. 4, pp. 454–466, 2002.

[58] D. Wesenberg, I. Kyriakides, and S. N. Agathos, “White-rot fungi and their enzymes for the treatment of industrial dye effluents,” *Biotechnol. Adv.*, vol. 22, no. 1, pp. 161–187, 2003.

[59] L. Pollegioni, F. Tonin, and E. Rosini, “Lignin-degrading enzymes,” *FEBS J.*, vol. 282, no. 7, pp. 1190–1213, 2015.

[60] D. Knop, D. Levinson, A. Makovitzki, A. Agami, E. Lerer, A. Mimran, O. Yarden, and Y. Hadar, “Limits of versatility of versatile peroxidase,” *Appl. Environ. Microbiol.*, vol. 82, no. 14, pp. 4070–4080, 2016.

[61] A. O. Falade, U. U. Nwodo, B. C. Iweriebor, E. Green, L. V. Mabinya, and A. I. Okoh, “Lignin peroxidase functionalities and prospective applications,”

MicrobiologyOpen, 2016.

[62] T. D. Bugg, M. Ahmad, E. M. Hardiman, and R. Singh, "The emerging role for bacteria in lignin degradation and bio-product formation," *Curr. Opin. Biotechnol.*, vol. 22, no. 3, pp. 394–400, 2011.

[63] M. Ahmad, J. N. Roberts, E. M. Hardiman, R. Singh, L. D. Eltis, and T. D. Bugg, "Identification of DypB from *Rhodococcus jostii* RHA1 as a lignin peroxidase," *Biochemistry*, vol. 50, no. 23, pp. 5096–5107, 2011.

[64] W. Zimmermann, "Degradation of lignin by bacteria," *J. Biotechnol.*, vol. 13, no. 2, pp. 119–130, 1990.

[65] C. R. Taylor, E. Hardiman, M. Ahmad, P. Sainsbury, P. Norris, and T. D. Bugg, "Isolation of bacterial strains able to metabolize lignin from screening of environmental samples," *J. Appl. Microbiol.*, vol. 113, no. 3, pp. 521–530, 2012.

[66] W. R. Finnerty, "The biology and genetics of the genus *Rhodococcus*," *Annu. Rev. Microbiol.*, vol. 46, no. 1, pp. 193–218, 1992.

[67] L. Martínková, B. Uhnáková, M. Pátek, J. Nešvera, and V. Křen, "Biodegradation potential of the genus *Rhodococcus*," *Environ. Int.*, vol. 35, no. 1, pp. 162–177, 2009.

[68] M. P. McLeod, R. L. Warren, W. W. L. Hsiao, N. Araki, M. Myhre, C. Fernandes, D. Miyazawa, W. Wong, A. L. Lillquist, D. Wang, M. Dosanjh, H. Hara, A. Petrescu, R. D. Morin, G. Yang, J. M. Stott, J. E. Schein, H. Shin, D. Smailus, A. S. Siddiqui, M. A. Marra, S. J. M. Jones, R. Holt, F. S. L. Brinkman, K. Miyauchi, M. Fukuda, J. E. Davies, W. W. Mohn, and L. D. Eltis, "The complete genome of *Rhodococcus sp*. RHA1 provides insights into a catabolic powerhouse.," *Proc. Natl. Acad. Sci. U.S.A.*, vol. 103, no. 42, pp. 15582–7, 2006.

[69] T. D. Bugg and R. Rahmanpour, "Enzymatic conversion of lignin into renewable chemicals," *Curr. Opin. Chem. Biol.*, vol. 29, pp. 10–17, 2015.

[70] R. Plaggenborg, J. Overhage, A. Loos, J. A. Archer, P. Lessard, A. J. Sinskey, A. Steinbüchel, and H. Priefert, "Potential of *Rhodococcus* strains for biotechnological vanillin production from ferulic acid and eugenol," *Appl. Microbiol. Biotechnol.*, vol. 72, no. 4, pp. 745–755, 2006.

[71] J. M. Landete, H. Rodriguez, J. A. Curiel, B. de las Rivas, J. M. Mancheño, and R. Muñoz, "Gene cloning, expression, and characterization of phenolic acid decarboxylase from *Lactobacillus brevis* RM84," *J. Ind. Microbiol. Biotechnol.*, vol. 37, no. 6, pp. 617–624, 2010.

[72] J. Klepacka and Ł. Fornal, "Ferulic acid and its position among the phenolic compounds of wheat," *Crit. Rev. Food Sci. Nutr.*, vol. 46, no. 8, pp. 639–647,

2006.

[73] S. Mathew and T. E. Abraham, “Ferulic acid: an antioxidant found naturally in plant cell walls and feruloyl esterases involved in its release and their applications,” *Crit. Rev. Biotechnol.*, vol. 24, no. 2–3, pp. 59–83, 2004.

[74] M. M. de O. Buanafina, “Feruloylation in grasses: Current and future perspectives,” *Mol. Plant*, vol. 2, no. 5, pp. 861–872, 2009.

[75] L. C. Bourne and C. Rice-Evans, “Bioavailability of ferulic acid,” *Biochem. Biophys. Res. Commun.*, vol. 253, no. 2, pp. 222–227, 1998.

[76] C. Mancuso and R. Santangelo, “Ferulic acid: pharmacological and toxicological aspects,” *Food Chem. Toxicol.*, vol. 65, pp. 185–195, 2014.

[77] S. Ou and K.-C. Kwok, “Ferulic acid: pharmaceutical functions, preparation and applications in foods,” *J. Sci. Food Agric.*, vol. 84, no. 11, pp. 1261–1269, 2004.

[78] R. J. Robbins, “Phenolic acids in foods: an overview of analytical methodology,” *J. Agric. Food Chem.*, vol. 51, no. 10, pp. 2866–2887, 2003.

[79] L. Barthelmebs, C. Diviés, and J.-F. Cavin, “Molecular characterization of the phenolic acid metabolism in the lactic acid bacteria *Lactobacillus plantarum*,” *Le Lait*, vol. 81, no. 1–2, pp. 161–171, 2001.

[80] S. RunCang, X. F. Sun, S. Q. Wang, W. Zhu, and X. Y. Wang, “Ester and ether linkages between hydroxycinnamic acids and lignins from wheat, rice, rye, and barley straws, maize stems, and fast-growing poplar wood.,” *Ind. Crops Prod.*, vol. 15, no. 3, pp. 179–188, 2002.

[81] R. D. Hatfield, J. Ralph, and J. H. Grabber, “Cell wall cross-linking by ferulates and diferulates in grasses,” *J. Sci. Food Agric.*, vol. 79, pp. 403–407, 1999.

[82] H. T. H. Nguyen, M. H. Reis, P. Qi, and S. A. Miller, “Polyethylene ferulate (PEF) and congeners: polystyrene mimics derived from biorenewable aromatics,” *Green Chem.*, vol. 17, no. 9, pp. 4512–4517, 2015.

[83] H. T. H. Nguyen, E. R. Suda, E. M. Bradic, J. A. Hvozdovich, and S. A. Miller, “Polyesters from bio-aromatics,” in *Green Polymer Chemistry: Biobased Materials and Biocatalysis*, American Chemical Society, 2015, pp. 401–409.

[84] L. Mialon, A. G. Pemba, and S. A. Miller, “Biorenewable polyethylene terephthalate mimics derived from lignin and acetic acid,” *Green Chem.*, vol. 12, no. 10, pp. 1704–1706, 2010.

[85] T. Li, L. Huo, C. Pulley, and A. Liu, "Decarboxylation mechanisms in biological system," *Bioorg. Chem.*, vol. 43, pp. 2–14, 2012.

[86] F. Jordan and H. Patel, "Catalysis in enzymatic decarboxylations: Comparison of selected cofactor-dependent and cofactor-independent examples.," *ACS Catal.*, vol. 3, no. 7, pp. 1601–1617, 2013.

[87] X. Sheng, M. E. Lind, and F. Himo, "Theoretical study of the reaction mechanism of phenolic acid decarboxylase," *FEBS J.*, vol. 282, no. 24, pp. 4703–4713, 2015.

[88] J.-F. Cavin, V. Dartois, and C. Diviès, "Gene cloning, transcriptional analysis, purification, and characterization of phenolic acid decarboxylase from *Bacillus subtilis*," *Appl. Environ. Microbiol.*, vol. 64, no. 4, pp. 1466–1471, 1998.

[89] N. P. Tran, J. Gury, V. Dartois, T. K. C. Nguyen, H. Seraut, L. Barthelmebs, P. Gervais, and J.-F. Cavin, "Phenolic acid-mediated regulation of the *padC* gene, encoding the phenolic acid decarboxylase of *Bacillus subtilis*," *J. Bacteriol.*, vol. 190, no. 9, pp. 3213–3224, 2008.

[90] G. Degrassi, P. P. De Laureto, and C. V. Bruschi, "Purification and characterization of ferulate and p-coumarate decarboxylase from *Bacillus pumilus*.," *Appl. Environ. Microbiol.*, vol. 61, no. 1, pp. 326–332, 1995.

[91] I.-Y. Lee, T. G. Volm, and J. P. Rosazza, "Decarboxylation of ferulic acid to 4-vinylguaiacol by *Bacillus pumilus* in aqueous-organic solvent two-phase systems," *Enzyme Microb. Technol.*, vol. 23, no. 3, pp. 261–266, 1998.

[92] J.-F. Cavin, L. Barthelmebs, J. Guzzo, J. Van Beeumen, B. Samyn, J.-F. Travers, and C. Diviès, "Purification and characterization of an inducible p-coumaric acid decarboxylase from *Lactobacillus plantarum*," *FEMS Microbiol. Lett.*, vol. 147, no. 2, pp. 291–295, 1997.

[93] H. Rodriguez, I. Angulo, B. de las Rivas, N. Campillo, J. A. Páez, R. Muñoz, and J. M. Mancheño, "*p*-Coumaric acid decarboxylase from *Lactobacillus plantarum*: Structural insights into the active site and decarboxylation catalytic mechanism," *Proteins: Struct., Funct., Bioinf.*, vol. 78, no. 7, pp. 1662–1676, 2010.

[94] L. Barthelmebs, B. Lecomte, C. Divies, and J.-F. Cavin, "Inducible metabolism of phenolic acids in *Pediococcus pentosaceus* is encoded by an autoregulated operon which involves a new class of negative transcriptional regulator," *J. Bacteriol.*, vol. 182, no. 23, pp. 6724–6731, 2000.

[95] L. Godoy, V. Garcia, R. Peña, C. Martinez, and M. A. Ganga, "Identification of the *Dekkera bruxellensis* phenolic acid decarboxylase (PAD) gene responsible for wine spoilage," *Food Control*, vol. 45, pp. 81–86, 2014.

[96] H.-K. Huang, M. Tokashiki, S. Maeno, S. Onaga, T. Taira, and S. Ito, "Purification and properties of phenolic acid decarboxylase from *Candida guilliermondii*," *J. Ind. Microbiol. Biotechnol.*, vol. 39, no. 1, pp. 55–62, 2012.

[97] M. W. Bhuiya, S. G. Lee, J. M. Jez, and O. Yu, "Structure and mechanism of ferulic acid decarboxylase (FDC1) from *Saccharomyces cerevisiae*," *Appl. Environ. Microbiol.*, vol. 81, no. 12, pp. 4216–4223, 2015.

[98] W. Gu, J. Yang, Z. Lou, L. Liang, Y. Sun, J. Huang, X. Li, Y. Cao, Z. Meng, and K.-Q. Zhang, "Structural basis of enzymatic activity for the ferulic acid decarboxylase (FADase) from *Enterobacter sp*. Px6-4," *PloS ONE*, vol. 6, no. 1, p. e16262, 2011.

[99] M. Goujon, H. McWilliam, W. Li, F. Valentin, S. Squizzato, J. Paern, and R. Lopez, "A new bioinformatics analysis tools framework at EMBL–EBI," *Nucleic Acids Research*, vol. 38, no. suppl_2, p. W695, 2010 [Online]. Available: + http://dx.doi.org/10.1093/nar/gkq313

[100] F. Sievers, A. Wilm, D. Dineen, T. J. Gibson, K. Karplus, W. Li, R. Lopez, H. McWilliam, M. Remmert, J. Söding, J. D. Thompson, and D. G. Higgins, "Fast, scalable generation of high-quality protein multiple sequence alignments using Clustal Omega," *Molecular Systems Biology*, vol. 7, no. 1, 2011 [Online]. Available: http://msb.embopress.org/content/7/1/539

[101] J. M. van Dijl and M. Hecker, "*Bacillus subtilis*: from soil bacterium to super-secreting cell factory.," *Microb. Cell Fact.*, vol. 12, p. 3, 2013.

[102] J. Rosazza, Z. Huang, L. Dostal, T. Volm, and B. Rousseau, "Review: biocatalytic transformations of ferulic acid: an abundant aromatic natural product," *J. Ind. Microbiol.*, vol. 15, no. 6, pp. 457–471, 1995.

[103] S. Mathew and T. E. Abraham, "Bioconversions of ferulic acid, an hydroxycinnamic acid," *Crit. Rev. Microbiol.*, vol. 32, no. 3, pp. 115–125, 2006.

[104] X. Li, J. Yang, X. Li, W. Gu, J. Huang, and K.-Q. Zhang, "The metabolism of ferulic acid via 4-vinylguaiacol to vanillin by *Enterobacter sp*. Px6-4 isolated from Vanilla root," *Process Biochem.*, vol. 43, no. 10, pp. 1132–1137, 2008.

[105] A. Frank, W. Eborall, R. Hyde, S. Hart, J. P. Turkenburg, and G. Grogan, "Mutational analysis of phenolic acid decarboxylase from *Bacillus subtilis* (Bs PAD), which converts bio-derived phenolic acids to styrene derivatives," *Catal. Sci. Technol.*, vol. 2, no. 8, pp. 1568–1574, 2012.

[106] Y. Hashidoko and S. Tahara, "Stereochemically specific proton transfer in decarboxylation of 4-hydroxycinnamic acids by 4-hydroxycinnamate decarboxylase from *Klebsiella oxytoca*," *Arch. Biochem. Biophysics*, vol. 359, no. 2, pp. 225–230, 1998.

[107] S. Mishra, A. Sachan, A. S. Vidyarthi, and S. G. Sachan, "Transformation of ferulic acid to 4-vinyl guaiacol as a major metabolite: a microbial approach," *Rev. Environ. Sci. Biotechnol.*, vol. 13, no. 4, pp. 377–385, 2014.

[108] B. M. Upton and A. M. Kasko, "Strategies for the conversion of lignin to high-value polymeric materials: Review and perspective," *Chem. Rev.*, vol. 116, no. 4, pp. 2275–2306, 2015.

[109] H. Cheng, R. A. Gross, and P. B. Smith, *Green polymer chemistry: biobased materials and biocatalysis*. American Chemical Society, 2015.

[110] Y. Zhu, C. Romain, and C. K. Williams, "Sustainable polymers from renewable resources," *Nature*, vol. 540, no. 7633, pp. 354–362, 2016.

[111] NNFCC, "Renewable Polymers: Bioplastics," *Renewable Materials Factsheet*. The National Non-Food Crops Centre, pp. 1–2, 2010.

[112] "American Chemical Society National Historic Chemical Landmarks. Foundations of Polymer Science: Wallace Carothers and the Development of Nylon." [Online]. Available: http://www.acs.org/content/acs/en/education/whatischemistry/landmarks/carotherspolymers.html. [Accessed: 04-Jan-2017]

[113] M. Jamshidian, E. A. Tehrany, M. Imran, M. Jacquot, and S. Desobry, "Poly-lactic acid: production, applications, nanocomposites, and release studies," *Compr. Rev. Food Sci. Food Saf.*, vol. 9, no. 5, pp. 552–571, 2010.

[114] D. Garlotta, "A literature review of poly (lactic acid)," *J. Polym. Environ.*, vol. 9, no. 2, pp. 63–84, 2001.

[115] Y. Chen, L. M. Geever, J. A. Killion, J. G. Lyons, C. L. Higginbotham, and D. M. Devine, "A review of multifarious applications of poly (lactic acid)," *Polym.-Plast. Technol. Eng.*, vol. 55, pp. 1057–1075, 2016.

[116] I. S. Tawakkal, M. J. Cran, J. Miltz, and S. W. Bigger, "A review of poly (lactic acid)-based materials for antimicrobial packaging," *J. Food Sci.*, vol. 79, no. 8, pp. R1477–R1490, 2014.

[117] A. Anjum, M. Zuber, K. M. Zia, A. Noreen, M. N. Anjum, and S. Tabasum, "Microbial production of polyhydroxyalkanoates (PHAs) and its copolymers: A review of recent advancements," *Int. J. Biol. Macromol.*, vol. 89, pp. 161–174, 2016.

[118] K. Sudesh, H. Abe, and Y. Doi, "Synthesis, structure and properties of polyhydroxyalkanoates: biological polyesters," *Prog. Polym. Sci.*, vol. 25, no. 10, pp. 1503–1555, 2000.

[119] Z. Li, J. Yang, and X. J. Loh, "Polyhydroxyalkanoates: opening doors for a sustainable future," *NPG Asia Mater.*, vol. 8, p. e265, 2016.

[120] Y. Poirier, C. Nawrath, and C. Somerville, “Production of polyhydroxyalkanoates, a family of biodegradable plastics and elastomers, in bacteria and plants,” *Nat. Biotechnol.*, vol. 13, no. 2, pp. 142–150, 1995.

[121] J. G. Linger, D. R. Vardon, M. T. Guarnieri, E. M. Karp, G. B. Hunsinger, M. A. Franden, C. W. Johnson, G. Chupka, T. J. Strathmann, P. T. Pienkos, and G. T. Beckham, “Lignin valorization through integrated biological funneling and chemical catalysis.,” *Proc. Natl. Acad. Sci. U.S.A.*, vol. 111, no. 33, pp. 12013–8, 2014.

[122] P. M. Visakh, “Polyhydroxyalkanoates (PHAs), their Blends, Composites and Nanocomposites: State of the Art, New Challenges and Opportunities,” in *Polyhydroxyalkanoate (PHA) based Blends, Composites and Nanocomposites*, Royal Society of Chemistry, 2015, pp. 1–17.

[123] R. A. Sheldon, “Green and sustainable manufacture of chemicals from biomass: state of the art,” *Green Chem.*, vol. 16, no. 3, pp. 950–963, 2014.

[124] E. de Jong, M. Dam, L. Sipos, and G. Gruter, “Furandicarboxylic acid (FDCA), a versatile building block for a very interesting class of polyesters,” in *Biobased monomers, polymers, and materials*, vol. 1105, Patrick B. Smith and Richard A. Gross, Ed. American Chemical Society Washington, DC, 2012, pp. 1–13.

[125] J. Zhang, J. Li, Y. Tang, L. Lin, and M. Long, “Advances in catalytic production of bio-based polyester monomer 2, 5-furandicarboxylic acid derived from lignocellulosic biomass,” *Carbohydr. Polym.*, vol. 130, pp. 420–428, 2015.

[126] A. A. Rosatella, S. P. Simeonov, R. F. M. Frade, and C. A. M. Afonso, “5-hydroxymethylfurfural (HMF) as a building block platform: Biological properties, synthesis and synthetic applications,” *Green Chem.*, vol. 13, no. 4, pp. 754–793, 2011.

[127] S. Thiyagarajan, A. Pukin, J. van Haveren, M. Lutz, and D. S. van Es, “Concurrent formation of furan-2, 5-and furan-2, 4-dicarboxylic acid: unexpected aspects of the Henkel reaction,” *RSC Adv.*, vol. 3, no. 36, pp. 15678–15686, 2013.

[128] S. M. McKenna, S. Leimkühler, S. Herter, N. J. Turner, and A. J. Carnell, “Enzyme cascade reactions: synthesis of furandicarboxylic acid (FDCA) and carboxylic acids using oxidases in tandem,” *Green Chem.*, vol. 17, no. 6, pp. 3271–3275, 2015.

[129] S. Thiyagarajan, W. Vogelzang, R. J. Knoop, A. E. Frissen, J. van Haveren, and D. S. van Es, “Biobased furandicarboxylic acids (FDCAs): effects of isomeric substitution on polyester synthesis and properties,” *Green Chem.*, vol. 16, no. 4, pp. 1957–1966, 2014.

[130] R. McKenna, L. Moya, M. McDaniel, and D. R. Nielsen, "Comparing *in situ* removal strategies for improving styrene bioproduction," *Bioprocess Biosyst. Eng.*, vol. 38, no. 1, pp. 165–174, 2015.

[131] J. Scheirs, "Historical overview of styrenic polymers," *Modern Styrenic Polymers: Polystyrenes and Styrenic Copolymers. Wiley*, pp. 1–24, 2003.

[132] H. G. Bayne, B. J. Finkle, and R. E. Lundin, "Decarboxylative conversion of hydroxycinnamic acids to hydroxystyrenes by *Polyporus circinata*.," *J. Gen. Microbiol.*, vol. 95, no. 1, pp. 188–90, 1976.

[133] H. Chung, J. E. Yang, J. Y. Ha, T. U. Chae, J. H. Shin, M. Gustavsson, and S. Y. Lee, "Bio-based production of monomers and polymers by metabolically engineered microorganisms," *Curr. Opin. Biotechnol.*, vol. 36, pp. 73–84, 2015.

[134] B. Thompson, M. Machas, and D. R. Nielsen, "Creating pathways towards aromatic building blocks and fine chemicals," *Curr. Opin. Biotechnol.*, vol. 36, pp. 1–7, 2015.

[135] B. Max, J. Carballo, S. Cortés, and J. M. Dominguez, "Decarboxylation of ferulic acid to 4-vinyl guaiacol by *Streptomyces setonii*," *Appl. Biochem. Biotechnol.*, vol. 166, no. 2, pp. 289–299, 2012.

[136] H. Zhang and G. Stephanopoulos, "Engineering *E. coli* for caffeic acid biosynthesis from renewable sugars," *Appl. Microbiol. Biotechnol.*, vol. 97, no. 8, pp. 3333–3341, 2013.

[137] R. McKenna and D. R. Nielsen, "Styrene biosynthesis from glucose by engineered *E. coli*," *Metab. Eng.*, vol. 13, no. 5, pp. 544–554, 2011.

[138] S.-Y. Kang, O. Choi, J. K. Lee, J.-O. Ahn, J. S. Ahn, B. Y. Hwang, and Y.-S. Hong, "Artificial *de novo* biosynthesis of hydroxystyrene derivatives in a tyrosine overproducing *Escherichia coli* strain," *Microb. Cell Fact.*, vol. 14, no. 1, p. 78, 2015.

[139] P. H. Toy, "Polystyrene," in *Encyclopedia of Reagents for Organic Synthesis*, John Wiley & Sons, Ltd, 2001.

[140] P. Giardina, V. Faraco, C. Pezzella, A. Piscitelli, S. Vanhulle, and G. Sannia, "Laccases: a never-ending story," *Cell. Mol. Life Sci.*, vol. 67, no. 3, pp. 369–385, 2010.

[141] S. Riva, "Laccases: blue enzymes for green chemistry," *Trends Biotechnol.*, vol. 24, no. 5, pp. 219–226, 2006.

[142] C. F. Thurston, "The structure and function of fungal laccases," *Microbiology*, vol. 140, no. 1, pp. 19–26, 1994.

[143] A. Hatakka, “Biodegradation of lignin,” *Biopolymers Online*, 2005.

[144] L. P. Christopher, B. Yao, and Y. Ji, “Lignin biodegradation with laccase-mediator systems,” *Front. Energy Res.*, vol. 2, p. 12, 2014.

[145] N. Bahrin, P. M. Lee, and K. Ngalib, “Isolation and purification of laccase from rice straw fermented with *Pleurotus sajor-caju*,” in *Science and Social Research (CSSR), 2010 International Conference on*, 2010, pp. 736–740.

[146] D. Areskogh, “Structural Modifications of Lignosulphonates,” PhD Thesis, KTH Royal Institute of Technology, 2011.

[147] M. A. West, A. C. Hickson, M.-L. Mattinen, and G. Lloyd-Jones, “Evaluating lignins as enzyme substrates: Insights and methodological recommendations from a study of laccase-catalyzed lignin polymerization,” *BioResources*, vol. 9, no. 2, pp. 2782–2796, 2014.

[148] F. Hollmann and I. W. Arends, “Enzyme initiated radical polymerizations,” *Polymers*, vol. 4, no. 1, pp. 759–793, 2012.

[149] D. Areskogh and G. Henriksson, “Immobilisation of laccase for polymerisation of commercial lignosulphonates,” *Process Biochem.*, vol. 46, no. 5, pp. 1071–1075, 2011.

[150] I. F. Fiţigău, F. Peter, and C. G. Boeriu, “Oxidative polymerization of lignins by laccase in water-acetone mixture,” *Acta Biochim. Pol.*, vol. 60, no. 4, pp. 817–822, 2013.

[151] N. Aktaş and A. Tanyolaç, “Reaction conditions for laccase catalyzed polymerization of catechol,” *Bioresour. Technol.*, vol. 87, no. 3, pp. 209–214, 2003.

[152] K. Rittstieg, A. Suurnäkki, T. Suortti, K. Kruus, G. M. Guebitz, and J. Buchert, “Polymerization of guaiacol and a phenolic β-O-4-substructure by *Trametes hirsuta* laccase in the presence of ABTS,” *Biotechnol. Prog.*, vol. 19, no. 5, pp. 1505–1509, 2003.

[153] X. Sun, R. Bai, Y. Zhang, Q. Wang, X. Fan, J. Yuan, L. Cui, and P. Wang, “Laccase-catalyzed oxidative polymerization of phenolic compounds,” *Appl. Biochem. Biotechnol.*, vol. 171, no. 7, pp. 1673–1680, 2013.

[154] D. Areskogh, P. Nousiainen, J. Li, G. Gellerstedt, J. Sipilä, and G. Henriksson, “Sulfonation of phenolic end groups in lignin directs laccase-initiated reactions towards cross-linking,” *Ind. Biotechnol.*, vol. 6, no. 1, pp. 50–59, 2010.

[155] G. S. Nyanhongo, T. Kudanga, E. N. Prasetyo, and G. M. Guebitz, “Enzymatic polymer functionalisation: advances in laccase and peroxidase derived lignocellulose functional polymers,” in *Biofunctionalization of*

Polymers and their Applications, Springer, 2010, pp. 47–68.

[156] D. Areskogh, J. Li, P. Nousiainen, G. Gellerstedt, J. Sipilä, and G. Henriksson, "Oxidative polymerisation of models for phenolic lignin end-groups by laccase," *Holzforschung*, vol. 64, no. 1, pp. 21–34, 2010.

[157] D. van de Pas, A. Hickson, L. Donaldson, G. Lloyd-Jones, T. Tamminen, A. Fernyhough, and M. L. Mattinen, "Characterization of fractionated lignins polymerized by fungal laccases," *BioResources*, vol. 6, no. 2, pp. 1105–1121, 2011.

[158] K. Rittstieg, A. Suurnakki, T. Suortti, K. Kruus, G. Guebitz, and J. Buchert, "Investigations on the laccase-catalyzed polymerization of lignin model compounds using size-exclusion HPLC," *Enzyme Microb. Technol.*, vol. 31, no. 4, pp. 403–410, 2002.

[159] M.-L. Mattinen, T. Suortti, R. Gosselink, D. S. Argyropoulos, D. Evtuguin, A. Suurnäkki, E. de Jong, and T. Tamminen, "Polymerization of different lignins by laccase," *BioResources*, vol. 3, no. 2, pp. 549–565, 2008.

[160] K. Piontek, M. Antorini, and T. Choinowski, "Crystal structure of a laccase from the fungus*Trametes versicolor* at 1.90-Å resolution containing a full complement of coppers," *J. Biol. Chem.*, vol. 277, no. 40, pp. 37663–37669, 2002.

[161] S. Kawai, T. Umezawa, M. Shimada, and T. Higuchi, "Aromatic ring cleavage of 4,6-di(tert-butyl)guaiacol, a phenolic lignin model compound, by laccase of *Coriolus versicolor*," *FEBS Lett.*, vol. 236, no. 2, pp. 309–311, 1988.

[162] P. Baldrian, "Fungal laccases - occurrence and properties.," *FEMS Microbiol. Rev.*, vol. 30, no. 2, pp. 215–42, 2006.

[163] A. M. Mayer and R. C. Staples, "Laccase: new functions for an old enzyme.," *Phytochemistry*, vol. 60, no. 6, pp. 551–65, 2002.

[164] G. Anderson, "Marine science, the high tide zone," 2003. [Online]. Available: http://www.marinebio.net/marinescience/03ecology/tphi.htm. [Accessed: 16-Feb-2017]

[165] A. Trepte, "Blue Mussel," 2007. [Online]. Available: https://commons.wikimedia.org/wiki/File:Blue_mussel_Mytilus_edulis.jpg

[166] J. H. Waite, "Surface chemistry: mussel power," *Nat. Mater.*, vol. 7, no. 1, pp. 8–9, 2008.

[167] C. R. Matos-Pérez, J. D. White, and J. J. Wilker, "Polymer composition and substrate influences on the adhesive bonding of a biomimetic, cross-linking polymer," *J. Am. Chem. Soc.*, vol. 134, no. 22, pp. 9498–9505, 2012.

[168] B. P. Lee, P. B. Messersmith, J. N. Israelachvili, and J. H. Waite, "Mussel-inspired adhesives and coatings," *Annu. Rev. Mater. Res.*, vol. 41, pp. 99–132, 2011.

[169] N. Holten-Andersen, H. Zhao, and J. H. Waite, "Stiff coatings on compliant biofibers: the cuticle of *Mytilus californianus* byssal threads," *Biochemistry*, vol. 48, no. 12, pp. 2752–2759, 2009.

[170] D. R. Miller, S. Das, K.-Y. Huang, S. Han, J. N. Israelachvili, and J. H. Waite, "Mussel coating protein-derived complex coacervates mitigate frictional surface damage," *ACS Biomater. Sci. Eng.*, vol. 1, no. 11, pp. 1121–1128, 2015.

[171] L. Li and H. Zeng, "Marine mussel adhesion and bio-inspired wet adhesives," *Biotribology*, vol. 5, pp. 44–51, 2016.

[172] K. Rischka, K. Richter, A. Hartwig, M. Kozielec, K. Slenzka, R. Sader, and I. Grunwald, "Bio-inspired polyphenolic adhesives for medical and technical applications," in *Biological Adhesive Systems*, von Byern, Janek, and Grunwald, Ingo, Ed. Springer, 2010, pp. 201–211.

[173] H. Lee, S. M. Dellatore, W. M. Miller, and P. B. Messersmith, "Mussel-inspired surface chemistry for multifunctional coatings," *Science*, vol. 318, no. 5849, pp. 426–430, 2007.

[174] G. Westwood, T. N. Horton, and J. J. Wilker, "Simplified polymer mimics of cross-linking adhesive proteins," *Macromolecules*, vol. 40, no. 11, pp. 3960–3964, 2007.

[175] D. Leibig, A. H. Müller, and H. Frey, "Anionic polymerization of vinylcatechol derivatives: Reversal of the monomer gradient directed by the position of the catechol moiety in the copolymerization with styrene," *Macromolecules*, vol. 49, no. 13, pp. 4792–4801, 2016.

[176] H. Hatakeyama, E. Hayashi, and T. Haraguchi, "Biodegradation of poly (3-methoxy-4-hydroxy styrene)," *Polymer*, vol. 18, no. 8, pp. 759–763, 1977.

[177] S. Coghe, K. Benoot, F. Delvaux, B. Vanderhaegen, and F. R. Delvaux, "Ferulic acid release and 4-vinylguaiacol formation during brewing and fermentation: indications for feruloyl esterase activity in *Saccharomyces cerevisiae*," *J. Agric. Food Chem.*, vol. 52, no. 3, pp. 602–608, 2004.

[178] H. Leisch, S. Grosse, K. Morley, K. Abokitse, F. Perrin, J. Denault, and P. C. Lau, "Chemicals from agricultural biomass: chemoenzymatic approach for production of vinylphenols and polyvinylphenols from phenolic acids," *Green Process. Synth.*, vol. 2, no. 1, pp. 7–17, 2013.

[179] C. E. Carraher, *Introduction to Polymer Chemistry, Third Edition*. Taylor & Francis, 2012.

[180] Z. Huang, L. Dostal, and J. Rosazza, "Purification and characterization of a ferulic acid decarboxylase from *Pseudomonas fluorescens*.," *J. Bacteriol.*, vol. 176, no. 19, pp. 5912–5918, 1994.

[181] H.-P. Chen, M. Chow, C.-C. Liu, A. Lau, J. Liu, and L. D. Eltis, "Vanillin catabolism in *Rhodococcus jostii* RHA1," *Appl. Environ. Microbiol.*, vol. 78, no. 2, pp. 586–588, 2012.

[182] N. Nakashima and T. Tamura, "A novel system for expressing recombinant proteins over a wide temperature range from 4 to 35°C," *Biotechnol. Bioeng.*, vol. 86, no. 2, pp. 136–148, 2004.

[183] N. Nakashima and T. Tamura, "Isolation and characterization of a rolling-circle-type plasmid from *Rhodococcus erythropolis* and application of the plasmid to multiple-recombinant-protein expression," *Appl. Environ. Microbiol.*, vol. 70, no. 9, pp. 5557–5568, 2004.

[184] G. Sezonov, D. Joseleau-Petit, and R. D'Ari, "*Escherichia coli* physiology in Luria-Bertani broth," *J. Bacteriol.*, vol. 189, no. 23, pp. 8746–8749, 2007.

[185] D. Salvachúa, E. M. Karp, C. T. Nimlos, D. R. Vardon, and G. T. Beckham, "Towards lignin consolidated bioprocessing: simultaneous lignin depolymerization and product generation by bacteria," *Green Chem.*, vol. 17, no. 11, pp. 4951–4967, 2015.

[186] L. Han, J. Feng, S. Zhang, Z. Ma, Y. Wang, and X. Zhang, "Alkali pretreated of wheat straw and its enzymatic hydrolysis," *Braz. J. Microbiol.*, vol. 43, no. 1, pp. 53–61, 2012.

[187] T. D. Bugg, R. Rahmanpour, and G. M. Rashid, "Bacterial enzymes for lignin oxidation and conversion to renewable chemicals," in *Production of Biofuels and Chemicals from Lignin*, Fang, Zhen and Smith, Jr., Richard L., Ed. Singapore: Springer, 2016, pp. 131–146.

[188] D. Kaneko, S. Wang, K. Matsumoto, S. Kinugawa, K. Yasaki, D. H. Chi, and T. Kaneko, "Mussel-mimetic strong adhesive resin from bio-base polycoumarates," *Polym. J.*, vol. 43, no. 10, pp. 855–858, 2011.

[189] B. Lochab, S. Shukla, and I. K. Varma, "Naturally occurring phenolic sources: monomers and polymers," *RSC Adv.*, vol. 4, no. 42, pp. 21712–21752, 2014.

[190] C. L. Jenkins, H. M. Siebert, and J. J. Wilker, "Integrating mussel chemistry into a bio-based polymer to create degradable adhesives," *Macromolecules*, vol. 50, pp. 561–568, 2017.

[191] H. J. Meredith, C. L. Jenkins, and J. J. Wilker, "Enhancing the adhesion of a biomimetic polymer yields performance rivaling commercial glues," *Adv. Funct. Mater.*, vol. 24, no. 21, pp. 3259–3267, 2014.

[192] M. A. North, C. A. Del Grosso, and J. J. Wilker, “High strength underwater bonding with polymer mimics of mussel adhesive proteins,” *ACS Appl. Mater. Interfaces*, vol. 9, no. 8, pp. 7866–7872, 2017.

[193] H. J. Meredith and J. J. Wilker, “The interplay of modulus, strength, and ductility in adhesive design using biomimetic polymer chemistry,” *Adv. Funct. Mater.*, vol. 25, no. 31, pp. 5057–5065, 2015.

[194] H. J. Cha, D. S. Hwang, S. Lim, J. D. White, C. R. Matos-Perez, and J. J. Wilker, “Bulk adhesive strength of recombinant hybrid mussel adhesive protein,” *Biofouling*, vol. 25, no. 2, pp. 99–107, 2009.

[195] S. Gouveia, C. Fernández-Costas, M. A. Sanromán, and D. Moldes, “Enzymatic polymerisation and effect of fractionation of dissolved lignin from *Eucalyptus globulus* Kraft liquor.,” *Bioresour. Technol.*, vol. 121, pp. 131–8, 2012.

[196] H. Hatakeyama and T. Hatakeyama, “Lignin structure, properties, and applications,” in *Biopolymers*, Springer, 2009, pp. 1–63.

[197] A. Isakova, P. D. Topham, and A. J. Sutherland, “Controlled RAFT polymerization and zinc binding performance of catechol-inspired homopolymers,” *Macromolecules*, vol. 47, no. 8, pp. 2561–2568, 2014.

[198] W. H. Daly and S. Moulay, “Synthesis of poly(vinylcatechols),” in *J. Polym. Sci., Polym. Symp.*, 1986, vol. 74, no. 1, pp. 227–242.

[199] S. Hornig, T. Heinze, C. R. Becer, and U. S. Schubert, “Synthetic polymeric nanoparticles by nanoprecipitation,” *J. Mater. Chem.*, vol. 19, no. 23, pp. 3838–3840, 2009.

[200] B. Yang, D. G. Kang, J. H. Seo, Y. S. Choi, and H. J. Cha, “A comparative study on the bulk adhesive strength of the recombinant mussel adhesive protein fp-3,” *Biofouling*, vol. 29, no. 5, pp. 483–490, 2013.

[201] BSI, “Adhesives—determination of tensile lap-shear strength of bonded assemblies,” London, UK, 2009.